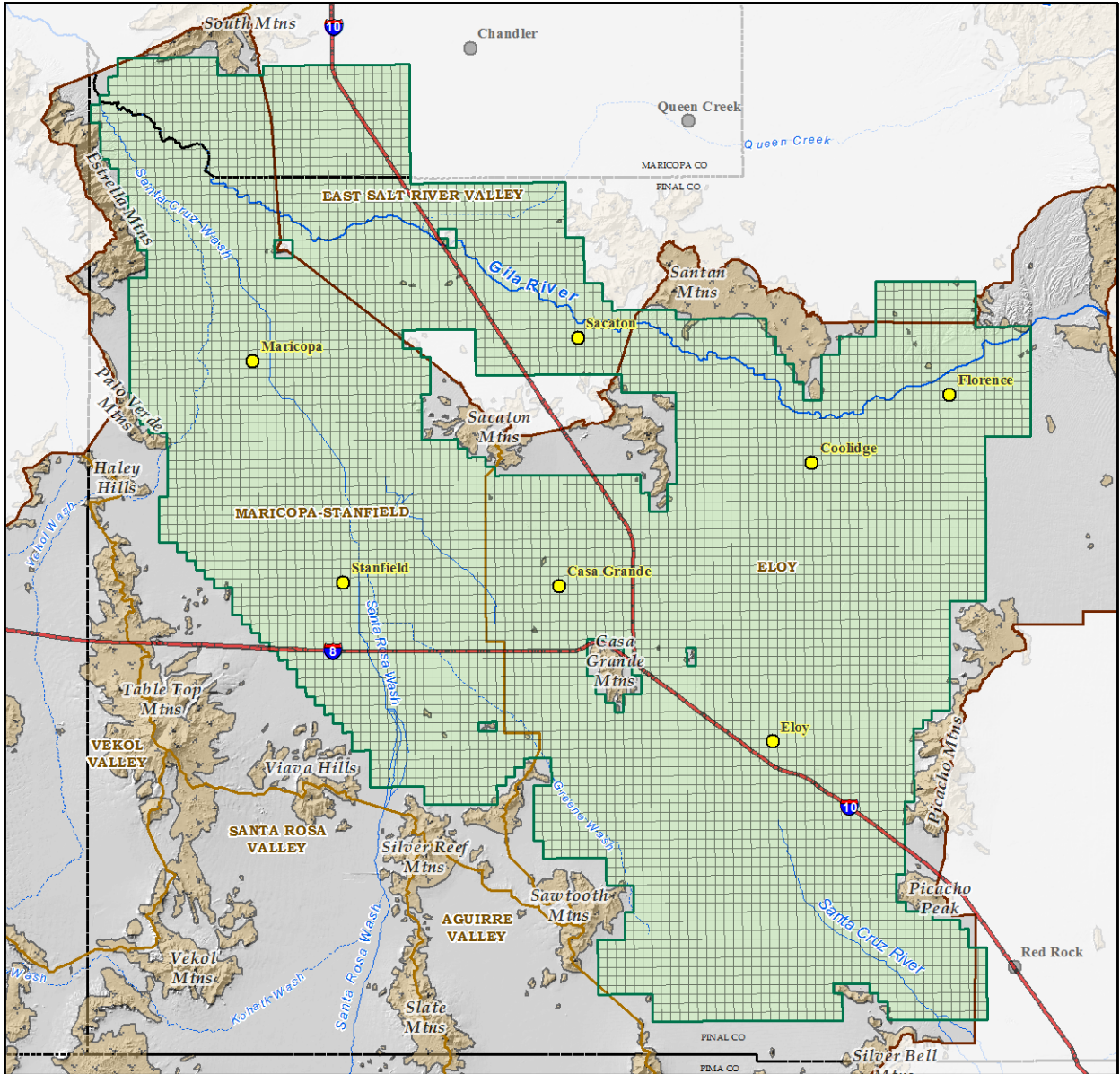


**ARIZONA DEPARTMENT OF WATER RESOURCES**  
**REGIONAL GROUNDWATER FLOW MODEL**  
**OF THE PINAL ACTIVE MANAGEMENT AREA, ARIZONA**  
**MODEL UPDATE AND CALIBRATION**



**Public Comment Draft 9/20/2013 - MODEL REPORT NO. 26**

**BY**

**SHUYUN LIU, KEITH NELSON, DIANNE YUNKER, WES HIPKE, FRANK CORKHILL**

**HYDROLOGY DIVISION - PHOENIX, ARIZONA**

# Table of Contents

<b>TABLE OF CONTENTS</b> .....	<b>II</b>
<b>LIST OF FIGURES</b> .....	<b>IV</b>
<b>LIST OF TABLES</b> .....	<b>VII</b>
<b>LIST OF APPENDICES</b> .....	<b>VII</b>
<b>LIST OF ACRONYMS</b> .....	<b>VIII</b>
<b>ABSTRACT</b> .....	<b>1</b>
<b>CHAPTER 1. GENERAL BACKGROUND</b> .....	<b>3</b>
INTRODUCTION .....	3
OBJECTIVE AND SCOPE .....	3
STUDY AREA .....	4
PREVIOUS INVESTIGATIONS .....	5
<b>CHAPTER 2. CONCEPTUAL MODEL</b> .....	<b>7</b>
HYDROGEOLOGIC UNITS .....	7
Upper Alluvial Unit (UAU) .....	8
Middle Silt and Clay Unit (MSCU) .....	9
Lower Conglomerate Unit (LCU) .....	11
Relationship between Hydrogeologic Units and Model Layers.....	12
LAND SUBSIDENCE AND EARTH FISSURES .....	13
HYDRAULIC PROPERTIES .....	16
Transmissivity and Hydraulic Conductivity .....	16
Storage Properties .....	23
CONCEPTUAL GROUNDWATER BUDGET .....	24
Inflows.....	25
Outflow.....	40
Conceptual Water Budget (1923 – 2009).....	43
<b>CHAPTER 3. NUMERIC MODEL</b> .....	<b>46</b>
MODEL DESCRIPTION AND FEATURES .....	46
MODFLOW PACKAGES.....	49
BOUNDARY CONDITIONS .....	51
MODEL DATA DEVELOPMENT .....	52
Water Levels .....	53
Aquifer Parameters.....	68
Pumping .....	69
Evapotranspiration .....	78
Stream flow Routing and Groundwater / Surface-Water Interactions .....	78
Natural Recharge.....	80
Incidental Recharge.....	82
Land Subsidence and Aquifer System Compaction.....	85

<b>CHAPTER 4. MODEL CALIBRATION .....</b>	<b>89</b>
CALIBRATION TARGETS AND STANDARDS .....	89
Water Level Targets .....	89
Land Subsidence Targets .....	91
Water Budget Comparisons .....	94
Residuals and Calibration Statistics .....	94
MODIFICATIONS OF MODEL INPUTS (STEADY-STATE AND TRANSIENT CALIBRATIONS).....	96
Agricultural Recharge .....	96
Canal Recharge .....	97
Stream Recharge .....	98
Other Recharge Components .....	98
Pumping .....	98
Hydraulic Conductivity .....	99
Vertical Conductance .....	100
Storage Coefficient.....	102
SUB-WT package parameters .....	102
CALIBRATION RESULTS .....	105
Steady-State Water Budget .....	105
Transient Water Budget .....	109
Head Residuals .....	112
Water Level Maps .....	115
Hydrographs .....	115
Simulated Inter-bed Storage (IB Storage).....	116
Observed and Simulated Subsidence .....	117
<b>CHAPTER 5. SENSITIVITY ANALYSIS.....</b>	<b>119</b>
SENSITIVITY RUNS.....	119
SENSITIVITY ANALYSIS METHODS.....	120
SENSITIVITY ANALYSIS PROCEDURES .....	121
SENSITIVITY RESULTS .....	122
Simulation without subsidence.....	122
Simulation using Non-Lagged Recharge .....	124
Vertical Hydraulic Conductivity (Kz).....	126
Recharge.....	128
Specific Yield (Sy).....	128
Pumping .....	132
Combined Pumping and Recharge.....	134
Combined Pumping and Specific Yield.....	136
Sensitivity Analysis of the SUB-WT Parameters .....	138
<b>6. MODEL SUMMARY AND RECOMMENDATIONS .....</b>	<b>140</b>
MODEL SUMMARY AND RESULTS .....	140
MODEL LIMITATIONS AND USES.....	142
RECOMMENDATIONS .....	143

## List of Figures

- Figure 1 Pinal AMA and Model Boundary
- Figure 2 Major Cities, Towns and Indian Reservations in the Pinal Model Area
- Figure 3 Pinal Model Area
- Figure 4 Wells With Logs and Hydrogeologic Data Used to Delineate the UAU (Layer 1)
- Figure 5 Depth to the Bottom (Thickness) of the UAU (Layer 1)
- Figure 6 Elevation of the Bottom of the UAU (Layer 1)
- Figure 7 Wells With Logs and Hydrogeologic Data Used to Delineate the MSCU (Layer 2)
- Figure 8 Depth to the Bottom of the MSCU (Layer 2)
- Figure 9 Elevation of the Bottom of the MSCU (Layer 2)
- Figure 10 Thickness of the MSCU (Layer 2)
- Figure 11 Wells With Logs and Hydrogeologic Data Used to Delineate the LCU
- Figure 12 Depth to the Bottom of the LCU (Layer 3)
- Figure 13 Elevation of the Bottom of the LCU (Layer 3)
- Figure 14 Thickness of the LCU (Layer 3)
- Figure 15 Geodetic Survey Points Within the Pinal Model Area
- Figure 16 Measured Subsidence Cross-Section A-A'
- Figure 17 Selected Aquifer Test Data in the Pinal Model Area
- Figure 18 Boundary Conditions in the Pinal Model Area
- Figure 19 Total Estimated Agricultural Acres, Agricultural Water Use and Agricultural Recharge (1923 – 2009) in the Pinal Model Area
- Figure 20 Comparison Of Total Agricultural Water Use Estimates in Pinal Model Area 1934 to 1983
- Figure 21 Total Estimated Agricultural Recharge in the Pinal Model Area 1923-2009 (Lagged and Non-Lagged)
- Figure 22 Major Irrigation Canals and Laterals in the Pinal Model Area
- Figure 23 Other Recharge Locations – Picacho Reservoir, Urban Irrigation, and USFs
- Figure 24 Pumping by Water Use for the Pinal Model Area from 1984 to 2009
- Figure 25 Pumping in the Pinal Model Area from 1923 to 2009
- Figure 26 Area of Riparian Evapotranspiration (ET)
- Figure 27 Pinal Model Grid
- Figure 28 Pinal, SRV and Hassayampa Model Locations Within the Central Arizona Model (CAM) Grid
- Figure 29 Hydrograph Locations in the Pinal Model Area
- Figure 30 1900 Composite Water Level Elevation Map - Pinal Model Area
- Figure 31 1900 Depth to Water - Pinal Model Area
- Figure 32 1941 Composite Water Level Elevation Map - Pinal Model Area
- Figure 33 1941 Depth to Water Map - Pinal Model Area
- Figure 34 1951 Composite Water Level Elevation Map - Pinal Model Area
- Figure 35 1951 Depth-to-Water Map - Pinal Model Area
- Figure 36. 1963 Composite Water Level Elevation Map - Pinal Model Area
- Figure 37 1963 Depth-to-Water Map - Pinal Model Area
- Figure 38 1976 Composite Water Level Elevation Map - Pinal Model Area
- Figure 39 1976 Depth-to-Water Map - Pinal Model Area
- Figure 40 1984 Water Level Elevations Per Model Layer
- Figure 41 1984 Depth-to-Water Map - Pinal Model Area
- Figure 42 1993 Composite Water Level Elevation Map - Pinal Model Area

Figure 43 1993 Depth-to-Water Map - Pinal Model Area.  
Figure 44 2003 Composite Water Level Elevation Map - Pinal Model Area  
Figure 45 2003 Depth-to-Water Map - Pinal Model Area  
Figure 46 2007 Water Level Elevation Maps Per Layer Pinal Model Area  
Figure 47 2007 Depth-to-Water Map - Pinal Model Area  
Figure 48 Pumping Sub-Areas in The Pinal Model  
Figure 49 Location of Pumping Wells in the Pinal Model Area  
Figure 50 Location of Evapotranspiration (ET) Cells in Pinal Model Area  
Figure 51 Natural Recharge Distribution - Pinal Model Area  
Figure 52 Major Agricultural Areas - Pinal Model Area  
Figure 53 Agricultural Recharge Maximum Extent - Pinal Model Area  
Figure 54 Maximum Distribution of Canal Recharge  
Figure 55 "Other" Recharge Distribution - Pinal Model Area  
Figure 56 Observed Land Subsidence in the Pinal Model Area 1952 to 1977  
Figure 57 Compressible Sediment Thickness Per Layer – Pinal Model Area  
Figure 58 Total Assigned Interbed Thickness for All Three Model layers  
Figure 59 Calibration Residuals for the Steady-State Simulation With the (SUB-WT) Package  
Figure 60 Calibration Residuals for 1941 Transient Simulation With the (SUB-WT) Package  
Figure 61 Calibration Residuals for 1952 Transient Simulation With the (SUB-WT) Package  
Figure 62 Calibration Residuals for 1963 Transient Simulation With the (SUB-WT) Package  
Figure 63 Calibration Residuals for 1976 Transient Simulation With the (SUB-WT) Package  
Figure 64 Calibration Residuals for 1984 Transient Simulation With the (SUB-WT) Package  
Figure 65 Calibration Residuals for 1988 Transient Simulation With the (SUB-WT) Package  
Figure 66 Calibration Residuals for 2007 Transient Simulation With the (SUB-WT) Package  
Figure 67 Plot of Observed Vs Computed Target Values (with SUB-WT) in the Pinal Model Area  
Figure 68 Plot of Observed Vs Residual Target Values (with SUB-WT) in the Pinal Model Area  
Figure 69 Predevelopment WL Contours - Conceptual and Model Simulated  
Figure 70 2007 Water Level Contours Per Layer Conceptual and Model Simulated  
Figure 71 Head Difference Between Layers for the Steady State Calibration  
Figure 72 Head Difference Between Layers for 1941  
Figure 73 Head Difference Between Layers for 1952  
Figure 74 Head Difference Between Layers for 1963  
Figure 75 Head Difference Between Layers for 1976  
Figure 76 Head Difference Between Layers for 1984  
Figure 77 Head Difference Between Layers for 1988  
Figure 78 Head Difference Between Layers for 2007  
Figure 79 Calibrated Hydraulic Conductivity for the UAU (Layer 1)  
Figure 80 Calibrated Hydraulic Conductivity for the MSCU (Layer 2)  
Figure 81 Calibrated Hydraulic Conductivity for the LCU (Layer 3)  
Figure 82 Calibrated Specific Yield for the UAU (Layer 1)  
Figure 83 Calibrated Specific Yield for the MSCU (Layer 2)  
Figure 84 Calibrated Specific Yield for the LCU (Layer 3)  
Figure 85 Calibrated Specific Storage for the MSCU (Layer 2)  
Figure 86 Calibrated Specific Storage for the LCU (Layer 3)  
Figure 87 Simulated Pinal Model Cumulative Change in Storage Plus Interbed Storage Change  
Figure 88 Simulated Net Storage Change and Interbed Storage Change

Figure 89 Simulated and Observed Subsidence 1952 to 1977  
Figure 90 Measured vs Simulated Subsidence Along Cross-Section A – A'  
Figure 91 Total Simulated Subsidence after 88 stress periods, from 1923 to 2009  
Figure 92 Observed Subsidence Between 2004 and 2009  
Figure 93 Hydrograph at location H76 Layer 2 Simulated Heads With and Without Subsidence  
Figure 94 Hydrograph at location H36 Layer 1 Simulated Heads Lagged and Non-Lagged Recharge  
Figure 95 Average head change (At SP 88) scaled multiplier of Kz per model layer  
Figure 96 Average head change (At SP88) with respect to scaled multiplier of Kz per model sub-basin  
Figure 97 Average head change (At SP 88) Percentage Change in Recharge By Model Layer  
Figure 98 Average head change (At SP 88) Percentage Change in Recharge By Sub-Basin  
Figure 99 Average head change (At SP 88) Sy Multiplier By Model Layer  
Figure 100 Average head change (At SP 88) Sy Multiplier By Sub-Basin  
Figure 101 Average head change (At SP 88) Pumping Multiplier By Model Layer  
Figure 102 Average head change (At SP 88) Pumping Multiplier By Sub-Basin  
Figure 103 Average Head Change (At SP 88) Combined Pumping and Recharge Change By Model Layer  
Figure 104 Average Head Change (At SP 88) Combined Pumping and Recharge By Sub-Basin  
Figure 105 Model-Wide Average change in Head (At SP 88) of the Individual vs. Combined Pumping and Recharge  
Figure 106 Average head change (At SP 88) the Combined Pumping and Specific Yield Change By Model Layer  
Figure 107 Average head change (At SP 88) the Combined Pumping and Specific Yield Change By Sub-Basin  
Figure 108 Model-Wide Average Change in Head (At SP 88) of the Individual vs. Combined Pumping and Specific Yield (Sy)  
Figure 109 Sensitivity of SUB-WT Parameters (Cc, Cr, Precon, Void Ratio) – Layer 1  
Figure 110 Sensitivity of SUB-WT Parameters (Cc, Cr, Precon, Void Ratio) – Layer 2  
Figure 111 Sensitivity of SUB\_SWT Parameters (Cc, Cr, Precon, Void Ratio) – Layer 3  
Figure 112 Sensitivity of SUB\_SWT Parameter (Cc) – All Layers  
Figure 113 Sensitivity of SUB-WT Parameter (Cr) – All Layers  
Figure 114 Sensitivity of SUB-WT Parameter (Precon) – All Layers  
Figure 115 Sensitivity of SUB-WT Parameter (Void Ratio) – All Layers  
Figure 116 Model-Wide Average Change in Head (At SP 88) Vertical Hydraulic Conductivity (Kz)  
Figure 117 Comparison of the Model-Wide Average Changes in Head (At SP 88) Between Pumping, Recharge and Specific Yield (Sy)  
Figure 118 Sensitivity Analysis of Fundamental Model Parameters and Stresses Compared to Base SUB-WT in the Pinal Model

## List of Tables

Table 1 Selected Aquifer Test Data in the Pinal Model Area.....	21
Table 2 Selected Underflow Estimates in the Pinal Model Area.....	26
Table 3 Estimated Gila River Flood Recharge in the Pinal Model Area 1934 to 2009.....	30
Table 4 Estimated Maximum Potential Recharge for San Carlos Project Canals and Laterals 1944 to 2009 .....	38
Table 5 Conceptual Water Budgets for the Pinal Model Area for Steady-State (Circa 1923) and Transient Period (1923 to 2009) .....	45
Table 6 Pinal Model Features and Characteristics.....	48
Table 7 Total Simulated Pumping in the Pinal Model Area 1923-2009 (by Sub-Area).....	71
Table 8 San Carlos Project Pumping to Agency and District Parts 1934 to 2009.....	73
Table 9 Estimated and Reported Pumping Data for GRIC 1923 to 2009.....	76
Table 10 Pinal Model Water Level Calibration Targets.....	93
Table 11 Pinal Model Simulated Steady-State Water Budget (With and Without the SUB-WT) ....	108
Table 12 Conceptual and Model Simulated Steady-State Water Budgets <sup>1</sup> .....	108
Table 13 Model Simulated 1923 – 2009 Water Budgets (With and Without SUB-WT).....	110
Table 14 Conceptual and Simulated (With SUB-WT) Pinal Model Water Budgets 1923 to 2009 .....	111
Table 15 Pinal Model Steady-State and Transient Residual Summary .....	114
Table 16 Model Sensitivity to Subsidence (Without SUB-WT) .....	123
Table 17 Model Sensitivity to Lagged and Non-Lagged Agricultural Recharge .....	125
Table 18 Model Sensitivity to Vertical Hydraulic Conductivity .....	127
Table 19 Model Sensitivity to Recharge.....	130
Table 20 Model Sensitivity to Specific Yield.....	131
Table 21 Model Sensitivity to Pumping .....	133
Table 22 Combined Model Sensitivity to Pumping and Recharge.....	135
Table 23 Combined Model Sensitivity to Pumping and Specific Yield.....	137

## List of Appendices

- Appendix A – Selected Pump Test Data In Pinal Model Area
- Appendix B – Leaky Aquifer Analyses For Selected Wells in Pinal Model Area
- Appendix C – Hydrographs
- Appendix D – Sensitivity Analyses Data

## List of Acronyms

AAWS	Assured and Adequate Water Supply
ADWR	Arizona Department of Water Resources
AMA	Active Management Area
AME	Absolute Mean Error
BAS	Basic Package
BCF	Block-Centered Flow Package
BLS	Below Land Surface
CAP	Central Arizona Project
CHB	Constant Head Boundary
CHD	Time-Variant Specified-Head Package
DIS	Discretization Package
DTW	Depth-to-Water
ET	Evapotranspiration
GFR	Grandfathered Right
GMG	Geometric Multigrid Solver Package
GRIC	Gila River Indian Community
GWSI	Groundwater Site Inventory
HOB	Hydraulic-Head Observation Package
HMS	Hydrologic Map Series
HYDMOD	MODFLOW Hydrograph Program
IGFR	Irrigation Grandfathered Rights
INSAR	Inferometric Synthetic Aperture Radar
K	Hydraulic Conductivity
LCU	Lower Conglomerate 1 Unit
MSCU	Middle Silt and Clay Unit
ME	Mean Error
RCH	Recharge Package
RMSE	Root Mean Squared Error
ROGR	Registry of Grandfathered Rights
SCIP	San Carlos Irrigation Project
SFR	Stream Flow Routing Package
SRP	Salt River Project
SRPMIC	Salt River Pima-Maricopa Indian Community
SRV	Salt River Valley
SUB-WT	Subsidence and Aquifer-System Compaction Package for Water-table Aquifers
UAU	Upper Alluvial Unit
USBR	United States Bureau of Reclamation
USF	Underground Storage Facilities
USGS	United States Geological Survey
VCONT	Vertical Conductance
WEL	Well Package
WWTP	Waste Water Treatment Plant

## Abstract

The Pinal Active Management Area (AMA) was established by the Groundwater Management Act of 1980. The Pinal AMA covers approximately 4,000 square miles in the south-central portion of the State between Phoenix and Tucson. The management goal of the Pinal AMA is to allow development of non-irrigation uses and to preserve existing agricultural economies in the AMA for as long as feasible, consistent with the necessity to preserve future water supplies for non-irrigation uses. Groundwater flow models have become an integral tool in understanding the complex interactions that affect regional aquifers and assisting in analysis of potential future conditions due to the effects of various stresses on aquifers ranging from changes in climate, urbanization, or management practices.

The first numerical groundwater flow model of the Pinal AMA was developed by the Arizona Department of Water Resources (ADWR) in 1990. The original model consisted of two layers, and simulated groundwater conditions at steady-state, circa 1900, and for a transient-state from 1985 to 1988. This report documents an extensive update of the 1990 model. The key elements of the model update include:

- (1) Standardization and refinement of the model grids, using uniform model grids of 0.5 mile<sup>2</sup>;
- (2) Increased model layering from two to three layers;
- (3) Extension of the northern model boundary to include the Gila River throughout the entire model domain;
- (4) Inclusion of most of the Gila River Indian Reservation within the model domain;
- (5) Model code updated to United States Geological Survey (USGS) - MODFLOW 2005 with inclusion of the subsidence package for land subsidence simulation.

- (6) Performed geologic data collection and analysis, and updated model geology;
- (7) Performed modeling data collection and database development of historic pumping, recharge, water levels, well constructions, hydraulic properties, and land subsidence.
- (8) Simulation of groundwater conditions from pre-development (circa 1922) to near present time (2009) with annual stress periods

The updated Pinal model simulated regional water level fluctuations over the past 87 years within industry standards (ASTM, 1996) through the evaluation of well hydrographs, water level contour maps, and the model water budgets. More importantly, this updated model was able to reasonably simulate the pronounced vertical gradients between different aquifer units in both the Maricopa-Stanfield and Eloy sub-basins. In addition, the model simulates the area of documented regional land subsidence in Pinal AMA, and the model simulated land subsidence rates reasonably match observed rates and trends over the historic period of record for leveling (survey) data. The simulated aquifer storage loss, due to inter-bed compaction, substantially improved model calibration and helped quantify this important, but previously un-simulated process.

# Chapter 1. General Background

## Introduction

The Arizona Department of Water Resources (ADWR) has updated its groundwater flow model of the Pinal Active Management Area (AMA). Since the AMA's inception in 1980, ADWR's focus within the Pinal AMA has been to maintain the existing agricultural economy for as long as feasible; and to also preserve future water supplies for non-agricultural uses.

The Pinal AMA has experienced significant population growth and changes in land use, water supplies, and other stresses to the regional aquifer since it was established in 1980. It is likely that water demand and supply will also vary considerably in the future. The updated Pinal AMA model provides a useful tool to assist in analyzing the potential future impact(s) of those changes.

## Objective and Scope

The purpose of the Pinal model update was to upgrade the existing Pinal AMA groundwater flow model to provide an effective tool to simulate future water management scenarios within the Pinal AMA. The Pinal model database also serves as a repository for a wide range of hydrologic and geologic data. This model study was divided into two phases. Phase I updated various features and components of the existing model. The model updates include:

- ✓ Revised geologic interpretation
- ✓ Increasing the model layers to three from two
- ✓ Refined model grid from 1 mile to 0.5 mile grid spacing
- ✓ Extending the active model boundary north to encompass the Gila River reach from the eastern edge of the Pinal AMA to west of South Mountain

- ✓ Updated groundwater budget components including pumpage and recharge
- ✓ Increased the transient model simulation period from 1923 to 2009
- ✓ Incorporated the latest MODFLOW code
- ✓ Inclusion of MODFLOW Subsidence package

Phase II included calibration of the model from steady-state conditions in the early 1900's to near-current conditions in 2009. The MODFLOW subsidence package was used to simulate observed land subsidence trends in the Pinal AMA. This report provides an overview of the Pinal model development and a detailed analysis of the updates that were made to the model.

### **Study Area**

The Pinal AMA is located in the basin and range physiographic province of Central Arizona. It is about 4,000 square miles in size, and includes five groundwater sub-basins: Maricopa-Stanfield, Eloy, Vekol Valley, Santa Rosa Valley, and Aguire Valley (Figure 1). The Pinal active model domain is approximately 1,513 square miles (mi<sup>2</sup>) in area and includes most of the Maricopa-Stanfield and Eloy sub-basins, the Ak-Chin Indian Reservation and the Gila River Indian Community (GRIC) area. The model domain covers areas with concentrated urban and agriculture development. Figure 2 shows the urban centers within the Pinal model as well as the three Indian communities: the Gila River Indian Community (GRIC), Ak-Chin Indian Community, and Tohono O'Odham.

The groundwater basin portion of the Pinal model is generally surrounded by mountains that form essentially impervious boundaries to groundwater flow (Figure 3). The active model domain is bounded on the south and southwest by the Silverbell, Sawtooth, Silver Reef Mountains, and the Viava Hills. Table Top Mountain, the Halley Hills, the Palo Verde and the Estrella mountains form the western model boundary. The model is bounded on the north by

South Mountain, the Sacaton and Santan Mountains. The Picacho Mountains and Picacho Peak form the eastern boundary. The Casa Grande Mountains are located in the middle of the model domain, partially separating the Maricopa-Stanfield and the Eloy sub-basins.

Two major ephemeral streams traverse the model area (Figure 3). The Gila River is located in the northern portion of the model area, and flows from east to west. During pre-development, the Gila River was perennial throughout the model area. Since the construction of Coolidge Dam and Ashurst-Hayden Dam, the flow in the Gila River has been generally regulated by upstream reservoir releases and diversions at Ashurst-Hayden Dam. The Santa Cruz River flows northwesterly through the model area, and has a poorly defined channel in the western part of the Eloy sub-basin. It only flows in response to intense rainfall. The confluence of the two streams is located in the northwest corner of the Pinal AMA.

### **Previous Investigations**

W.T. Lee (1904) investigated the underground waters in Gila Valley, and documented hydrogeologic information for the Gila Valley including geology, wells, water levels, and groundwater quality. Groundwater underflows were also estimated in this study. In 1940, Smith conducted a study to quantify the groundwater supply in Eloy. The U.S. Geological Survey (USGS) investigated the groundwater resources in Santa Cruz Basin (Turner and others, 1943), in Gila River Basin and adjacent areas (Halpenny and others, 1952), and in Western Pinal County (Hardt and Cattany, 1965). Anderson (1968) constructed an electrical-analog model to assess the impact of groundwater pumping on the groundwater system in Central-Arizona using known aquifer characteristics and the pumping history between 1923 and 1964. The US Bureau of Reclamation (1976) published a regional geology and groundwater resources report for the Central Arizona Project (CAP) for Maricopa and Pinal counties.

Based on previous work that had been done in central Arizona and using the USGS MODFLOW code, ADWR developed a three-dimensional numerical model for Pinal AMA which simulated transient flow conditions between 1985 and 1988 (Corkhill and Hill, 1990). In 1991 Thomsen and Eychaner of USGS developed a two-dimensional steady-state numerical model to simulated pre-development hydrologic conditions in the Gila River Corridor. This modeling effort was undertaken to better understand groundwater conditions before the Gila River surface water diversion was started upstream from the GRIC area, and to aid in the evaluation of water right claims. In 2001, Pool and others at the USGS conducted an investigation into the hydrogeologic conditions in the Picacho Basin, and documented their conceptualizations of the hydrogeologic system. In 2004, ADWR estimated groundwater inflow and outflow components and derived a conceptual groundwater budget for the Pinal AMA from 1980 to 2002. Burgess and Niple was subsequently retained to conduct a professional review of the conceptual water budget developed by ADWR to evaluate the various water budget components in terms of general accuracy and overall applicability (Burgess and Niple, 2004).

## **Chapter 2. Conceptual Model**

The original ADWR Pinal model (Wickham and Corkhill, 1989 and Corkhill and Hill, 1990) serves as a basic framework for this updated model. Within the past 20 years, diligent data collection efforts have yielded significant additional data to provide a better understanding of the geology, hydrogeology, and groundwater development in the Pinal AMA. In addition to the new data, the USGS-MODFLOW code has been updated and expanded with the addition of new features and modules, such as the stream flow routing package and the subsidence package. In this updated model study, the original conceptual model has been reviewed and revised; each component of the updated conceptual model is discussed in detail in the following sections.

### **Hydrogeologic Units**

Since the completion of the original Pinal AMA model in 1990, the amount of information from wells drilled in the Pinal model area has increased significantly. During this model update, thousands of well logs including driller's logs, particle size logs, geologist logs, and geological logs were reviewed. Out of all the logs studied, 1,993 logs were used; 1,882 of which were driller's logs. Information derived from these logs was used to refine geologic interpretations in the Pinal model area. Detailed information on the geology update can be found in the Regional Groundwater Flow Model of the Pinal Active Management Area Provisional Report Geology Update (Dubas and Liu, 2010). This section summarizes the new findings and revisions from the updated geology interpretation.

Within the Pinal model area, the Maricopa-Stanfield and Eloy sub-basins are separated by a shallow, buried bedrock ridge referred to in this report as Casa Grande Ridge. This ridge

trends in a north-south direction from the Sacaton Mountain to the Silver Reef Mountain and is about 150 feet below the land surface.

The four major hydrogeologic units identified in the Phase One report for the Pinal AMA Regional Groundwater Flow Model (Wickham and Corkhill, 1989) were also used in the updated geology interpretation. From top to bottom, these units are the Upper Alluvial Unit (UAU), Middle Silt and Clay Unit (MSCU), Lower Conglomerate Unit (LCU), and Hydrogeologic Bedrock Unit (HBU). General descriptions of these units were provided in the ADWR Pinal AMA Regional Groundwater Flow Model Phase One Report (Wickham and Corkhill, 1989) and in the Regional Groundwater Flow Model of the Pinal Active Management Area Provisional Report Geology Update (Dubas and Liu, 2010). Numerous logs were reviewed to refine the geologic structure and properties simulated in this model. However, some logs were not used due to various factors including: the quality of the log/data, discretization and scale issues, and smoothing of data to assist model convergence (especially along the model boundaries) or in areas where a hydrogeologic unit pinches out. General descriptions and an overview of the three main water-bearing units that are simulated in the model are summarized below.

#### ***Upper Alluvial Unit (UAU)***

The UAU consists primarily of unconsolidated to slightly consolidated inter-bedded sand and gravels with some finer grained materials existing as lenses. Cementation is low to non-existent (Wickham and Corkhill, 1989). Review of driller's logs indicates that in some areas of Eloy, in the lower part of the UAU, there is a transition zone where relatively coarse alluvial materials are inter-bedded with finer-grained material. This transition zone was previously included in the UAU according to the Phase One Report for the Pinal AMA Regional Groundwater flow model (Wickham & Corkhill, 1989).

Simulation of land subsidence was one of the objectives of this model update. Delineation of the spatial extent of finer materials that are susceptible to aquifer compaction is critical. Therefore, when updating the geology, the transition zone which contains layers of finer grained materials was grouped with the MSCU unit for a better simulation of land subsidence. The revised interpretation is based on the fact that hydraulic parameters of the transition zone are much more similar to those of MSCU. Compared to the original Pinal model, the revised geology for this study shows a thinner UAU overlying a thicker MSCU in areas where the transition zone is present.

Numerous driller's logs were reviewed for UAU contact delineation. Figure 4 shows the locations of logs that were reviewed to estimate the UAU contact. The data deficient areas are limited to basin margins and the northwest corner of the model area (Figure 4). Figures 5 and 6, illustrate depth to the bottom of UAU, which is the same as the layer thickness, and the UAU bottom elevation, respectively. The UAU generally has a greater thickness in the basin centers (Figure 5). The maximum UAU thickness was estimated to be about 450 feet in the Eloy sub-basin.

#### ***Middle Silt and Clay Unit (MSCU)***

The MSCU is a fine grained unit that consists primarily of silt, clay, and sand (Wickham and Corkhill, 1989). During the Pinal Model geology update, the criteria used to define the MSCU unit were compared for consistency with criteria used in the SRV regional model geologic update (Dubas and Davis, 2006). Specifically, the MSCU was defined by counting the frequency and thickness of fine-grained samples. The MSCU was required to contain at least 40 percent of clay and/or silt and have a total thickness of at least 60 feet. Based on this criterion,

the transition zone existing in some areas of Eloy sub-basin that was previously included in UAU (Wickham and Corkhill, 1989) is now interpreted to be part of the MSCU.

Figure 7 shows the locations of logs reviewed for estimating the MSCU contact. The locations of the geological data points give a clear indication of areas of data deficiency, specifically in the centers of the major basins and the northwest corner of the model area. However, this may be due more to the fact that most wells drilled in those locations do not penetrate the bottom of the MSCU, rather than due to the lack of well data itself. Areas where the simulated depth and thickness of the MSCU has been adjusted due to data deficiencies or model stability concerns are discussed later in the report.

As indicated in Figure 7, there is little or no MSCU in the Casa Grande Ridge area (center of the model area), along the Gila River corridor (between the Sacaton and San Tan Mountains, and east of Florence), at the basin margins, and in the southeastern corner of the model area. Figures 8, 9, and 10 illustrate the simulated depth to the bottom of MSCU, MSCU bottom elevation and MSCU thickness, respectively. In general, the thickness of MSCU increases from the basin margins towards the basin centers, and decreases towards the Casa Grande Ridge. The MSCU is more extensive and much deeper in the Eloy sub-basin than in Maricopa-Stanfield sub-basin. The maximum thickness of MSCU was estimated to be nearly 6,000 feet in the center of the Eloy sub-basin. In the northwestern portion of the model area, the MSCU is comparatively thick, however the unit pinches out towards the east. It should be noted that for modeling purposes, the simulated MSCU thickness in the center of the Eloy sub-basin was truncated at depth of 2800 ft. Details on MSCU bottom truncation are discussed later in the report.

### *Lower Conglomerate Unit (LCU)*

The LCU is characterized by semi-consolidated to consolidated coarse sediments consisting of granite fragments, cobbles, boulders, sands and gravels with varying degree of cementation (Wickham and Corkhill, 1989). This unit is the deepest water bearing unit in the model area and generally overlies impermeable bedrock.

During the Pinal model geology update, the estimated thickness of the LCU was modified for modeling purposes in the Casa Grande ridge area. Review of driller's logs in the Casa Grande Ridge area revealed that there was little or no LCU deposited over a portion of the ridge area (Dubas and Liu, 2010). The same observation was also noted in the study performed by Hardt and Cattany (1965). Figure 11 shows the area where no evidence of the LCU was found in drillers logs. In the absence of the LCU, the thick fractured bedrock in this area has been recognized as an important source of water in this bedrock high area. Consequently, a decision was made to include 200 feet of fractured bedrock in the LCU in the Casa Grande Ridge area (Figure 11). The 200 feet is used to account for the average depth of wells in this area that penetrate the top portion of the fractured bedrock.

Figure 11 also shows the locations of wells with driller logs used to delineate the LCU bottom elevation. As seen on this figure, there are many areas where there are insufficient data to define the bottom of the LCU with any level of confidence. Available driller logs data are concentrated in areas where the bedrock is relatively shallow. Little or no log data are available in basin centers of both the Maricopa-Stanfield and Eloy sub-basins. In these data gap areas, the estimated bottom depth of the LCU is primarily based on depth-to-bedrock data presented in the Arizona Geological Survey study by Richard, Reynolds, Spencer, and Pearthree (2000).

Figures 12, 13, and 14 illustrate simulated depth to the bottom of the LCU, LCU bottom elevation and LCU thickness, respectively. The estimated thickness of the LCU ranges from less than 50 feet to over 8,000 feet. The LCU is thicker in the northwest portion of the model area, and in the centers of Maricopa-Stanfield and Eloy sub-basins. The greatest thickness is occurs in the area southwest of Eloy. The LCU is thinner in the Casa Grande Ridge area and in the Gila River corridor east of Gila Butte. Areas where the simulated depth and thickness of the LCU has been adjusted due to data deficiencies or model stability concerns are discussed later in the next section of this report.

#### ***Relationship between Hydrogeologic Units and Model Layers.***

Three model layers were used to represent the three hydrogeologic units. Model Layer 1 was used to represent the UAU, Layer 2 to represent the MSCU, and Layer 3 to represent the LCU. No modifications were made to the estimated thickness or bottom elevation of the UAU when translating that unit's structure into Layer 1.

Two modifications were made in translating the geologic structure of the MSCU into model Layer 2. The first modification involved assigning a minimum thickness to model Layer 2 in areas where the MSCU thins significantly or pinches out, such as in the Casa Grande Ridge area and along the basin margins. In areas where the MSCU pinches out, or is less than 50 feet in thickness, a minimum thickness of 50 feet was assigned to model Layer 2 cells. In such areas, the original combined thickness of the UAU, MSCU and LCU was maintained by subtracting 50 feet from the top elevation of the underlying Layer 3 (LCU) model cells. Hydraulic properties representative of the LCU were assigned to the Layer 2 model cells in those areas. This modification created a "continuous" Layer 2 throughout the model area, and improved the model's numerical stability by reducing large changes in model layer thicknesses between

horizontally adjacent model cells. The modification also allowed the model to better simulate observed hydraulic gradients in the all model layers in areas where the MSCU abruptly thins or pinches out.

The MSCU in the Eloy sub-basin is very thick, especially in the basin center. Since the total thickness of the model is truncated at a depth of 3,000 feet bls, the bottom of Layer 2 was limited, where applicable, to a maximum depth of 2,800 feet bls. Similar to the modifications made in areas where the MSCU thins or pinches out, this modification improves the model's numerical stability and provides lateral continuity, where applicable, for horizontal groundwater flow in Layer 3. The model area affected by the truncation of the MSCU is shown in Figure 7.

Only one modification besides the inclusion of the weathered/fractured bedrock in the Casa Grande Ridge area was made when translating the LCU structure into model Layer 3. Where applicable, in the centers of both the Maricopa-Stanfield and Eloy sub-basins, the bottom of the LCU was truncated at a depth of 3,000 feet bls. Figure 11 shows the area affected by the truncation of the LCU.

### **Land Subsidence and Earth Fissures**

Land subsidence is the downward movement or sinking of the Earth's surface caused by removal of underlying support (Slaff, 1993). An earth fissure is a crack at or near the earth's surface that is caused by land subsidence (Slaff, 1993). Differential aquifer compaction results in the development of earth fissures. Land subsidence can be caused by natural processes and/or human activities. The major activity that has caused historic land subsidence and earth fissures observed in Pinal model area is groundwater pumping.

The Pinal AMA has an agricultural dominated economy, and groundwater has been the primary source for irrigation before Central Arizona Project (CAP) water became available in

1987. Groundwater pumping increased greatly since the 1930s in the AMA, reaching a peak level of about 1.4 million acre-feet in 1953. Groundwater pumping continued at that relatively high level until the late 1980s. Over the period of groundwater development, long-term pumping has greatly exceeded natural recharge. As a result, groundwater levels have declined substantially in both the Maricopa-Stanfield and Eloy sub-basins. The declining water levels have caused a reduction in hydrostatic pressure and an increase in the effective stress that is applied to the aquifer system. The increases in vertical effective stress cause the compaction of the fine-grained materials, thus resulting in land subsidence (Pool and others, 2001).

Land subsidence in the Pinal area has been investigated and documented by many previous studies. Land subsidence was first detected in 1934 when the USGS conducted first-order leveling and subsequent checks on bench marks along the 1905 primary level line from Casa Grande to near Picacho Peak (Figure 15) and about 0.5 feet of land subsidence was measured in the area west of Eloy at that time (Robinson and Peterson, 1962). Later surveys were conducted by National Geodetic Survey in 1948, 1952, 1960, and 1967; by Arizona Department of Transportation in 1961 and 1964; by the U.S. Bureau of Reclamation in 1964; and by the USGS in 1977 (Laney and others, 1978).

From 1952 to 1977, data shown in Laney's 1978 report indicated that about 120 square miles in the Eloy and Stanfield area had subsided by more than 7 feet. The amount of subsidence increased substantially since 1952 and was greatest near the town of Picacho (Laney and others, 1978). Figure 16 is a land subsidence cross-section covering the central portion of the Eloy sub-basin that was reproduced from data shown in Laney's report. This figure shows the increase of the subsidence rate over time along the primary level line in Eloy (Laney and others, 1978). As shown on Figure 16, the point of the greatest land subsidence was observed to migrate

southeastward over time from the west of Eloy to Picacho (Laney and others, 1978). More than 15 feet of land subsidence was measured as of 1985 south of the City of Eloy. The land subsidence was measured to be about 11.9 feet by 1977 in the Maricopa-Stanfield sub-basin near Stanfield (Laney and others, 1978).

Although groundwater levels in much of the Pinal model area have recovered significantly since 1987 due to reduced pumping and the use of CAP water, a USGS study (Evans and Pool, 2000) shows that the effects of historic pumping on the aquifer systems are still evident as aquifer compaction and land subsidence continue. The amount of historic water level decline and the thickness of the fine-grained materials (silt and clay) control the rate and the duration of the aquifer compaction. The large thicknesses of MSCU, identified in both the Eloy and Maricopa-Stanfield sub-basins, result in the long term residual aquifer compaction and subsequent land subsidence (Burgess and Niple, 2004). Residual aquifer compaction continued in the Eloy and Maricopa-Stanfield sub-basins during the period from 1989 through 1996, with measured subsidence ranging from 0.032 feet to 0.22 feet (Evans and Pool, 2000).

Earth fissures in the Pinal model area are located at basin edges or near the periphery of the subsidence areas. The first earth fissure recorded in Arizona was discovered in 1927, about 3 miles southeast of Picacho (Robinson and Patterson, 1962). These fissures eventually connect to form linear systems, the longest fissure has been observed to be about 9 mile in length near Picacho Peak (Wickham and Corkhill, 1989). Most fissures have no apparent vertical offset. However, a few fissures have been observed that have vertical offsets. The most prominent fissure with vertical offset is near the Picacho Mountains (Laney and others, 1977).

To obtain a better understanding of land subsidence caused by aquifer compaction, Epstein (1987) developed a one-dimension model to simulate the aquifer compaction at an

extensometer site near Eloy from 1965 to 1983. The model simulated the compaction changing with time using boundary stress values, hydraulic conductivity, layer thickness and specific storage (compressibility values). Model results indicate that virgin specific storage, pre-consolidation stress and clay thickness are critical hydrologic and geologic factors for land subsidence. Hydrologic thresholds defining when/where consolidation starts/occurs are also important model parameters. Many depositional units within the Pinal AMA are millions of years old. However it remains unclear where, and to what extent, existing fine-grained units may have been pre-consolidated in the geologic past.

Aquifer compaction is an important geologic process that affects the groundwater system in the Pinal model area and is an important component for the Pinal groundwater flow model. Aquifer compaction yields an additional source of water by dewatering fine-grained materials within the MSCU. However in fine-grained materials, compaction, related to dewatering is, to a large extent, irreversible and may result in a permanent loss of groundwater storage capacity. In addition, the compaction of fine-grained material may result in a reduction in hydraulic conductivity over time (Haneberg and others, 1998, and Rivera, and others, 1991).

## **Hydraulic Properties**

### ***Transmissivity and Hydraulic Conductivity***

The capability of the aquifer system to transmit water is characterized by hydraulic properties including transmissivity (T) and hydraulic conductivity (K). Transmissivity and hydraulic conductivity are usually estimated by conducting aquifer tests. In absence of aquifer tests, transmissivities are often estimated based on grain-size analyses and well specific capacity tests.

## **Grain-size Analyses**

During the development of Pinal AMA Regional Groundwater Flow Model (Wickham and Corkhill, 1989), the initial hydraulic parameters for each geologic unit were generated using the Drillers' Log Program (DLP) (Long and Erb, 1980). The DLP estimated hydraulic conductivity values for the UAU were estimated to range from 100 gpd/ft<sup>2</sup> (13 feet/day) to 1,150 gpd/ft<sup>2</sup> (154 feet/day) with an average of 436 gpd/ft<sup>2</sup> (58 feet/day). The hydraulic conductivity of the MSCU was estimated to range from 1 gpd/ft<sup>2</sup> (0.1 feet/day) to less than 25 gpd/ft<sup>2</sup> (<3.3 feet/day) with an average of 16 gpd/ft<sup>2</sup> (2.1 feet/day). For LCU, the hydraulic conductivity was estimated to range from 4 gpd/ft<sup>2</sup> (0.5 feet/day) to 998 gpd/ft<sup>2</sup> (133 feet/day). The average hydraulic conductivity of the LCU was estimated to be 254 gpd/ft<sup>2</sup> (34 feet/day).

The hydraulic conductivity, based on grain-size analyses, for most alluvial materials in the upper portions of the regional aquifer system in the Picacho basin (essentially the same area as the Eloy sub-basin) was estimated to range from about 30 to 60 feet/day (Pool and others, 2001). Lower conductivity zones occur in the fine-grained sediments southwest of Eloy and south of Coolidge. Higher values, ranging from 70 to 100 feet/day are associated with coarse-grained stream sediments along the Gila River, south of the Casa Grande Mountains, east of Eloy and the area between the Silverbell Mountains and Picacho Peak (Pool and others, 2001).

## **Specific Capacity Data**

Hardt and Cattany (1965) studied the specific capacity (gpm/foot of drawdown) distribution from well tests in the western portion of Pinal County. Hardt and Cattany (1965) divided the western portion of Pinal County into four areas that include; the Casa Grande-Florence area, the Eloy area, the Maricopa-Stanfield area, and the Gila River area. In their study, specific capacities determined from completion tests of 539 wells drilled from 1945 to 1950 were

analyzed. Among the total number of wells studied, 405 wells have depths less than 600 feet. Therefore, these data generally represent aquifer characteristics in the UAU and upper portion of the MSCU. High specific capacities were calculated along the Gila River and in the northern half of the Casa Grande-Florence area. In the Eloy area, high specific capacities were estimated in the area between Silverbell and Picacho Peak and westward toward the Sawtooth Mountains, east of Eloy toward the Picacho Mountains, and along the south side of the Casa Grande Mountains. In the Maricopa-Stanfield area, large specific capacities were calculated from Stanfield south to Santa Rosa Wash and eastward to the Casa Grande Ridge, from the Haley Hills northeast to Maricopa, and along the south western part of the Sacaton Mountains.

Based on Jacob's non-equilibrium equation the transmissivity of an aquifer can be estimated by multiplying specific capacity data by an empirical constant that may range from about 2,000 for confined aquifers to 1,500 for unconfined aquifers as presented by Driscoll (1986). A constant of 1,700 was used by Hardt and Cattany (1965) to estimate transmissivity in their study. Using that method, aquifer transmissivity for the depths penetrated by wells was estimated to range from about 8,000 to 180,000 gpd/ft (1,070 ft<sup>2</sup>/d to 20,064 ft<sup>2</sup>/d) in Casa Grande-Florence area, from 7,000 to 300,000 gpd/ft (936 ft<sup>2</sup>/d to 40,107 ft<sup>2</sup>/d) in Eloy; from 5,000 to 270,000 gpd/ft (668 ft<sup>2</sup>/d to 36,096 ft<sup>2</sup>/d) in Maricopa-Stanfield; and 37,000 to 245,000 gpd/ft (4,947 ft<sup>2</sup>/d to 32,754 ft<sup>2</sup>/d) in Gila River area (Hardt and Cattany, 1965).

Although the specific capacity method could possibly underestimate transmissivities due to well efficiency, pumping duration, and depth of penetration into the aquifer, the variations in average transmissivities reveal the spatial pattern of aquifer characteristics and provide insight on the transmissivity distribution for model calibration.

## Aquifer Tests

Aquifer tests are frequently performed to more accurately evaluate aquifer hydraulic properties. Appendix A summarizes all the aquifer test results in the Pinal model area that were available to ADWR (Figure 17). The reported hydraulic properties are ranked based on their quality. Low rank was given to estimates derived from specific capacity test, pumping tests of short duration, and non-ideal aquifer tests.

Nearly all the aquifer tests were initially analyzed based on an assumption of confined aquifer condition. Consequently, the Theis (1935) and Cooper-Jacob (1946) methods were used in previous studies to analyze drawdown data, and the Theis Recovery method was applied for analyzing recovery data. The reported hydraulic conductivity and storage properties were assigned to different hydrogeologic units (model layers) based on well construction data and the interpreted geology for the model cell where the well was located. Fewer pumping test results were available for the UAU. The single hydraulic conductivity estimate for the Maricopa-Stanfield area was more representative of the K value in the MSCU since the pumping well was screened in both UAU and MSCU (Figure 17). Hydraulic conductivity values for the MSCU are primarily available in both Eloy and Maricopa-Stanfield sub-basin basin centers (Figure 17). Several hydraulic conductivity estimates were obtained for the LCU, but no data were available in the area south of Eloy, due to the large thickness of MSCU in that area, no well is deep enough to penetrate the LCU (Figure 17).

The aquifer system in the Pinal model area is generally characterized by multiple aquifers separated by thick aquitards in some areas. During aquifer tests, water levels measured in aquifers may have been affected to varying degrees by vertical leakage through the overlying and underlying aquitards. Based on this fact, leaky aquifer solutions such as Hantush and Jacob

(1955), Hantush (1960), and Moench (1985) were often considered to be more representative and applicable for analysis of aquifer test data for the study area, than conventional confined aquifer solutions; such as, Theis (1935) or Cooper–Jacob (1946). Therefore, in locations where leaky aquifer conditions were believed to exist, aquifer test data were independently evaluated by ADWR (Figure 17) using leaky aquifer solutions (Nelson, 2011). Estimated hydraulic conductivity values (K) were based on the assumption that  $K=T/B$ , where B equals to the screen interval length, and T is estimated the transmissivity. All non-leaky and leaky aquifer solutions were optimized using non-linear regression techniques (Duffield and Rumbaugh, 1991). It should be noted that the leaky-aquifer solutions were evaluated using drawdown data (ddn) only. Comparisons between the observed drawdown and calculated using selected solutions are shown in graphs and presented in Appendix B.

The leaky solutions estimated by ADWR reevaluation were compared with confined aquifer solutions evaluated by Arizona Water Company (AWC). Differences of K values from different solutions are also compared and summarized in Table 1 for each area. Results indicate that the use of leaky aquifer solutions tends to yield lower values of T (and K) than the use of the confined aquifer solutions. Residual errors associated with the leaky aquifer test solutions of Hantush and Jacob (1955), Hantush (1960), and Moench (1985) are generally lower than the confined aquifer solutions of Theis (1935) and Cooper-Jacob (1946). These results suggest that leakage through the aquitard may be impacting heads under pumping stress and that the estimated K values are generally lower than previously determined.

**Table 1 Selected Aquifer Test Data in the Pinal Model Area  
West and Southwest Maricopa-Stanfield Area**

Location	<i>Non-Leaky Solutions of Theis; Theis recovery and Cooper-Jacob (feet/day)</i>					
	AWC ddn	AWC recovery	ADWR ddn	ADWR recovery	ADWR (Theis)	<b>Average; +/- SD</b>
D-6-3_23bac	96.7	67.8	94	68	77.4	<b>80.8 +/- 13.9</b>
D-5-3_17dcc	68.4		43.2		35.3	<b>48.97 +/- 17.3</b>
Confined average						<b>64.9 +/- 21.6</b>
	<i>Leaky-Aquifer Solutions of Hantush (1955; 1960) and Moench (1985) (feet/day)</i>					
			Hantush no S	Hantush et al With S	Moench With S	
D-6-3_23bac			23.4	51.6	59.2	<b>44.7 +/- 5.37</b>
D-5-3_17dcc			30.9	30	11.44	<b>24.1 +/- 13.1</b>
Leaky average						<b>34.4 +/- 17.8</b>

**Central Maricopa-Stanfield Area**

Location	<i>Non-Leaky Solutions of Theis; Theis recovery and Cooper-Jacob (feet/day)</i>					
	AWC ddn	AWC recovery	ADWR ddn	ADWR recovery	ADWR (Theis)	<b>Average; +/- SD</b>
D-5-3_26cca	15.9	26.5	16	24.5	3	<b>17.2 +/- 9.28</b>
	<i>Leaky-Aquifer Solutions of Hantush (1955; 1960) and Moench (1985) (feet/day)</i>					
			Hantush no S	Hantush et al With S	Moench With S	
D-5-3_26cca			1.53	2.03	2.98	<b>2.18 +/- 0.67</b>

**Coolidge Area**

Location	<i>Non-Leaky Solutions of Theis; Theis recovery and Cooper-Jacob (feet/day)</i>					
	AWC ddn	AWC recovery	ADWR ddn	ADWR recovery	ADWR (Theis)	<b>Average; +/- SD</b>
D-5-8_20acd	8.4	10.3	8	7.35	7.8	<b>8.37 +/- 1.14</b>
D-5-7_14cab			40.2	38.9	41.3	<b>40.1 +/- 26.5</b>
D-5-7_36acc	17.5	37.5	16.2		22.2	<b>23.3 +/- 9.78</b>
Confined average						<b>31.7</b>
	<i>Leaky-Aquifer Solutions of Hantush (1955; 1960) and Moench (1985) (feet/day)</i>					
			Hantush no S	Hantush et al With S	Moench With S	
D-5-8_20acd				6.14	4.74	<b>5.44 +/- 0.99</b>
D-5-7_14cab			35.7	31.2	20.9	<b>29.3 +/- 7.6</b>
D-5-7_36acc			21.9	11.1	11.8	<b>14.9 +/- 6.02</b>
Leaky average						<b>16.5</b>

**Gila River Coolidge Area**

Location	<i>Non-Leaky Solutions</i> of Theis; This recovery and Cooper-Jacob (feet/day)					
	AWC ddn	AWC recovery	ADWR ddn	ADWR recovery	ADWR (Theis)	Average; +/- SD
D-4-8_25cdc	2.5	2.1	4.05	2.53		<b>2.8 +/- 0.86</b>
Location	<i>Leaky-Aquifer Solutions</i> of Hantush (1955; 1960) and Moench (1985) (feet/day)					
			Hantush no S	Hantush et al With S	Moench With S	
D-4-8_25cdc			1.24	1.85		<b>1.55</b>

**Picacho/Eloy/Toltec Area**

Location	<i>Non-Leaky Solutions</i> of Theis; This recovery and Cooper-Jacob (feet/day)					
	AWC ddn	AWC recovery	ADWR ddn	ADWR recovery	ADWR (Theis)	Average; +/- SD
D-8-8_27add			10.3	44	2.88	<b>19.1 +/- 21.9</b>
D-7-7_03cdd	17.5	31.9	17.5	24.8	17.6	<b>21.9 +/- 6.43</b>
D-7-7_03ccc	27.8	20.6	11.6	22.8	7.3	<b>18.0 +/- 8.39</b>
D-8-8_15ccd			3.66	4.62	5.12	<b>4.47 +/- 0.74</b>
D-8-6_26dbb	33.3	16.1	22.6	13.4	11.5	<b>19.4 +/- 8.84</b>
Confined Average						<b>16.6 +/- 6.9</b>
Location	<i>Leaky-Aquifer Solutions</i> of Hantush (1955; 1960) and Moench (1985) (feet/day)					
			Hantush no S	Hantush et al With S	Moench With S	
D-8-8_27add			1.57	2	1.78	<b>1.78 +/- 0.16</b>
D-7-7_03cdd			16.2	10.8	10.3	<b>12.4 +/- 0.35</b>
D-7-7_03ccc			3.69	4.7	6.62	<b>5.0 +/- 1.36</b>
D-8-8_15ccd			7.66	3.73	3.6	<b>5 +/- 0.09</b>
D-8-6_26dbb			9.9	8.55		<b>9.23</b>
Leaky Average						<b>6.69 +/- 4.3</b>

**Casa Grande Area**

Location	<i>Non-Leaky Solutions</i> of Theis; This recovery and Cooper-Jacob (feet/day)					
	AWC ddn	AWC recovery	ADWR ddn	ADWR recovery	ADWR (Theis)	Average; +/- SD
D-6-6_36aca	24.2	13.5	18.3	9.76	10.34	<b>15.2 +/- 6.1</b>
D-6-6_25bdb	15.4	17.4	18.5		18.5	<b>17.5 +/- 1.5</b>
D-6-6_25aca	17.6	13.5	18.6	10.9	17.3	<b>15.6 +/- 3.3</b>
Confined average						<b>16.1 +/- 4.0</b>
Location	<i>Leaky-Aquifer Solutions</i> of Hantush (1955; 1960) and Moench (1985) (feet/day)					
			Hantush no S	Hantush et al With S	Moench With S	
D-6-6_36aca			9.091	9.07	4.3	<b>7.49 +/- 3.37</b>
D-6-6_25bdb			9.71	9.2	9.11	<b>9.34 +/- 0.06</b>
D-6-6_25aca			13.4	14.1	9.09	<b>12.2 +/- 4.28</b>
Leaky average						<b>9.7 +/- 2.8</b>

For model calibration purposes, the estimated K values from the different solutions provide a range for calibrating the hydraulic conductivity zones within the model. The inclusion of K estimates from the leaky-aquifer solutions decrease the ensemble mean value of K.

### ***Storage Properties***

The capacity for the aquifer system to store and yield water is described by the aquifer storage properties. Storage properties in unconfined aquifers are defined by the specific yield ( $S_y$ ) which is the volume of water yielded per unit area per unit change in the water table. Water is yielded to wells primarily by the draining of pore space in unconfined aquifers. Storage properties in confined aquifers are expressed by the specific storage ( $S_s$ ) and storage coefficient ( $S_c$ ). The specific storage multiplied by the thickness of a confined aquifer is equal to the confined aquifer's storage coefficient. The storage coefficient is the volume of water yielded per unit area of aquifer per unit change in the potentiometric surface of the aquifer. Water is yielded to wells in confined aquifers from the compression of pore space and the expansion of water.

Initial specific yield distributions for each model layer were based on estimates from the ADWR Pinal AMA Regional Groundwater Flow Model (Corkhill and Hill, 1990). The specific yield of the UAU was estimated to vary from .05 to .20 (5 to 20 percent) with an average of about .11. The specific yield of the MSCU was estimated to vary from .03 to .07, with an average of about .04. For the LCU, the specific yield was estimated to vary from .03 to .18, with an average of about .09.

In the Picacho (Eloy sub-basin area) basin, specific yield was estimated based on water level changes, measured gravity and subsidence along a primary level line (Pool and others, 2001). Specific yield was estimated to be less than 0.05 at Eloy, about 0.1 and 0.15 east and west of Eloy, respectively, and 0.15 to 0.25 near Casa Grande.

In confined aquifers water is mainly yielded from elastic and inelastic compression of saturated pore space. Elastic compression of an aquifer generally yields far less water than inelastic compression for the same amount of applied stress (potentiometric surface decline). Holzer (1981) observed that the aquifer in the Eloy area deformed elastically before water level declines reached a pre-consolidation stress of about 100 feet (a value of 80 feet was used for the calibrated model), and deformation occurred inelastically at greater stress. Inelastic storage coefficients estimated from Holzer's (1981) study of water level decline and subsidence in wells near Eloy ranged from  $3.73 \times 10^{-2}$  to  $5.31 \times 10^{-2}$ ; elastic values ranged from  $.91 \times 10^{-3}$  to  $5.38 \times 10^{-3}$ . Those values are considered to represent maximum values of storage coefficient because the water levels represent conditions that existed after the recovery from seasonal pumping levels and probably aren't indicative of maximum stress (Pool and others, 2001). Pool's 2001 study found that the average specific-storage for the area along the Eloy primary leveling line varied from about  $7.2 \times 10^{-6} \text{ ft}^{-1}$  (elastic range) for the period from 1905-1948 to  $2.7 \times 10^{-5} \text{ ft}^{-1}$  for the period from 1948-1964 (inelastic range) and  $4.5 \times 10^{-5} \text{ ft}^{-1}$  (inelastic range) for the period from 1964-1977. The apparent increase in specific storage with time was probably caused by stresses that are greater than those indicated by annual water levels and stresses that occur throughout greater thicknesses of compressible sediments with time (Pool and others, 2001).

The storage properties estimated by previous studies served as initial values for the current Pinal model update. During model calibration, some initial estimates were adjusted as needed.

### **Conceptual Groundwater Budget**

Major components of inflow to and outflow from the aquifer system in the model area were analyzed to compile conceptual water budgets for both steady-state (circa 1922) and transient

periods (1923-2009). Estimated groundwater storage change is calculated as the difference between system inflows and outflows. The following sections provide details of that analysis.

### ***Inflows***

#### **Groundwater Underflow**

Groundwater underflow enters and leaves the Pinal model area in several locations (Figure 18). Underflow entering the model area at natural or artificial boundaries was identified at the following locations:

- Between Silverbell Mountains and Picacho Peak
- Between Picacho Peak and Picacho Mountains
- Between Picacho Mountains and Tortilla Mountains (Cactus Forest area)
- Between West Silverbell Mountains and Sawtooth Mountains (Aguirre Valley area)
- Santa Rosa Wash
- Vekol Wash
- East SRV, Chandler area southeast of South Mountain

Table 2 provides a comparison of selected underflow estimates, both boundary and non-boundary (internal) fluxes, from previous studies and model efforts. The estimates of underflow provided a range of potential values that were used to guide the model calibration process. The transient groundwater fluxes vary in magnitude and direction with time. For instance, underflow changes both in flow direction and volume along the model boundary located southeast of the South Mountain. In this study, the total conceptual underflow entering the model area was estimated to range from about 45,000 to 55,000 acre-feet per year for the pre-development and post-development eras, respectively.

**Table 2 Selected Underflow Estimates in the Pinal Model Area**  
**(All Estimates are Rounded to Nearest 100 Acre-Feet Per year)**

Underflow Components	USGS Turner, and others (1943)	USGS Thomsen and Eychaner (1991)	USGS Thomsen and Porcello (1991)	USGS Freethey and Anderson (1986)	USGS Pool, and others (2001)	ASLD Hardt and Cattany (1965)	Pre-Development Average	ADWR Freihoefer, and others (2009)	ADWR Mason and Ikeya (1998)	ADWR Mason and Hipke (2013)	ADWR Wickham and Corkhill (1989)	ADWR Corkhill And Hill (1991)	Post Development Average
	Pre-development or Early Development							Post-development					
<b>S. Picacho Peak Inflow</b> (between Silverbell Mtms & Picacho Peak)	23,000 to 24,000	19,000		15,000 to 30,000	20,000 to 23,000	25,000	23,000			11,600 to 32,700	35,300	29,000	28,800
<b>N. Picacho Peak Inflow</b> (between Picacho Peak & Picacho Mtms)					4,000 to 8,000		6,000						6,000*
<b>Cactus Forest Inflow</b> (between Picacho Mtms & Tortilla Mtms)	2,500			<1,000	5,500 to 11,000		3,900				2,800		2,800
<b>Aguirre Inflow</b> (between Silverbell Mtms and Sawtooth Mtms)	2,500			1,000 to 5,000			2,800				4,100	2,900	3,500
<b>Santa Rosa Wash Inflow</b> (near Vaiva Vo)	1,500			1,000 to 5,000			2,300						1,500*
<b>N. Vekol Wash Inflow</b> (between Table Top Mtms. And Halley Hills)	500			<1,000			800						500*
<b>East SRV Inflow</b> (southeast of South Mountain )			6,500 to 7,000				6,800		11,600				11,600
<b>Total Estimated Groundwater Inflow</b>							44,800						54,700
<b>Florence Outflow</b> (between Santan and Tortilla Mtms)			(500)				(500)	(2,800)			(4,200)	(3,300)	(3,400)
<b>Sierra Estrella and South Mountain Gap Outflow</b>		(10,000)		(15,000) to (30,000)			(16,300)						(16,300)*
<b>Total Estimated Groundwater Outflow</b>							(16,800)						(19,700)

\*Estimated from Pre-development values

## Natural Recharge

The natural recharge components in this study include stream infiltration recharge and mountain front recharge. The study area is a semi-arid region with an average annual precipitation rate of 8.5 inches. As a result, the natural recharge is generally limited except during wet years, when recharge could become significant.

### Mountain Front Recharge

Most of the mountains surrounding the model area are low-relief with the exception of the Picacho Mountains and the Table Top Mountains located southwest of Stanfield. A limited amount of mountain front recharge was estimated, ranging from 129 to 562 acre-feet per year (AFY) (Wickham and Corkhill, 1989). The Pinal budget review performed by Burgess and Niple in 2004 confirmed that mountain front recharge in Pinal model area should be no more than 500 AFY. Consequently, mountain front recharge was estimated to be about 500 AFY along the Picacho Mountains.

### Stream Infiltration Recharge

The Gila River and Santa Cruz River are the two main rivers that interact with the groundwater system of the Pinal model area. Recharge from the infiltration of surface water flow in Gila and Santa Cruz Rivers provides the primary source natural recharge, especially during wet years.

#### *Gila River*

The Gila River is the most important source of surface water in the Pinal model area. The Gila enters the model area northeast of Florence, and flows in a westerly direction through the

GRIC, and exits the model area through the gap between South Mountain and the Sierra Estrella Mountains.

The Gila River was perennial in the model area during the pre-development era. The mean annual flow of the Gila River upstream from GRIC was estimated to be 500,000 AFY and the median annual flow was estimated at 380,000 AFY during the pre-development era (Thomsen and Eychaner, 1991). Gila River infiltration during pre-development was estimated to be 94,000 AFY (Thomsen and Eychaner, 1991).

During early stages of development, there was an increase in the number of diversions on the Gila River system upstream of the model area. Surface water was controlled and managed on the main stem of the Gila by the construction of dams. Ashurst-Hayden Dam is a diversion structure on the Gila River and was built in 1922. Coolidge Dam is a storage structure and was completed in 1928, upstream of the model area. Water released from the Coolidge Dam is normally diverted at Ashurst-Hayden Dam for delivery to the San Carlos Irrigation Project (SCIP). Records of Gila River surface water spilled and sluiced at the Ashurst-Hayden Dam from 1930 to present are available in the SCIP annual reports (SCIP, 1934-2009). After the construction of Ashurst-Hayden Dam, the Gila River became ephemeral along most of its reach between Ashurst-Hayden Dam and Pima Butte. The reduction in annual streamflow below Ashurst-Hayden Dam essentially eliminated recharge from the Gila except in wet years, when major spills may occur.

Following the construction of dams on the Gila River recharge from the infiltration of surface flows has been estimated as the difference between gaged inflows and outflows in the model area. The inflow refers to the annual volume of Gila River surface water reported by the SCIP to be spilled and sluiced at the Ashurst-Hayden Dam. Gila River outflows were estimated

using the USGS gage 09479500 near Laveen for the period of 1940 to 1995 and the USGS gage 09479350 near Maricopa for years after 1995. When outflow data were missing, or if outflow was larger than inflow due to ungaged additions to flow from minor tributaries, effluent recharge facilities or other sources, Gila River recharge was estimated to be 65% of the Gila River inflow. Table 3 presents the maximum potential Gila River Recharge estimated for the period from 1934 to 2009. The estimated mean and median annual Gila River recharge for the period from 1934 to 2009 were 40,260 acre-feet and 9,964 acre-feet, respectively. The standard deviation was about 98,837 acre-feet with a minimum of 244 acre-feet occurring in 2009 and a maximum of about 745,000 acre-feet occurring in 1993. The second largest recharge year was 1983, when approximately 353,000 AF was estimated to have been recharged. Relatively large recharge was also estimated in 1965, 1984, 1985 and 1992. Estimated Gila River recharge was low from the 1940s to mid-1960s. Estimated recharge was low after 1993, except for 2006, when recharge was estimated to be around 93,000 AF.

**Table 3 Estimated Gila River Flood Recharge in the Pinal Model Area 1934 to 2009**  
**(Units = Acre-Feet)**

<b>1934</b>	3,145		<b>1960</b>	15,852		<b>1986</b>	29,493
<b>1935</b>	65,332		<b>1961</b>	1,131		<b>1987</b>	730
<b>1936</b>	10,347		<b>1962</b>	6,327		<b>1988</b>	8,122
<b>1937</b>	15,691		<b>1963</b>	9,503		<b>1989</b>	3,112
<b>1938</b>	6,074		<b>1964</b>	8,008		<b>1990</b>	16,162
<b>1939</b>	14,460		<b>1965</b>	131,767		<b>1991</b>	47,202
<b>1940</b>	16,641		<b>1966</b>	17,754		<b>1992</b>	203,636
<b>1941</b>	12,845		<b>1967</b>	66,681		<b>1993</b>	745,223
<b>1942</b>	2,918		<b>1968</b>	9,654		<b>1994</b>	12,082
<b>1943</b>	11,743		<b>1969</b>	1,985		<b>1995</b>	77,865
<b>1944</b>	10,273		<b>1970</b>	9,089		<b>1996</b>	5,283
<b>1945</b>	596		<b>1971</b>	1,743		<b>1997</b>	1,482
<b>1946</b>	5,008		<b>1972</b>	111,696		<b>1998</b>	8,858
<b>1947</b>	6,923		<b>1973</b>	27,971		<b>1999</b>	722
<b>1948</b>	3,580		<b>1974</b>	3,899		<b>2000</b>	25,942
<b>1949</b>	8,732		<b>1975</b>	10,749		<b>2001</b>	1,329
<b>1950</b>	7,402		<b>1976</b>	4,468		<b>2002</b>	290
<b>1951</b>	2,029		<b>1977</b>	22,706		<b>2003</b>	1,473
<b>1952</b>	6,378		<b>1978</b>	85,309		<b>2004</b>	1,969
<b>1953</b>	1,587		<b>1979</b>	3,599		<b>2005</b>	27,003
<b>1954</b>	45,775		<b>1980</b>	110,187		<b>2006</b>	93,863
<b>1955</b>	47,670		<b>1981</b>	11,783		<b>2007</b>	14,961
<b>1956</b>	2,320		<b>1982</b>	9,600		<b>2008</b>	20,026
<b>1957</b>	1,739		<b>1983</b>	353,187		<b>2009</b>	244
<b>1958</b>	21,436		<b>1984</b>	141,371			
<b>1959</b>	15,744		<b>1985</b>	190,279			

Annual Gila River recharge was estimated at maximum potential levels. Recharge for some years was adjusted during model calibration. The relative distribution of Gila River recharge to different reaches of the river was handled differently during “wet” and “dry” years. During dry years, Gila River recharge was non-linearly distributed only from Ashurst-Hayden Dam to Pima Butte with higher infiltration rates assigned in up-gradient reaches. During flood years, however, the estimated total recharge was applied to the entire reach of Gila River which was within the model area. This distribution approach was supported by observed water level

trends as water level recovered significantly during flood years even in reaches west of Pima Butte where shallow groundwater conditions exist.

#### *Santa Cruz River*

The Santa Cruz River is ephemeral, and flows into the Pinal model area between Picacho Peak and the Silverbell Mountains. It runs northwesterly toward its confluence with the Gila River near the Sierra Estrella Mountains. Natural flow in Santa Cruz River is limited and runoff rarely reaches the Eloy sub-basin, except in wet years (Wickham and Corkhill, 1989). For example, in 1983 a major storm event occurred in southeastern Arizona that caused the Santa Cruz River to overflow its banks in many areas (USGS, 1989). In the Pinal AMA large areas were inundated by the flood waters.

Today, the natural flow of the Santa Cruz is augmented by effluent released into the Santa Cruz channel from the wastewater treatment facility located at Ina and Rogers Road (in the Tucson AMA). After 1980, effluent became the main source of recharge from the Santa Cruz with the addition of runoff during wet years. The portion of recharge from the Santa Cruz occurring inside the Pinal model domain was estimated from the ADWR Tucson AMA groundwater flow model (Mason and Hipke, 2013).

In the model, Santa Cruz River recharge was distributed differently for drought years and flood years. During flood years estimated Santa Cruz River recharge is larger and distributed along the complete reach which extends from Eloy sub-basin to the Maricopa-Stanfield sub-basin (USGS, 1989). During dry years, estimated Santa Cruz river recharge is low, and only distributed to a limited reach within the Eloy sub-basin.

## **Incidental Recharge**

Incidental recharge is defined as water that recharges the regional aquifer during the course of its use for agricultural, industrial, or municipal purposes. On average, incidental recharge is responsible for more than 90 percent of the total estimated recharge to the groundwater system in the Pinal model area. In this study, incidental recharge components include agricultural recharge, canal recharge, urban irrigation recharge, artificial lake recharge, artificial recharge, and effluent recharge.

### **Agricultural Recharge**

The Pinal AMA has an agricultural dominated economy. Consequently, agricultural recharge is a large and important source of water to the Pinal regional aquifer. Agricultural recharge represents water returned to the regional aquifer when water used for irrigation percolates below the plant root zone rather than being utilized by consumptive use or evapotranspiration. Agricultural recharge is generally estimated to be the product of the total agricultural water use and the irrigation inefficiency ( $1 - \text{irrigation efficiency}$ ). The irrigation efficiency is defined to be the ratio of the total irrigation requirement to the total amount of water applied. Figure 19 presents the estimated agricultural recharge, total agricultural water supply and total irrigated acres since 1923.

### **Agriculture Recharge 1984~2009**

Arizona annual agricultural statistics data provide crop acreage, crop types, and other related data for all the counties in Arizona since 1941 (Arizona Agricultural Statistics, 1966 and 1966-2009). Most of the irrigated acres and crop types published for Pinal County are located in the Pinal model area. Using crop-specific consumptive use rates and other special crop-specific

water need data (ADWR, 1999) the total irrigation requirement for the period of 1984 to 2009 was calculated.

In the Pinal AMA, comprehensive groundwater withdrawal, surface water diversion and CAP water use data have been available since 1984. Groundwater and surface water are both used for irrigation purposes, with groundwater being the primary source, prior to CAP water becoming available in 1987. Before the availability of CAP water surface water use was historically restricted to the Eloy sub-basin on the San Carlos Irrigation District lands (Wickham and Corkhill, 1989) and to the GRIC lands through SCIP project. Since 1987, CAP water became an additional source for agricultural use, resulting in groundwater pumping being decreased accordingly. Analyses of these data provide an estimate of the total water supplied for irrigation use. Precipitation over 8.5 inches per year was also taken into account when determining the total potential water supply for irrigation. A combination of water supply from all the possible sources yields the estimated total amount of agricultural water use for each year during the period of 1984 to 2009.

The ratio of the estimated total irrigation requirement obtained from the Arizona Agricultural Statistics data to the estimated total of irrigation water supply gives the approximate irrigation efficiency for each year. The estimated inefficiency for the period of 1984 to 2009 varied from 0.21 to 0.42, and the 22-year average is 0.34. Based on the calculated trends, irrigation inefficiency was estimated at 0.35 from 1984 to 1989, 0.30 from 1990 to 1993, and 0.35 from 1994 to 2006.

Several irrigation districts are located in Pinal model area; Maricopa-Stanfield Irrigation and Drainage District (MSIDD), Central Arizona Irrigation and Drainage District (CAIDD), and Hohokam Irrigation District (HID). For this time period ADWR (the Pinal AMA office)

documented and summarized the total agricultural water use for each of the irrigation districts, the AK-Chin Indian Reservation area and non-irrigation district farming operations. Total agriculture water use for the SCIP project area is available in the SCIP annual reports. The total of agriculture water use in the Non-SCIP part of GRIC area was estimated based on large farming well pumping (Freihoefer, and others, 2009). Agricultural recharge for each area was then estimated by multiplying the assigned irrigation inefficiency with the total irrigation water use for each year. During this period, conceptual agricultural recharge ranged from 194,000 AFY in 1993 to about 441,000 AFY in 2008, and the average recharge was about 280,000 AFY.

#### Agriculture Recharge 1934~1983

Based on annual Arizona Agricultural Statistics reports, using the crop-specific water consumption rate and the published acres for each crop type, the total irrigation requirement for the period of 1941-1983 was calculated. A trend analysis of the long term irrigation history indicates that the average irrigation requirement was about 3.13 acre-feet per acre.

During the period of 1934 to 1940, information was limited. No information was available for each crop type and its corresponding acreage. Instead, only a lump sum estimate of the total irrigation acreage was available. Consequently, the total irrigation requirement for this period was approximated by the multiplying the estimated average irrigation requirement (3.13 acre-feet/acre) with the reported total irrigation acres.

It was assumed that the estimated average irrigation efficiency of 0.66 obtained during the period of 1984 to 2009 was also valid for the period of 1934 to 1983. The total agricultural water demand during the period of 1934 to 1983 was then estimated by dividing the total irrigation water requirement by the irrigation efficiency of 0.66. As a cross-check, the total agricultural water demand was also estimated by using the water budget method. Prior to 1983,

water sources for irrigation included groundwater, surface water diverted for the SCIP project and precipitation greater than 8.5 inches per year. Figure 20 compares the total agriculture water used estimated from the two different methods. In general, there is a reasonably good match between the two methods. Based on this analysis, the irrigation efficiency of 0.66 was deemed to be a reasonable estimate for this period, and the inefficiency of 0.34 was subsequently used with the total agricultural water demand to estimate agricultural recharge for this period. Agricultural recharge increased significantly since 1941 because of the groundwater withdrawal, and the recharge fluctuated around 400,000 AFY from 1940s to 1982. Estimated agricultural recharge decreased significantly in 1983, possibly related to the flood that year and also due to the land fallowing related to the PIK program (Wickham and Corkhill, 1989).

#### Agriculture Recharge 1923~1933

Data are very sparse for this period. The only data available are the estimated total number of irrigated acres. As a result, the total annual irrigation demand was estimated using parameters developed for the period from 1934 to 1983, with an average water duty of 3.13 acre-feet per acre and an irrigation efficiency of 0.66. The estimated agricultural recharge during this period is shown on Figure 21.

#### Lagged Agriculture Recharge

In the Pinal model area, groundwater pumping increased significantly from the 1940s, and water levels were observed to decline rapidly. By the early 1950s, depths to water were about 200 feet in many parts of the Eloy and Maricopa-Stanfield sub-basins. However, depths to water were around 350 feet in the southwest section of the Maricopa-Stanfield sub-basin. Water levels continued to decline, due to the ever increasing groundwater overdraft, and only started to

recover in some areas by the mid to late 1970s and early 1980s when annual pumping rates began to significantly decrease from earlier levels.

The combination of deep water tables and the slow seepage of excess agricultural irrigation water percolating downward through the vadose zone created a time lag for the arrival of agricultural recharge to the water table in many parts of the Pinal model area. A lag factor for travel time through the vadose zone was estimated to be between 15 and 20 years based on the average DTW and estimated percolation rates (Burgess and Niple, 2004).

In the Pinal model, lagged agricultural recharge was assumed to percolate downward to the water table at a constant rate of about 15 to 20 feet/year. In agricultural areas with deep water tables only a portion of the estimated annual agriculture recharge for a given year was assumed to reach the water table. The balance of the agricultural recharge for that year was assumed to arrive at the water table in later years. The agricultural recharge distribution in the Pinal model was shifted in time to reflect the lag effect. Specifically, annual agricultural recharge estimates that were input to the Pinal model were lagged after 1948 until 1983. During the period from 1948 to 1983, agricultural recharge was simulated at less than the conceptual estimate. The lag-delayed recharge was assumed to arrive at the water table between 1984 and 2009 (Figure 21). Although the agricultural recharge distribution was shifted in time, the cumulative sum of the estimated agricultural recharge remained unchanged over the 87 year model simulation period. Therefore, lagging only changed the simulated arrival time of the agricultural recharge at the aquifer, and did not create an additional source of recharge.

### **Canal Recharge**

Canal recharge represents the estimated amount of water that seeps from canals and laterals, eventually percolating to the regional aquifer. Canal seepage in the Pinal model area

includes seepage through the CAP main aqueduct and laterals and the SCIP main canal and laterals (Figure 22).

The CAP main aqueduct and laterals are lined canals, and the seepage rate is much smaller than unlined canals. For the CAP main aqueduct, the canal recharge was estimated using canal length, the wetted perimeter and the canal seepage rate. The seepage rate was estimated to be 0.015 feet/day (Burgess and Niple, 2004). For CAP laterals it was assumed that 2.5 percent of total water delivered is system loss, and 20 percent of the system loss was attributed to canal lateral seepage. In this study, the CAP lateral recharge was combined with agricultural recharge for each irrigation district due to their relatively small volumes and the convenience of distribution. The canal recharge resulted from seepage through the CAP main aqueduct was estimated to be 1,710 AFY.

The SCIP main canals and laterals are unlined canal. Based on SCIP annual reports, these canals can have 30 to 50 percent seepage losses. Main canal losses were obtained from the SCIP annual reports. Losses for the laterals were calculated through a water budget method based on total water delivered and the total water applied to the field. The estimated canal losses from the SCIP main canal and laterals were simulated in the model as a separate component of recharge. No loss to evaporation was considered. Therefore, the estimated SCIP canal recharge represents the maximum potential canal recharge. Table 4 presents the estimated maximum potential SCIP canal recharge that ranged from about 40,000 AFY in 1934 to slightly more than 231,000 AFY in 1981. Greater than average canal recharge was estimated during the wet period from 1979 to 1996. This wet period includes the 1983 and 1993 flood years, when deliveries of Gila River surface water to the SCIP were greater than in other years.

**Table 4 Estimated Maximum Potential Recharge for San Carlos Project Canals and Laterals 1944 to 2009**

Year	Maximum Potential Recharge (AF/Yr)	Year	Maximum Potential Recharge (AF/Yr)
1934	39,343	1972	75,582
1935	78,617	1973	126,057
1936	71,460	1974	150,780
1937	88,611	1975	151,290
1938	66,464	1976	100,269
1939	52,658	1977	55,993
1940	52,138	1978	133,741
1941	92,221	1979	180,338
1942	129,394	1980	212,240
1943	124,868	1981	231,441
1944	111,880	1982	159,498
1945	92,711	1983	115,953
1946	55,670	1984	166,752
1947	55,389	1985	168,453
1948	63,690	1986	178,584
1949	114,189	1987	142,907
1950	82,162	1988	168,950
1951	44,612	1989	158,048
1952	113,768	1990	48,196
1953	48,859	1991	103,383
1954	63,688	1992	128,971
1955	65,688	1993	131,178
1956	58,521	1994	160,199
1957	46,518	1995	164,805
1958	112,216	1996	185,290
1959	84,119	1997	116,546
1960	117,264	1998	119,502
1961	48,104	1999	79,747
1962	101,040	2000	66,835
1963	80,806	2001	98,826
1964	62,492	2002	69,970
1965	68,695	2003	57,658
1966	113,694	2004	61,816
1967	116,125	2005	115,177
1968	121,059	2006	109,403
1969	122,062	2007	104,766
1970	103,404	2008	126,530
1971	52,914	2009	126,444

## **Picacho Reservoir Recharge**

The Picacho Reservoir is an irrigation water storage facility operated by the San Carlos Irrigation Project (Figure 23). The operating loss at the Picacho Reservoir was reported for some of the years in the SCIP reports. When loss data were not available, the operating loss was estimated to be 55 percent of the reservoir's inflow. The total operating loss of the reservoir was then separated into two components: 62 percent of the loss to evapotranspiration and 38 percent to reservoir seepage. The percentages for seepage and evapotranspiration are rough estimates, developed by ADWR's Pinal AMA office for the period of 1981 to 1993.

## **Effluent Recharge**

The effluent recharge in this study mainly consists of recharge generated by the Casa Grande Wastewater Treatment Facility (Figure 23). The reclaimed effluent generated by Casa Grande Wastewater Treatment Facility is delivered to various users including golf course, an electric power generating station, farmlands and discharged to Santa Cruz River bed (Burgess and Niple, 2004). The Pinal AMA office estimated the volume of effluent recharge based on the estimated effluent volume of effluent applied to farm lands and the irrigation efficiency for the period 1980 to 2009. The effluent recharge was estimated to range from 1,230 AFY to 1,496 AFY. Due to limited information, effluent recharge was assumed to remain constant at 1,399 AFY after 2000.

## **Artificial Recharge**

Currently, there are 4 active Underground Storage Facility (USF) recharge projects in Pinal AMA. They are: 1) North Florence Recharge Facility; 2) the Arizona City Sanitary District Recharge Facility; 3) Sun Lakes at Casa Grande Effluent Recharge Facility; and 4) the Eloy Reclaimed Water Recharge Project (Figure 23). These facilities recharged reclaimed

effluent through recharge basins or wells. The recharge volume at the Eloy Reclaimed Water Recharge Project ranged from 194 AFY to 814 AFY, and is much larger than those at other recharge facilities. The recharge volumes at the other three facilities are very small and are generally less than 100 AFY.

There is also a currently inactive recharge facility in Pinal model domain. The Hohokam Water Recharge Facility #1 was expired in 2004. CAP water was recharged at this facility once in 2003 (739.50 AFY).

### **Urban Irrigation Recharge**

Urban irrigation recharge represents an estimated amount of return flow resulting from flood irrigation water applied to urban areas such as parks, golf courses, or other turf areas. In the Pinal AMA ADWR assumes that 4 percent of the total municipal and industrial water use may be attributed to urban irrigation recharge. This is a small inflow component in the study area (Figure 23).

### ***Outflow***

System outflows are defined as flow components within the Pinal model area that remove water from the aquifer. Those components include groundwater underflow, pumping, riparian evapotranspiration, and groundwater discharge to stream channels.

### **Groundwater Underflow**

Groundwater underflow flows northwest from the Pinal model area between the South Mountains and Sierra Estrella Mountains and to the north between the Santan and Tortillita Mountains north of Florence (Figure 18). Estimated pre-development groundwater fluxes at these two locations were about 16,000 AFY and less than 1,000 AFY, respectively. Modern fluxes are estimated to have changed only slightly between the Sierra Estrellas and South

Mountain and were estimated to be about 3,400 AFY north of Florence. Changes in fluxes near Florence were primarily due to changes in groundwater gradients.

### **Groundwater Pumping**

Groundwater pumping is the dominant groundwater outflow component in the Pinal model area. The groundwater pumping simulated in the Pinal model is divided into 4 major time periods and data sources: 1) USGS estimated groundwater pumping (1923 to 1983) for the lower Santa Cruz basin; 2) SCIP reported pumping on the GRIC area (the Agency Part) and on the non-GRIC area (the District Part) (1935~2009); 3) ADWR estimated non-SCIP GRIC pumping (1923 to 2009); and 4) ADWR reported pumping for non-SCIP, non-GRIC groundwater users stored in the Registry of Grandfathered Rights (ROGR) database for the period of 1984 through 2009.

The historical pumping from 1923 to 1983 was estimated by the USGS was based on electrical and gas power-consumption reports. This groundwater pumping includes historical pumping on both Indian and non-Indian lands in the lower Santa Cruz Basin (Anning and Duet, 1994).

The majority of the pumping in Pinal model area has been for agricultural purposes, with municipal and industrial groundwater uses accounting for a very small percentage of total groundwater pumping (Figure 24). The municipal and industrial volumes were determined from ADWR's ROGR database. Agricultural irrigation pumping is a combination of the data from the ROGR database and the data and estimates for the SCIP and GRIC pumping within the model area.

Figure 25 illustrates the groundwater pumping history in the Pinal model area. The total pumping reflected in this figure differs slightly from the pumping totals for the Pinal AMA since

it does not include pumping outside of the model area, and some of the pumping in the model area falls within the Phoenix AMA (East Salt River Valley sub-basin). As shown on this figure, the total groundwater pumping was limited in early times, less than 150,000 AFY before 1930. Groundwater withdrawals started to increase rapidly reaching 260,000 AFY in the mid- 1930s and exceeding 1,000,000 AFY in 1949. The maximum groundwater withdrawal of 1,400,000 AFY occurred in 1953. The total annual pumping volume averaged about 1,000,000 AFY until the late 1960s and dropped to about 600,000 AFY by the mid-1980s. Groundwater pumping has remained in the range of about 400,000 to 600,000 AFY since CAP water became fully available and utilized since about 1990.

### **Evapotranspiration**

Evapotranspiration (ET) is a result of phreatophyte growth, primarily along the Gila River riparian corridors and the Santa Cruz River near its confluence with the Gila River (Figure 26). Evapotranspiration also occurs in the Picacho Reservoir area, however evapotranspiration from the Picacho Reservoir may come primarily from perched groundwater that is not directly connected to the regional aquifer system.

During pre-development, ET was the dominant outflow component since the depth-to-water was very shallow, especially along the Gila River Corridor. ET was estimated to be about 96,000 AFY during pre-development (Thomsen and Eychaner, 1991). Evapotranspiration along the Gila River from near Coolidge to the Salt River (approximately 7 miles past the northwest boundary of the model) probably ranged from 100,000 to 150,000 AFY (Turner and others, 1943). The overall volume of evapotranspiration generated in riparian areas decreased greatly as groundwater was developed and water levels declined. Currently riparian ET in the Pinal model area mainly occurs on the western portion of the GRIC (Corkhill and others, 1993). Conceptual

estimates of current evapotranspiration within the Pinal model area for the riparian and shallow water table areas near the confluence of the Santa Cruz and Gila Rivers is about 23,000 AFY.

### **Stream Discharge**

Discharge of groundwater into the channel of the Gila River occurred frequently prior to the period of surface water and groundwater development in the model area. Lee (1904) reported that shallow groundwater was discharged to the Gila River channel in the western third of the GRIC reservation and near Coolidge. According to Lee (1904) about 51 CFS (about 37,000 AFA) of baseflow was diverted near Gila Crossing in the western portion of the GRIC. Based on their study and modeling of pre-development conditions, Thomsen and Eychaner estimated the groundwater discharge to the Gila and Santa Cruz Rivers in the western third of the GRIC reservation was about 18,700 AFY (Thomsen and Eychaner, 1991). The pre-development groundwater discharge to the Gila River near Coolidge was estimated to be 2,600 AFY (Thomsen and Eychaner, 1991). Since pre-development, water levels have declined rapidly due to increased groundwater pumping, and stream discharge has also decreased, except in wet years.

### ***Conceptual Water Budget (1923 – 2009)***

A conceptual steady-state water budget for Pinal model is shown in Table 5. The estimated total inflow for the pre-development (steady-state) system was about 140,000 AFY. The estimated total steady-state outflow was about 135,000 AFY. Ideally the total inflow and outflow of a steady-state water budget should be equal. However, since each component of the steady-state budget was estimated independently, the inflows and outflows do not match exactly. Under pre-development conditions, infiltration of surface flow from the Gila River was the

predominant source of recharge, and evapotranspiration from riparian areas and areas of shallow groundwater was the dominant outflow component.

Complete conceptual water budgets were not prepared for the period of groundwater development from 1923 to 2009 due to the lack of independent estimates of head-dependent groundwater discharge to the Gila and Santa Cruz Rivers. However, most of the major components of inflow and outflow between 1923 and 2009 are shown in Table 5. As indicated in Table 5, groundwater recharge from agricultural irrigation was the largest component of recharge during the transient period and groundwater pumping was the largest outflow component. The model simulated groundwater budget is discussed later in model calibration section.

**Table 5 Conceptual Water Budgets for the Pinal Model Area for Steady-State (Circa 1923) and Transient Period (1923 to 2009)**  
**Figures Are Average Annual Estimates For the Time Period (All Figures Are Rounded to Nearest 100 Acre-Feet)**

Time	SS <sup>2</sup>	1923-1929	1930- 1939	1940-1949	1950-1959	1960-1969	1970-1979	1980- 1989	1990-1999	2000-2009
<b>Inflows</b>										
Groundwater Underflow (Total For all Model Boundaries) <sup>1</sup>	45,600	47,000	48,000	49,000	50,000	51,000	52,000	53,000	54,000	54,700
Agricultural Recharge (non-lagged)	0	44,600	120,800	239,100	393,600	459,000	350,200	308,000	283,000	324,700
Canal Recharge (SCIP and CAP)	0	0	66,200	89,200	72,000	95,100	114,100	170,800	125,500	95,400
Picacho Reservoir Recharge	0	0	5,400	6,700	4,800	6,000	6,000	7,300	5,100	2,500
Mountain Front Recharge	500	500	500	500	500	500	500	500	500	500
Gila River Flood Recharge	94,000	24,100	17,300	7,900	15,200	15,800	28,000	90,400	111,300	18,000
Santa Cruz River Recharge (flood and effluent from TAMA)	0	0	0	6,000	13,800	10,000	31,700	36,500	23,700	26,500
Effluent and Artificial Recharge	0	0	0	0	0	0	0	1,300	1,400	1,900
Urban Irrigation	0	0	0	0	0	0	0	800	900	1,800
<b>Total of Estimated Inflow Components</b>	<b>140,100</b>	<b>116,200</b>	<b>258,200</b>	<b>398,400</b>	<b>549,900</b>	<b>627,410</b>	<b>582,500</b>	<b>668,600</b>	<b>605,400</b>	<b>526,000</b>
<b>Outflows</b>										
Groundwater Underflow (Total For all Model Boundaries) <sup>1,3</sup>	16,800	17,000	17,300	17,600	17,900	18,200	18,500	18,800	19,100	19,700
Pumping	0	83,600	244,600	635,400	1,142,500	1,036,900	917,300	702,600	445,600	490,900
Evapotranspiration (Gila & Santa Cruz areas only on GRIC) <sup>3</sup>	97,100	64,300	29,000	23,000	23,000	23,000	23,000	23,000	23,000	23,000
Gila and Santa Cruz River Groundwater Discharge <sup>3,4</sup>	21,300	NA	NA	NA	NA	NA	NA	NA	NA	NA
<b>Total of Estimated Outflow Components</b>	<b>135,200</b>	<b>164,900</b>	<b>290,900</b>	<b>676,000</b>	<b>1,183,400</b>	<b>1,078,100</b>	<b>958,800</b>	<b>744,400</b>	<b>487,700</b>	<b>533,600</b>

1 Estimates for periods from 1923-1999 based on interpolation between SS and 2000-2009 average rates

2 Conceptual estimates of SS Inflows and Outflows were independently developed and do not balance exactly

3 The close physical proximity between areas of groundwater underflow at the northwest model boundary, riparian ET and groundwater discharge to the channels of the Gila River and Santa Cruz Wash can be problematic for numerical model simulation. Although these components of groundwater discharge may be independently estimated from available data, each component's individual simulation using a groundwater model is complicated due to their interactive head-dependency.

4 NA = Not Available. Independent estimate of this head-dependent recharge component were not made for transient calibration period

## Chapter 3. Numeric Model

### Model Description and Features

The active model area for the Pinal model covers the major portions of the Eloy and Maricopa-Stanfield sub-basins in the Pinal AMA and a portion of the East Salt River Valley sub-basin in the Phoenix AMA (Figure 27). The active portion of Pinal model is approximately 1,510 mi<sup>2</sup> in area, and is included within ADWR's Central Arizona model domain which includes the Pinal, Salt River Valley (SRV) and Hassayampa model areas (Figure 28). The Pinal model was developed in the UTM Zone 12 North (NAD 1983 HARN) coordinate system. The model simulates steady-state (circa 1922) and transient flow conditions from 1923 to 2009. The transient period was divided into 87 annual stress periods between 1923 and 2009 with each stress period representing one year. Each stress period was divided into 10 time steps that had a time step multiplier of 1.2. The model units of length and time are feet and days, respectively.

Based on the conceptual model, three model layers were used to simulate the three different hydrogeologic units. Specifically, Layer 1 represents the UAU, Layer 2 represents the MSCU, and Layer 3 represents the LCU. Each layer is discretized into model cells of a half mile by a half mile. The Pinal model has 106 rows and 103 columns (10,918 total cells), with 6,052 active cells per model layer.

The model simulates groundwater inflow and outflow components. Inflow components include: groundwater underflow, natural recharge from mountain front and stream channel infiltration, and incidental recharge. Incidental recharge includes agricultural recharge, canal seepage, artificial lake recharge, effluent recharge, artificial recharge and urban irrigation recharge. Outflow components consist of groundwater underflow, evapotranspiration from

riparian vegetation along the Santa Cruz and Gila Rivers, stream discharge, and groundwater pumping. The numerical model was based upon the conceptualization of the aquifer system presented in Chapter 2. The general characteristics of the Pinal regional groundwater flow model are presented in Table 6.

The model code used to simulate groundwater flow in the Pinal model area was the USGS Modular Three-Dimensional Finite Difference Groundwater Flow Model (MODFLOW-2005, version 1.8) (Harbaugh, 2005), Groundwater Vistas Version 6 (Rumbaugh, 2011) and ArcGIS version 10 (ESRI, 2011) were used to process model data.

**Table 6 Pinal Model Features and Characteristics**

<b>Model Component</b>	<b>Description</b>	<b>Units</b>
Steady-state	Circa 1922	
Transient Period	1923 – 2009	Time = Days, Length = Feet
Model Grid	106 Rows x 103 Columns, 3 Layers	Model Cells = 0.25 mi <sup>2</sup>
Model Origin (Lower Left)	UTM, Zone 12, HARN 1983, Feet	X = 977,786.624 Y = 11,802,136.07
Model Cell Types	No Flow, Constant Head, Variable Head	
Boundary Conditions	Specified Head and Specified Flux	
DIS Package	Specifies aquifer tops and bottoms, space and time discretization	
BAS Package	Specifies starting water levels and active model domain	
Layer- Property Flow (LPF) – Rewetting Active	Specifies hydrologic parameters and allows rewetting of cells that go dry prior to or during a simulation	Rewetting Threshold = 0.1Foot (see Nelson, 2012)
Layer 1 – 6052 active cells	Layer Type 1 – Unconfined Aquifer, T = K x Saturated Thickness, Kh:Kz varies in space	K = Feet / Day
Layer 2 – 6,052 active cells	Layer Type 3 – Confined / Unconfined Aquifer, T = K x Saturated Thickness; Kh:Kz ratio varies in space	K = Feet / Day
Layer 3 – 6,052 active cells	Layer Type 3 – Confined / Unconfined Aquifer, T = K x Saturated Thickness, Kh:Kz ratio varies in space	K = Feet / Day
SUB-WT	Subsidence and Aquifer–System Compaction Package, Specifies compression index, recompression index, inter-bed thickness, and pre-consolidation stress,	
Specific Yield	Volume of water yielded per unit area per unit change of water level in unconfined aquifer	Dimensionless
Specific Storage	Volume of water yielded per area per unit change in a confined aquifer’s potentiometric surface	1/feet
Pumpage	Assigned to all simulated well locations	Feet <sup>3</sup> / Day
Recharge	Applied to specified uppermost active cells	Feet / Day
Evapotranspiration	Assigned rates per cell; Extinction Depth 30feet	Feet / Day
Stream Flow	Simulated groundwater flux between perennial stream reaches and aquifers	
Numerical Solver	Geometric Multigrid Solver (GMG)	Rclose = 500 to 2E3 ft <sup>3</sup> /d Hclose = 100 to 200 ft

## MODFLOW Packages

The Pinal groundwater flow model utilizes eleven data input packages and a numerical solver that are available in MODFLOW-2005. The packages are: Basic (BAS), Discretization (DIS), Layer-Property Flow (LPF), Well (WEL), Recharge (RCH), Stream (STR), Evapotranspiration (EVT), Subsidence and Aquifer-System Compaction Package (SUB-WT), Output Control (OC), the Time-Variant Specified-Head Package (CHD), Hydrograph program (HYDMOD). The numerical solver utilized was the Geometric Multigrid Solver (GMG). The brief discussion below describes how each package was used in model the Pinal regional aquifer.

1. The BASIC (**BAS**) package designates the active model domain and the starting water levels (steady state) for each active cell. The package defines cells as no-flow, variable head, or constant head.
2. The Discretization (**DIS**) package establishes the layout of the model. The package assigns the number of model rows, columns, model layers, and the physical dimensions of each model cell and the layer tops and bottoms. The DIS package also assigns the model time and length units, and time discretization which includes the number of stress periods and time steps and the length of each stress period.
3. The Layer-Property Flow (**LPF**) package defines the cell-centered hydraulic parameters of the model. The hydraulic parameters defined in the LPF package are the cell-specific horizontal and vertical hydraulic conductivities, and storage properties including specific yield, and specific storage terms. The LPF also controls the rewetting option. In the model the CONSTANTCV NOCVCORRECTION option was used when the SUB-WT package was used to avoid numerical instability issues. For more information on

additional options selected for the implementation of the LPF package in the Pinal model see (Nelson, 2012).

4. The Well (**WEL**) package was used to simulate the amount of water that was withdrawn from or added to a model, usually by a well. The Well package is sometimes also used to simulate positive or negative constant flux boundary conditions. Wells are assigned specified pumping rates for each stress period and are located within the model based on a row and column designation.
5. The Recharge (**RCH**) package was used to simulate various sources of natural, incidental or artificial recharge to specified cells within the model.
6. The Stream Flow Routing (**STR**) package simulates the routing of surface flow in rivers, streams, canals, or ditches as well as the leakage between surface water features and the aquifer system. The leakage is a function of the hydraulic properties and physical dimensions of the stream channel and the difference between the stream stage and hydraulic head in the adjacent aquifer.
7. The Evapotranspiration (**ET**) package was used to simulate groundwater outflow that is transpired by riparian vegetation or direct evaporation of groundwater at the land surface.
8. The output control (**OC**) package determined when and how to save model output such as heads, draw-downs, and cell-by-cell flow (mass balance) data.
9. The Time-Variant Specified-Head (**CHD**) package was used to simulate time-varying specified heads. The package allows boundary head cells to be assigned different values at different times during the model simulation, which allows boundary fluxes to vary through time based on the hydraulic gradient between the specified-head and variable heads within the model.

10. The Subsidence and Aquifer-System Compaction (**SUB-WT**) Package was used to simulate land subsidence and aquifer compaction. This package simulates groundwater storage changes and compaction in discontinuous inter-beds or in extensive confining units, and accounts for stress-dependent changes in storage properties.
11. Hydraulic-Head Observation (**HOB**) option within the BAS package was used to compare simulated heads with observed water levels (heads). The HOB option allows observed heads to be weighted based on their accuracy, and the resulting head residuals to be statistically evaluated. However, head weighting was not used with the HOB in the Pinal model study. The HOB is a post-processing feature within MODFLOW.
12. Hydrograph program (**HYDMOD**) generates time-series data (i.e. hydrographs) from MODFLOW's simulated heads at designated well locations within the Pinal model domain. The HYDMOD is a post-processing feature within MODFLOW.
13. Numerical solvers are used by MODFLOW to solve the large system of linear finite-difference groundwater flow equations needed to calculate movement of water into and out of the model cells. The model solver, Geometric Multigrid (**GMG**) package, was used in the transient simulation. During the model calibration it was necessary to vary the GMG solver closure criterion, Rclose and Hclose, from 500 to 2E3 ft<sup>3</sup>/d and from 100 to 200 feet to obtain reasonable mass balance errors.

### **Boundary Conditions**

The groundwater underflow into and out of the Pinal model domain is simulated through boundary conditions. Three types of boundaries were simulated in the Pinal model: specified head, specified flux, and no-flow. Groundwater underflow at specified head boundaries was proportional to both the hydraulic gradient and the conductance between boundary head cells and

the adjacent variable head cells. The Pinal model simulated the history of groundwater development in the AMA for more than 87 years. During that time the water levels and hydraulic gradients changed greatly in many locations, and head-dependent boundary fluxes (at constant head boundaries) varied proportionately.

Specified head boundaries were assigned between Picacho Peak and the Silverbell Mountains to simulate groundwater underflow into the model domain from the Tucson AMA. Groundwater underflow out of the model domain through Florence Gap (east of the Santan Mountains) and the gap between South Mountain and the Sierra Estrella Mountains were also simulated through specified head boundaries. Specified head conditions were also used in the northeastern portion of the model domain (in the southwest Chandler - GRIC area, southeast of the South Mountains) to simulate groundwater underflow from the East Salt River Valley sub-basin.

Specified flux boundaries were used at other locations where underflow into the model is comparatively low in volume and relatively constant over time. These boundaries include Aguirre Valley, Santa Rosa Wash, Vekol Wash, Picacho Pass, and north of the Picacho Mountains (Cactus Forest area). Inactive model cells simulate “no-flow” boundaries where groundwater flow into or out of the model does not occur. Figure 18 shows the locations and types of boundaries employed in the model. The calibrated underflow for each boundary generally fell within the range of conceptual estimates (Table 2).

### **Model Data Development**

Data used for the Pinal model update were derived from various sources. Several USGS hydrogeologic investigations and model reports provided pertinent data for early model simulation periods and the establishment of the geologic and hydrogeologic framework. Data

collected by ADWR was the most significant data source used for model development. The primary ADWR databases include: ADWR Groundwater Site Inventory (GWSI), Wells 55, Wells 35, and Registry of Grandfathered Rights (ROGR) databases. Previous ADWR model reports for the Pinal, Phoenix and Tucson areas also provided significant data for the model update. SCIP annual reports provided supplemental data for the SCIP area and the GRIC. Hydrologic studies conducted by consulting firms in support of the Assured and Adequate Water Supply (AAWS) and Underground Storage Facility (USF) recharge applications provided additional information on driller's logs, geophysical logs, aquifer test analyses, and other related data. A discussion of sources of data used to develop the ADWR model datasets is presented below.

### ***Water Levels***

Water level data were obtained mainly from the ADWR GWSI database. Water level data from various USGS studies were an important supplemental source for the pre-development and early transient model simulation periods. Groundwater levels were analyzed for a number of years to show spatial and temporal changes and trends.

Over the years of significant groundwater development (since 1940), large vertical hydraulic gradients have developed between aquifer units in many parts of the Maricopa-Stanfield and Eloy sub-basins where fine-grained sediments restrict vertical groundwater flow. In areas where significant vertical hydraulic gradients exist, and sufficient data are available, unit-specific water level maps should be developed to aide in model calibration. Developing unit-specific water level maps requires a careful study of available water level, lithologic (well logs and other geologic data) and well construction data. Unfortunately, in the Pinal model area much of the data that is required to construct comprehensive, unit-specific water level maps does not exist. Additionally, most wells that provide observational data penetrate and/or are open to

multiple aquifer units, and the water levels measured in such wells represent a “composite” or blend of water level of several aquifers instead of one specific aquifer unit. Due to the inherent difficulties in developing a time-series of unit-specific water level maps this study focused on developing unit-specific water level contours only for years 1984 and 2007. However, water level contour maps derived by USGS studies for pre-development (circa 1900) (Thomsen and Baldys, 1985), for 1941 (Turner and others, 1943), for 1952 (Halpenny and others, 1952), and for 1963 (Hardt and Cattany, 1965) were digitized and reviewed to obtain general knowledge on historic water level changes and trends.

To assist in the model calibration, 89 hydrographs were generated across the study area. Preference was given to wells with relatively long periods of record and wells that provided coverage over the entire model domain. Within the study area a few piezometers were installed to monitor vertical gradient between aquifers of interest. These wells are of importance to this model calibration as they provided key information on the historic development of vertical gradients. Figure 29 illustrates the distribution of hydrograph wells across the study area. Hydrographs were used to compare how the model simulated head (or vertical gradient) matched the observed trend over time. A detailed discussion on the hydrographs is presented later in the model calibration section. The hydrographs are included in Appendix C.

### **Historical Development of Groundwater Systems**

#### ***Pre-development 1900 to 1922***

Prior to 1923, the aquifer system in Central Arizona was considered to be in an equilibrium state (Anderson, 1968). Thomsen and Baldys (1985) performed a hydrologic study in Central Arizona, analyzed groundwater levels measured between 1897 to 1905, and used these data to derive a groundwater level contour map for pre-development (Figure 30). The water

level contour map derived by Thomsen and Baldys (1985) was digitized and used in this modeling effort as a composite water level map representing groundwater conditions in the pre-development aquifer system. Although vertical gradients may have existed during pre-development in some locations, such gradients were assumed to be minor on a regional scale, and the composite heads discretized from the pre-development water level map were used for starting heads for the steady-state model calibration. The 82 data points used for constructing the contour map were also used as water level calibration targets for the three model layers during steady-state.

During pre-development, depths to water ranged from 8 to 70 feet below land surface for most of the model domain. Relatively greater depths to water (more than 100 feet) were observed in the south/ southeastern portion of the Eloy sub-basin and in the southern portion of the Maricopa-Stanfield sub-basin, west of Casa Grande (Figure 31). During the pre-development era, groundwater generally flowed in a northwesterly direction from southeast of Eloy through the Casa Grande and Maricopa areas toward the gap between South Mountain and the Sierra Estrella Mountains (Figure 30). In the northern portion of the model domain, groundwater flowed from east to west generally following the Gila River flow direction.

### ***1923 to 1941***

Comparatively brief periods of significant well construction occurred at different times within the study area. Well construction started in the Casa Grande-Florence area around 1925, followed by the Eloy area in 1936 and 1937, and the Maricopa-Stanfield area from 1939 to 1941 (Turner and others, 1943). Figure 32 shows a composite groundwater contour map using the available data and the groundwater map constructed in Turner's study (1943). This map was digitized and used in this modeling effort. Comparisons of this contour map to that constructed

for pre-development (Figure 30), reveal only minor changes in regional groundwater levels and flow directions. The depth-to-water map for 1941 (Figure 33) shows slight deepening of the water levels in both the Eloy and Maricopa-Stanfield sub-basins as a result of the increased pumping.

### ***1941 to 1984- Period of Declining Water Levels***

This period covers one of the most important periods during the history of groundwater development history in the Pinal model area. Groundwater pumping increased greatly from early the 1940s and reached a maximum level of about 1,400,000 AFY in 1953 and maintained high levels until the early 1980s. The long-term pumping during this period caused significant changes to the aquifer system. Water levels declined rapidly, cones of depression formed near pumping centers, significant vertical hydraulic gradients developed between aquifer units, in many areas the UAU and MSCU were dewatered, groundwater flow directions changed and aquifer compaction and regional land subsidence occurred. Groundwater conditions during this period are discussed in more detail below.

### **1941 to 1951**

Water level continued to decline model-wide with the increased groundwater withdrawals. However, the rate of decline varies significantly within the model area. The rate of decline can also vary between the aquifer units, depending on which aquifer the water was being withdrawn from. Figures 34 and 35 are a composite water level map and depth-to-water map for 1951 (Halpenny and others, 1952). The groundwater contour map developed by Halpenny and others (1952) was digitized and used in this modeling effort. These maps provide an overview of the changes to the aquifers.

In the Maricopa-Stanfield area, depths to water ranged from about 50 feet near Maricopa to greater than 300 feet along the western edge of the Maricopa-Stanfield sub-basin. The depth-to-water decreased from basin edges to basin center, and also decreased northwesterly from the Casa Grande area towards Maricopa.

In the area between Casa Grande and Florence (Casa Grande- Florence Area), the depth-to-water ranged from about 50 feet along the Gila River Corridor to over 150 feet southeast of Florence. In the immediate vicinity of Casa Grande, the depth-to-water ranged from 40 feet to 70 feet.

In the Eloy Area, the depth-to-water ranged from near 100 feet to over 200 feet south and southeast of Eloy. Water levels declined about 50 feet to 70 feet in the past 10 years in most the area around Eloy.

Groundwater flow directions did not change significantly from 1941 to 1951. Regional groundwater depressions developed in pumping centers throughout the model area. In the eastern portion of the Maricopa-Stanfield sub-basin, the horizontal hydraulic gradient increased substantially along the Casa Grande ridge (Figure 34).

### **1951 to 1963**

During this period, groundwater withdrawal rate was at a very high level and generally ranged from about 1,000,000 AFY to 1,200,000 AFY with the exception of 1,400,000 AFY in 1953. The long-term elevated pumping caused water level to continue to decline at an accelerated rate. A composite water level map (Figure 36) and depth-to-water map (Figure 37) were constructed for 1963 based on the available data (Hardt and Cattany, 1965). These maps were digitized and used in this modeling effort.

The 1963 composite water level map (Figure 36) shows significant change in flow directions compared to earlier years. Significant local and sub-regional cones of depression continued to deepen in both the Maricopa-Stanfield and Eloy sub-basins. With the greater pumping the water level differentiation between the layers became more pronounced.

As shown in Figure 37, in 1963 in the Maricopa-Stanfield sub-basin, the depth-to-water ranged from about 100 feet near Maricopa to more than 500 feet in the western part of sub-basin. At the center of the cone of depression there was about 200 feet of decline observed during the 12 year period. West of the Sacaton Mountains the depth-to-water was about 400 feet, approximately a 200 feet decline over this period. The hydraulic gradient continued to increase along the eastern edge of the Maricopa-Stanfield sub-basin (Casa Grande ridge area), where the depth-to-water increased from about 70 feet to almost 300 feet within a couple of miles. The change gradient in the LCU was even more significant going from 70 feet to 500 feet in the same area.

The depth-to-water varied between Casa Grande and Maricopa within the Maricopa-Stanfield sub-basin. Specifically, the depth-to-water varied from about 300 feet along the eastern edge of the sub-basin to 250 feet at the basin center and continued to decrease reaching about 100 feet near Maricopa. A large cone of depression formed in the southwest portion of the Maricopa-Stanfield area, and significant vertical hydraulic gradients developed in areas where large thicknesses of fine-grained materials were present.

In the Casa Grande-Florence area, depths to water ranged from about 75 feet to over 100 feet along the Gila River Corridor west of Coolidge. The average water level decline for this period was around 50 feet for the area. Between Casa Grande and the Sacaton Mountains, the depth-to-water ranged from 150 to 230 feet, and the average water level decline was about 80

feet during the 12 year period. In the area west of Casa Grande, the depth-to-water ranged from 45 feet to 77 feet. Water levels changed little in this area during the time period.

In the Eloy Area, the depth-to-water ranged from about 130 feet near the Silver Reef Mountains to about 340 feet south and southeast of the Town of Eloy. In the area northeast of the Silver Reef Mountains, water level declines of about 30 feet to 80 feet occurred. Water level declines ranged from about 80 feet in the northern part of the Eloy sub-basin to 140 feet in the southern part.

### **1963 to 1976**

During this period, groundwater withdrawals decreased slightly. Pumping generally ranged from about 800,000 AFY to 1,000,000 AFY, and exceeded 1,000,000 AFY for only a few years. Water levels declined continuously. Figure 38 is a composite water level elevation map for 1976 and Figure 39 is a depth-to-water maps for 1976. The 1976 composite groundwater elevation contours are similar to contours shown on maps prepared for the same time period by Konieczki and English (1979) and Wickham and Corkhill (1989).

The depth-to-water ranged from over 120 feet near Maricopa to more than 350 feet along the southwestern edge of the Maricopa-Stanfield sub-basin. Hydrographs in the southwestern portion of the sub-basin showed depths to water of over 700 feet for the LCU. The water level decline over this time period ranged from 80 feet to 200 feet in that portion of the sub-basin. Large water level declines (more than 150 feet) also occurred southwest of the Sacaton Mountains, where the depth-to-water exceeded 400 feet. The steep hydraulic gradient was still present in the area along the eastern edge of the sub-basin where depths to water increased rapidly from 50 feet to over 250 feet (over 400 feet in the LCU) in a couple of miles.

In the Casa Grande- Florence area, depths to water ranged from about 103 feet to over 200 feet along the Gila River Corridor, and the average decline for this period was around 50 feet. In the little basin between Casa Grande and the Sacaton Mountains, the depths to water ranged from 170 to 300 feet, and the average water level decline was approximately 100 feet in the this 14 year period. In the area west of Casa Grande, the depth-to-water ranged from 45 feet to 65 feet. Water level changed little in this area over the 14 year period. South of Coolidge, water levels declined by about 30 feet during this time period.

During this time period vertical hydraulic gradients became more pronounced in the area northeast of the Silver Reef Mountains. In this area, depths to water ranged from 100 feet to over 150 feet, however, wells completed only in the MSCU and LCU showed depths to water over 428 feet. In the area just north of the Silver Reef Mountains, water levels increased about 50 feet, however water levels declined more than 150 feet in the area immediately southeast of the water level rise. Water levels declined by about 100 feet in the southern part of the Eloy sub-basin. In the northern portion of the sub-basin declines of about 30 feet were observed. Canal recharge in this area appears to have had an effect on the depth-to-water over this time period, especially in the UAU.

By 1976 the general direction of groundwater flow was still similar to earlier periods. However, water levels generally continued to drop in most areas during the period, except in the area around Casa Grande and to the south where water level elevations showed an increase.

#### **1976 to 1984**

With the availability of a significant amount of water level data and well information a more detailed analysis of groundwater levels was conducted to differentiate between the different hydrogeologic units. Water levels, well construction data and geology data were combined into a

single database. Water levels were assigned, where possible, to different hydrogeologic units based on available information. This analysis resulted in water level maps for each of the three model layers.

Some of the wells were screened only in one hydrogeologic unit and water levels were assigned to the appropriate model layer. However, many wells were screened through multiple model layers. For these wells, the percentage of the perforation interval in each model layer was first calculated; water levels were then assigned to the model layer containing more than 60 percent of the saturated perforated interval. For wells that only have depth data available, water levels were assigned to the lowermost model layer penetrated by the well. It was frequently found that no well construction information was available for many of the observation wells, and water levels were assigned to model layers based on water level trend analysis. In the areas where a significant vertical hydraulic gradient was noted, it was not uncommon for the water level measurements from wells that were open to multiple hydrogeologic units to show a blending of the water levels from the different aquifers. Composite water levels from such wells were not used for layer-specific contouring or model calibration. Upon the completion of the water level analysis, 593 water levels were selected for model layer 1, about 556 water levels were used for model layer 2 and about 412 water levels were used for model layer 3 to represent the groundwater conditions for the three different aquifers in 1984.

The detailed water level maps for the individual model layers are shown in Figure 40. It should be noted that the water level contours that were developed are highly interpretive, especially in areas where the data were sparse for a particular layer. The UAU map indicates areas of dewatering along most of the edges of the basin and in the southern portion of the Maricopa-Stanfield sub-basin.

Figure 40 shows 1984 groundwater conditions in the MSCU. No vertical hydraulic gradients were observed in the area around Casa Grande, and the groundwater mound observed in the UAU of similar size was also shown in the MSCU. West of the mound, the MSCU was dewatered, and a small cone of depression formed near the Town of Maricopa. In the southern portion of the Eloy sub-basin, a large groundwater depression was formed from three smaller cones. One cone formed immediately south of the Casa Grande Mountains; the second formed east of the Sawtooth Mountains and the third was located west of the Picacho Mountains. In the northern part of the Eloy sub-basin, water table was relatively flat. A small cone of depression was formed southeast of the Sacaton Mountains.

Figure 40 also shows groundwater conditions in LCU in 1984. The groundwater mound in the Casa Grande area was also observed in LCU. West of the groundwater mound, there was a very steep hydraulic gradient in the Casa Grande Ridge area where water levels dropped over 500 feet within a couple of miles. The steep hydraulic gradient in this area results from a complex combination of factors that complicate interpretation of data. The complicating factors include: the western limit of the zone of saturation in the UAU, possible perching conditions in the UAU, the pinchout of the MSCU to the east and difficult to evaluate vertical hydraulic gradients due limited unit-specific observation wells in the area

By 1984, groundwater pumping had created a deep cone of depression in the southwestern portion of the Maricopa-Stanfield sub-basin that dewatered the UAU and MSCU aquifers in that area. The development of the cone of depression in the LCU in this area caused the direction of groundwater flow in the Maricopa area to shift from a previously northwestern direction to a generally southern direction. A small cone of depression was also observed in the area between Casa Grande and the Sacaton Mountains. In the Eloy sub-basin, a large cone of

depression was located that extended along the southwestern boundary of the sub-basin. The western boundary of the cone showed a significant gradient to the west with water levels rising over 300 feet in a little over a mile. Significant vertical hydraulic gradients were observed in 1984 in this area among the three model layers. South of Eloy, LCU water level data were essentially unavailable and groundwater interpretations of LCU groundwater levels were based solely on water level trend analysis of available data from the UAU and MSCU. In the area along the Gila River there was very little, to no vertical hydraulic gradient observed between hydrogeologic units.

A generalized depth to water map was developed based on the water level contour map in Layer 1 (Figure 41). Overall, the basin experienced rising water levels in most of the areas. In the Maricopa-Stanfield sub-basin the southern portion of the basin showed signs of recovering slightly from the previous periods of heavy pumping. The cone of depression south of Maricopa did not change dramatically some areas rose slightly (+/- 10 feet) and some areas dropped slightly (+/- 10 feet).

The Eloy sub-basin showed water level recoveries ranging between 20 feet in the northern portion, to 100 feet in the southern portion of the sub-basin. 1984 is the first year that a distinct groundwater mound was delineated around the Picacho Reservoir, approximately half way between the towns of Coolidge and Eloy. The groundwater mound in the area around Casa Grande that existed since 1941 was still present in 1984. Water level recovery was observed in this area and depths to water ranged from 25 feet to 50 feet. The mound was sustained by agricultural recharge, canal seepage and other possible sources.

### ***1984 to 2007- Period of Rising Water Levels***

Groundwater pumping generally declined during this period, and ranged from 400,000 AFY to 600,000 AFY for most of the years except for the wet years of 1992 and 1993 when pumping was less than 300,000 AFY. The decrease of pumping was primarily attributed to the use of CAP water which became available since 1987, and to an overall decrease in agricultural activity and water use compared to earlier time periods. Water levels were observed to rise in most of the model area.

### **1984 to 1993**

Water level and depth-to-water maps were constructed for 1993 for the UAU aquifer (Figures 42 and 43). Water levels rose throughout most of the model area during this period. Dramatic changes occurred along the Gila River corridor, where water levels rose to 50 feet or less below land surface. The rise along the Gila Corridor was largely due to the high volume flood flows that occurred in 1992 and 1993. By 1993, the cone of depression in the Maricopa-Stanfield sub-basin located near the Town of Maricopa experienced significant water level recovery over this period, rising over 50 feet. There was not a significant change in the southern portion of the Maricopa-Stanfield sub-basin, at least in the upper layer of the aquifer. Along the southwestern edge of the sub-basin the extent of areas of with depths to water that exceeded 350 feet expanded into the sub-basin.

The northern portion of the Eloy sub-basin showed continued water level rises over this period by more than 50 feet, augmented by the increase in recharge from the flood events. The groundwater mound located in the vicinity of the Picacho Reservoir continued to expand. South of the Town of Eloy water levels declined by over 100 feet over this time period. The groundwater mound to the west of Casa Grande also showed slight declines over this period.

The general flow directions at the end of this period were similar to 1984. However, there were subtle changes as the water levels began to rise and the cones of depression became less pronounced. This was especially apparent in the center of the Eloy and Maricopa-Stanfield sub-basins.

### **1993 to 2003**

Water level and depth-to-water maps were constructed for 2003 for the UAU (Figures 44 and 45). During this period water levels continued to rise over most of the model area. However, water levels declined by about 50 feet along the Gila river corridor from highs caused by significant flooding in 1993. Between Coolidge and Florence groundwater level declines of over 100 feet were observed. By 2003, the cone of depression in the Maricopa-Stanfield sub-basin located near the Town of Maricopa rose over 100 feet in some places.

Water levels continued to rise by over 50 feet in the northern portion of the Eloy sub-basin, west of Coolidge. The groundwater mound located near the Picacho Reservoir also continued to expand. In the southern portion of the sub-basin, water levels generally rose by about 50 feet. The groundwater mound located west of Casa Grande declined slightly during the period. Groundwater flow directions were generally unchanged from earlier periods.

### **2003 to 2007**

Hydrogeologic unit-specific water level maps (Figure 46) and a depth-to-water map (Figure 47) were developed for 2007. Water levels that represent a blend of multiple model layers were not used in the analysis. Upon the completion of analysis, 502 water levels were assigned to model Layer 1, 480 water levels to Layer 2, and 295 water levels to model Layer 3.

The comparison of depth-to-water maps for 2003 (Figure 45) and 2007 (Figure 47) shows that water levels continued to rise throughout most of the model area. The groundwater mound in

the southern portion of the Maricopa-Stanfield sub-basin expanded. Water levels continued to rise in the Eloy sub-basin. The extent of the groundwater mound located near the Picacho Reservoir expanded slightly. The cone of depression northeast of the Town of Eloy was no longer apparent on the 2007 map. The groundwater mound located west of Casa Grande showed a slight rise compared to 2003.

The UAU water levels shown in Figure 46 indicate that the dewatered areas of UAU were similar to the 1984 dewatered area. A small cone of depression was evident in the MSCU near the Town of Maricopa. The water level data for Layers 1 and 2 indicate the presence of a groundwater mound located near the Picacho Reservoir. The large regional groundwater depression (composed of three separate cones) that was noted in 1984 in the southern portion of the Eloy sub-basin was still present in 2007. The eastern and southern cones were smaller in extent and experienced water level rises of approximately 50 feet. The large cone of depression on the west side of the sub-basin had a similar shape and size to the cone that was observed in 1984. However, the water level in cone had recovered by about 50 feet since 1984.

The LCU water level map for Layer 3 (Figure 46) showed an overall rise in water levels compared to the 1984 map. The groundwater mound west of the Casa Grande area did not change appreciably during the 23 year period. Likewise, the steep hydraulic gradient in the Casa Grande Ridge area remained essentially unchanged. The large cone of depression in the southwest portion of the Maricopa-Stanfield area was still present. However, water levels in the cone recovered more than 100 feet since 1984. The large cone of depression located on the southeastern edge of the Eloy sub-basin showed water level recoveries of over 50 feet. The steep gradient to the west of this feature was reduced from 300 feet per mile to 200 feet over the same distance. As with the Layer 3 map for 1984, the 2007 water levels south of Eloy, are solely

interpreted based on water level trend analysis since no wells in that area penetrate the deep LCU aquifer. Water levels along the Gila River generally showed a recovery trend from 1984 levels, usually rising no more than 50 feet.

### **Summary of Water Level Changes**

Analysis of water level observations indicates that the impacts of groundwater development varied from area to area. The largest water level declines occurred and an extensive cone of depression was formed in the southwest portion of the Maricopa-Stanfield sub-basin. The UAU and MSCU aquifers were dewatered along basin margins, and a steep hydraulic gradient developed west of the Casa Grande Ridge area. Vertical hydraulic gradients developed between aquifers since late 1940s, and groundwater flow direction reversed in Maricopa-Stanfield sub-basin.

In the Eloy sub-basin, groundwater responses to pumping varied from north to south. Water levels in the northern part of the sub-basin declined less than in the southern part because of lower groundwater withdrawals and greater amounts of natural recharge from floods (for example, 1983 and 1993). In the southern part of the Eloy sub-basin, water levels declined much more in the MSCU and LCU than in the UAU. Noticeable vertical hydraulic gradients developed between the UAU and MSCU/LCU starting in the late 1960s and became more significant as development progressed. There was a delay of about 20 years for the vertical hydraulic gradient to become apparent between the aquifer systems in the southern part of the Eloy sub-basin compared to the southwestern part of the Maricopa-Stanfield sub-basin. It is possible that water released from extensive aquifer compaction observed in the southern part of the Eloy sub-basin contributed to the delay of development of vertical gradients in that area.

The Casa Grande area experienced relatively minor water level declines over time, compared to either the Maricopa-Stanfield or Eloy sub-basins. Hydrographs shown in Appendix C illustrate the spatial and temporal characteristics of water level changes related to groundwater development. Further discussion of the hydrographs is provided in the section on model calibration.

### ***Aquifer Parameters***

In this study, aquifer parameters including hydraulic conductivities (k) and storage values were initially based on conceptual values developed by previous studies. In areas where aquifer test results were available, the estimated K values were used as primary information. In areas where aquifer test data were unavailable, transmissivities or conductivities estimated through other means were used as initial estimates. There were no field data available within the Pinal model area that provided information on vertical hydraulic conductivities. A Kh:Kz ratio of 10:1 was assigned to areas where large thickness of clay did not exist, and vertical hydraulic gradients were minimal. The Kh:Kz ratio was initially assigned to range from 100:1 to 10000:1 for areas where extensive clay is present. These Kh:Kz ratios were adjusted during model calibration.

The initial specific yield values were based on those estimated in Pinal 1990 model (Corkhill and Hill, 1990) for both the Maricopa-Stanfield and Eloy sub-basins. In the model area where Pinal model and SRV model overlap, the specific yield was based on the recent updated SRV model. Specific storage was initially assigned to range from  $10^{-6}$ /feet to  $10^{-5}$ /feet based on previous studies.

The subsidence package (SUB-WT) required parameters including compression index and recompression index, the thickness of clay, and pre-consolidation stress. The compression index and recompression index are empirical parameters, and were initially estimated based on literature review (Leake and Galloway, 2007). The clay thickness was based on the updated

geology interpretation. The pre-consolidation stress was initially estimated to be 90 feet based on other aquifer compaction studies performed in the Eloy area (Pool and others, 2001).

### ***Pumping***

Groundwater pumping is the dominant groundwater outflow component in the Pinal model area. The groundwater pumping simulated in the Pinal model was divided into 4 major time periods, and data sources include: 1) USGS estimated groundwater pumping (1923 to 1983) for the lower Santa Cruz basin; 2) SCIP reported pumping on the GRIC area (the Agency Part) and on the non-GRIC area (the District Part) (1935~2009); 3) ADWR estimated non-SCIP GRIC pumping (1923 to 2009); and 4) ADWR reported pumping for non-SCIP, non-GRIC groundwater users stored in the Registry of Grandfathered Rights (ROGR) database for the period of 1984 through 2009.

### **USGS Estimated Historical Pumping 1923 to 1983**

The total groundwater pumping from 1915 to 1983 in the Lower Santa Cruz (LSC) basin was estimated by the USGS based on electrical power and gas consumption records. The estimated total pumping in the LSC was used in this study as a conceptual limit for the total pumping in the Pinal model area. For modeling purposes, the entire model domain was divided into three subareas: the Maricopa-Stanfield, Eloy, and the Casa Grande-Gila River- Florence (CGF). Figure 48 shows the boundary of the three sub-areas. The total groundwater pumping for the LSC was divided among the three subareas from 1940 to 1951 by Halpenny and others (1952), and from 1952 to 1963 in Hardt and Cattany's study (1965). In this study, the pumping totals estimated by Halpenny and others (1952) and Hardt and Cattany (1965) were used for each of the three subareas during the period of 1940 to 1963. The estimated pumping percentage for each sub-area during the period of 1940 to 1963 provides a general trend for distributing the total pumping to the three sub-areas during the time from 1964 to 1983. The distribution of the total

LSC pumping to the three sub-areas during the early years was based on the groundwater development history in each sub-area. The largest percentage of groundwater pumping was assigned to Casa Grande-Florence areas before 1940. Groundwater development started several years earlier in Eloy than in Maricopa-Stanfield. Therefore more pumping was assigned to Eloy in early years than to Maricopa-Stanfield subarea. The total estimated pumping for the Maricopa-Stanfield sub-area was divided into Ak-Chin and non-Ak-Chin areas. The total pumping for Casa Grande-Florence-Sacaton area consists of three components including GRIC non-SCIP project pumping, SCIP project pumping, and Casa Grande-Florence-other well pumping. Table 7 shows the estimated historic groundwater pumping for each sub-area.

Once the annual pumping for each sub area was determined, the next task was to distribute the pumping to different well locations throughout each subarea. ADWR 55 and ADWR 35 well databases were queried for groundwater pumping wells in the Pinal model area, and the total number of pumping wells for each sub-area was summarized for each year. The pumping for each subarea was then distributed based on the number of pumping wells. This approach was used to initially distribute the total pumping over the model area (Figure 49).

**Table 7 Total Simulated Pumping in the Pinal Model Area 1923-2009 (by Sub-Area)**

(Acre-Feet/Year)

Year	CGF	Eloy	MS	Year	CGF	Eloy	MS
1923	82,823	9,994	3,905	1967	404,755	318,378	392,986
1924	85,131	10,340	4,255	1968	327,458	257,488	325,181
1925	86,443	10,457	4,805	1969	368,398	296,541	376,241
1926	88,395	11,253	4,905	1970	318,487	250,079	319,577
1927	90,236	11,229	5,005	1971	292,256	229,617	296,902
1928	91,944	12,454	5,305	1972	297,029	222,561	279,023
1929	92,818	13,108	5,555	1973	357,411	278,778	347,662
1930	110,702	18,313	6,755	1974	420,201	327,286	414,154
1931	124,094	28,801	8,004	1975	357,994	284,512	365,349
1932	148,015	28,556	9,458	1976	365,550	283,113	351,801
1933	164,398	37,038	9,708	1977	373,439	291,226	363,969
1934	170,181	50,372	15,558	1978	284,827	212,218	257,715
1935	172,894	68,980	18,755	1979	270,024	209,145	259,814
1936	164,413	85,882	31,101	1980	357,193	253,169	287,886
1937	164,619	102,142	36,700	1981	395,635	280,573	321,887
1938	172,143	101,614	46,612	1982	315,785	246,657	293,775
1939	166,501	123,811	60,000	1983	184,285	136,224	174,007
1940	162,683	140,207	70,910	1984	266,769	166,403	225,032
1941	192,065	152,165	75,125	1985	251,976	185,680	237,777
1942	202,048	200,888	101,005	1986	248,766	169,277	181,154
1943	207,789	191,237	110,965	1987	268,871	183,851	175,114
1944	230,647	182,256	115,965	1988	303,728	164,010	139,874
1945	262,400	203,388	141,165	1989	332,997	153,408	131,104
1946	285,114	223,415	151,115	1990	262,624	88,571	114,146
1947	287,309	265,363	151,115	1991	264,114	109,722	152,904
1948	320,914	364,465	261,065	1992	172,779	52,580	87,916
1949	314,667	424,723	361,365	1993	179,967	23,077	84,400
1950	288,298	375,294	341,479	1994	240,566	59,995	109,596
1951	275,643	384,015	371,709	1995	245,316	73,750	133,752
1952	285,611	305,246	365,791	1996	289,299	124,235	165,041
1953	387,742	459,539	552,084	1997	304,276	87,595	104,829
1954	372,695	409,724	422,261	1998	261,148	92,857	100,205
1955	356,367	396,881	452,693	1999	267,169	103,223	105,668
1956	348,396	365,814	390,788	2000	261,418	101,868	99,067
1957	348,370	366,916	390,919	2001	263,973	88,775	93,215
1958	372,354	369,516	461,121	2002	235,492	111,890	114,956
1959	380,318	366,962	460,898	2003	252,088	139,048	150,628
1960	377,165	338,197	390,969	2004	233,473	127,534	155,873
1961	361,239	306,117	491,352	2005	235,938	95,897	106,143
1962	321,222	245,871	490,583	2006	222,591	116,300	113,981
1963	299,192	265,090	440,505	2007	237,604	139,364	125,404
1964	389,756	328,816	434,146	2008	231,147	158,542	178,482
1965	312,750	260,085	336,588	2009	218,292	143,154	159,216
1966	321,764	259,288	335,706				

CGF=Casa Grande-Florence; Eloy; MS=Maricopa-Stanfield

As discussed earlier, groundwater levels declined significantly from the 1940s to 1983. As a result, wells were deepened and started to tap deeper aquifers. The vertical pumping distribution for each well is a function of time and water level changes (as they relate to changing aquifer transmissivity). Due to the generally shallow construction depths of early wells, it is believed that a large percentage of the groundwater pumped came from the upper part of the regional aquifer system during the early years of groundwater development. Water levels declined with time, the percentage of pumping from the upper aquifer decreased while the contribution from the deeper aquifer increased accordingly.

In this study, the years of 1938, 1952 and 1964 were selected as critical years for defining the vertical pumping distribution. Groundwater pumping was assumed to occur mainly from the UAU before 1938. With water level decline, the saturated thickness of the UAU became smaller or reduced to zero due to the UAU dewatering. As the UAU dewatered and overall pumping increased, more pumping was assigned to the MSCU and LCU (the well-specific MSCU:LCU pumping ratio was proportional to the MSCU:LCU transmissivity ratio) The vertical pumping percentages for intervening non-critical years were linearly interpolated. The spatial and vertical distributions of annual pumping were adjusted as needed during the model calibration.

### **SCIP Pumping**

Annual groundwater pumping on the San Carlos Irrigation Project (SCIP) is not directly reported to ADWR. However, annual well-specific pumping is reported in the SCIP annual reports for project wells located on the GRIC (the Agency Part) and for wells located off the GRIC (the District Part). Table 8 summarizes the pumping rates pumping locations for each year. The vertical distribution of GRIC pumping was assigned using the same methodology used to assign other pumping volumes. The percentage of pumping for each layer was estimated for

each well for selected critical years, and the vertical percentage among layers for intervening non-critical years were linearly interpolated.

**Table 8 San Carlos Project Pumping to Agency and District Parts 1934 to 2009**

<b>Year</b>	<b>Agency</b>	<b>District</b>	<b>Year</b>	<b>Agency</b>	<b>District</b>
1934	44,322	105,809	1972	34,390	33,021
1935	51,793	116,058	1973	30,731	44,325
1936	83,794	145,403	1974	34,132	55,147
1937	34,531	36,137	1975	26,993	40,148
1938	70,661	96,815	1976	51,722	40,900
1939	64,316	78,584	1977	60,221	31,050
1940	57,169	63,762	1978	26,508	29,458
1941	30,908	78,528	1979	18,092	21,129
1942	99,960	167,776	1980	21,888	37,055
1943	113,968	185,566	1981	28,039	50,144
1944	113,878	167,580	1982	24,290	44,397
1945	58,806	111,297	1983	22,668	41,503
1946	46,192	58,797	1984	20,944	41,745
1947	71,290	50,961	1985	17,982	29,325
1948	73,020	56,832	1986	23,248	43,717
1949	66,095	49,773	1987	27,213	27,385
1950	81,024	61,427	1988	35,974	33,063
1951	54,623	44,814	1989	43,831	32,507
1952	52,088	49,467	1990	45,534	24,666
1953	72,890	44,164	1991	24,277	26,507
1954	56,094	41,022	1992	4,896	5,845
1955	54,404	48,160	1993	11,528	8,269
1956	65,252	53,881	1994	19,165	22,391
1957	39,056	34,300	1995	20,374	18,363
1958	24,615	39,969	1996	27,955	28,694
1959	46,105	48,419	1997	51,203	32,352
1960	38,823	40,432	1998	30,410	23,606
1961	48,303	25,191	1999	46,298	33,134
1962	39,357	41,157	2000	40,953	34,161
1963	34,605	36,611	2001	40,534	25,822
1964	39,965	34,210	2002	45,902	26,646
1965	37,025	29,578	2003	48,682	21,778
1966	28,726	37,988	2004	38,857	18,240
1967	33,204	40,539	2005	27,500	19,765
1968	31,389	37,505	2006	31,704	18,657
1969	28,905	41,755	2007	35,184	21,905
1970	31,960	42,849	2008	41,617	18,182
1971	50,784	32,061	2009	43,891	21,758

## **GRIC Pumping**

The pumping on the Gila River Indian Community (GRIC) includes pumping on and off SCIP (Agency) lands. The portion of pumping on SCIP agency was reported in SCIP annual reports. Non-SCIP pumping on the GRIC was not reported and had to be estimated. This non-project pumping can be broken down into two components, the large farming well pumping and municipal / industrial (M&I) pumping. The GRIC M&I pumping is a small component. A letter sent to ADWR on behalf of the GRIC provided a list of pumping wells on GRIC lands and well specific pumping capacities (GRIC, circa 1980). The total pumping capacity for M&I wells was estimated to be around 2,500 AFY. ADWR estimated 1,900 AFY of annual groundwater pumping for municipal or utility use, and 900 AFY for industry or commercial use, a combined GRIC M&I total pumping of 2,800 AFY (ADWR, 1996). In addition, the non-irrigation water use on the GRIC was estimated to be 7,467 AFY in 1974 by Gookin & Associates in 1980, and this estimate was referenced in a hydrologic study conducted for the GRIC (Stetson Engineers, 1981). In this study, the volume of M&I pumping on the portion of GRIC inside the Pinal model area was estimated to range from 500 AFY in 1960 to 3,000 AFY in 2009.

Pumping from non-SCIP large farming wells (LFW) located on the GRIC was estimated using a water budget approach. The methodology consisted of first estimating the total annual agriculture water use requirement for the GRIC by multiplying the total irrigated acres in GRIC and the irrigation requirement factor of 4.74 Acre-feet/acre. It should be noted that the total irrigation acres consist of the irrigated acres on SCIP project land (the Agency part) and those off the project lands. The irrigated SCIP project lands were reported in the SCIP annual report from 1934 to 2009. The number of irrigation acres on GRIC non-project lands and total irrigation acres for both on-project and off-project lands from 1951 to 1976 were provided in a report from

Stetson Engineers (1981). ADWR also documented the total irrigation acres on GRIC from 1978 to 1988 in its 1993 SRV model report (Corkhill, and others, 1993). For years when total irrigated acres were missing or incomplete, the total irrigated acres on the GRIC were estimated based on available data and trends.

It was assumed that groundwater was the sole source for non-project land irrigation use before 1989. Some CAP water was used for irrigation on GRIC non-project lands for a few years after 1990. The volume of CAP water used in conjunction with the GRIC Groundwater Saving Facilities was available from 2006 to 2009. The CAP water used for irrigation purposes were used to offset the groundwater pumping through large farming wells from the total agricultural water requirement. Not all the GRIC large farming wells are located inside the model domain. The portion of pumping inside the model domain was approximated. Table 9 presents the estimated, GRIC non-project pumping, and total GRIC pumping. The GRIC portion of the SCIP pumping was simulated at SCIP wells, the GRIC non-project pumping was distributed to a list of wells provided in the BIA reports.

The vertical distribution of GRIC pumping was assigned using the same methodology used to assign other pumping volumes. The percentage of pumping for each layer was estimated for each well for selected critical years, and the vertical percentages among layers for intervening non-critical years were linearly interpolated.

### **ROGR Pumping 1984 to 2009**

Annual, well-specific pumping data and general well information are available for wells required to report their annual pumping to ADWR since 1984. Well-specific pumping totals are reported by groundwater users in their annual ROGR reports, and well construction data, well

**Table 9 Estimated and Reported Pumping Data for GRIC 1923 to 2009**

Year	LFW	M&I	SCIP(Agency)	Year	LFW	M&I	SCIP(Agency)
1923	12,329	0		1967	73,652	1,000	33,204
1924	12,329	0		1968	71,507	1,000	31,389
1925	12,329	0		1969	75,974	1,000	28,905
1926	12,329	0		1970	74,453	1,000	31,960
1927	12,329	0		1971	70,779	1,500	50,784
1928	12,329	0		1972	74,486	1,500	34,390
1929	12,329	0		1973	74,815	1,500	30,731
1930	12,329	0		1974	92,778	1,500	34,132
1931	12,328	0		1975	74,264	1,500	26,993
1932	16,439	0		1976	78,563	2,000	51,722
1933	16,438	0		1977	76,007	2,000	60,221
1934	16,439	0	44,322	1978	73,097	2,000	26,508
1935	20,548	0	51,793	1979	83,486	2,000	18,092
1936	20,548	0	83,794	1980	92,646	2,500	21,888
1937	20,548	0	34,531	1981	93,966	2,500	28,039
1938	20,548	0	70,661	1982	58,644	2,500	24,290
1939	20,548	0	64,316	1983	51,230	2,500	22,668
1940	20,548	0	57,169	1984	41,367	2,500	20,944
1941	32,877	0	30,908	1985	36,501	2,500	17,982
1942	32,877	0	99,960	1986	39,781	2,500	23,248
1943	32,877	0	113,968	1987	41,774	2,500	27,213
1944	32,877	0	113,878	1988	54,394	2,500	35,974
1945	32,877	0	58,806	1989	53,425	2,500	43,831
1946	32,877	0	46,192	1990	12,201	2,500	45,534
1947	32,877	0	71,290	1991	53,425	2,500	24,277
1948	32,877	0	73,020	1992	53,425	2,500	4,896
1949	32,877	0	66,095	1993	53,425	2,500	11,528
1950	32,877	0	81,024	1994	53,425	2,500	19,165
1951	41,096	0	54,623	1995	53,425	2,500	20,374
1952	41,096	0	52,088	1996	53,425	2,500	27,955
1953	41,096	0	72,890	1997	41,278	2,500	51,203
1954	41,096	0	56,094	1998	53,425	2,500	30,410
1955	41,096	0	54,404	1999	39,140	2,500	46,298
1956	43,274	0	65,252	2000	6,661	3,000	40,953
1957	46,286	0	39,056	2001	53,425	3,000	40,534
1958	41,063	0	24,615	2002	0	3,000	45,902
1959	48,296	0	46,105	2003	0	3,000	48,682
1960	51,152	500	38,823	2004	6,618	3,000	38,857
1961	47,334	500	48,303	2005	53,425	5,000	27,500
1962	50,367	500	39,357	2006	37,110	5,000	31,704
1963	53,248	500	34,605	2007	35,422	5,000	35,184
1964	52,890	500	39,965	2008	23,050	5,000	41,617
1965	61,644	1,000	37,025	2009	24,841	5,000	43,891
1966	69,731	1,000	28,726				

LFW = Large Farm Wells (Non-SCIP); M&I=Municipal and Industrial

logs and water level are available for many wells from the ADWR's Wells 55, Wells 35 and GWSI databases. In general, annual well-specific pumping volumes from the ROGR database were vertically distributed to model layers using three methods: 1) based on the perforated interval cited by GWSI, 2) based on well depth if perforation data were not available, and 3) if well depth was unavailable then the average well depth of wells in the vicinity of was used. For methods 2 and 3 it was assumed that the well was perforated over the entire well depth. Updated Pinal model geology data, 2007 water level data, and the initial hydraulic conductivity distribution for each model layer were used together in conjunction with the well construction data to derive the initial vertical distribution of ROGR pumping.

Annual well-specific pumping data were combined (as required for specific time periods) from one or more of the four major pumping data sources: 1) USGS 1923 to 1983 historical data; 2) SCIP (Agency and District) annual reports; 3) GRIC (non-SCIP) data and estimates; 4) ADWR 1984 to 2009 reported ROGR data. The well-specific vertical pumping distribution was determined for each well using available geologic, water level and well construction data. The WELL package was used to simulate pumping from each well per model layer based on the methods cited above. When necessary, simulated pumping was reassigned to deeper model layers to maintain estimated pumping rates. Figure 49 illustrates the locations of pumping wells simulated during the transient calibration period.

### ***Evapotranspiration***

Evapotranspiration occurs along the Gila River riparian zone and the Santa Cruz River near the confluence of Gila River as a result of phreatophyte growth. The ET maximum extent was determined based on the USGS study (Thomsen and Eychaner, 1991), and it covered about 830 model cells in the Pinal model. Figure 50 shows the maximum extent of ET simulated in Pinal model. The ET component was estimated to be 96,000 AFY at pre-development. The ET package requires three types of data: ET rate, extinction depth, and surface elevation. The ET rate for the 830 model cells was first calibrated during the steady-state model so that the model simulated total ET volume at steady-state reasonably match the conceptual value of 96,000 AFY based on the USGS study. The maximum ET rate per model cell was kept constant for the transient periods. The ET extinction depth was simulated at a constant value of 30 feet. The land surface elevation at the center of the model cell based on DEM data was used for the ET surface elevation. With groundwater level decline over time, the simulated ET volume during the transient model calibration decreased significantly after the steady-state time.

### ***Stream flow Routing and Groundwater / Surface-Water Interactions***

Streamflow and groundwater / surface water interactions were simulated using the stream (STR) package developed by Prudic (1989). The stream package simulates head-dependent groundwater recharge and discharge for the Gila and Santa Cruz Rivers within the model area (Figure 51). The Stream package simulates head-dependent losing and gaining reaches throughout the stream network by simulating the differences in elevations between the stream stage and the water table immediately adjacent to the stream during a given stress period. In the Pinal model, stream stage was calculated and head-dependent recharge from stream channel infiltration (losing conditions) could occur if the calculated stage was above the water table and surface flow of sufficient quantity was available in the stream segment. Groundwater discharge

to the stream (gaining conditions) could occur if the water table was at a greater elevation than the calculated stream stage.

The Gila River channel was simulated in the model using 150 model cells (or stream reaches), and the Santa Cruz River was simulated using 39 model cells for non-wet years (Figure 51). During the pre-development era, the Gila River was perennial and the mean annual flow of Gila River upstream from the GRIC was estimated to be about 500,000 AFY and the median annual flow of 380,000 AFY (Thomsen and Eychaner, 1991). For the steady-state model simulation, the mean annual runoff of 500,000 AFY was input to the stream package at the location where the Gila first enters the active model area (at the most upstream reach east of Florence). Head-dependent, steady-state groundwater recharge and discharge conditions at gaining and losing reaches were subsequently simulated for the pre-development era. Stream bed conductance terms were calibrated during the steady-state model simulation to help match independent estimates of groundwater discharge and recharge from Thomsen and Eychaner's (1991) pre-development model.

As discussed in Chapter 2, the Gila River natural flow was controlled, managed, and diverted by upstream dam structures since early the 1920s. Due to the ephemeral nature of the river, and also due to relatively short duration of historic flood events (a few days to a few weeks) compared to the length of model stress periods (one year) it was not possible to accurately simulate recharge from specific historical flood events (during the transient model simulation period) using the stream flow routing package. Instead, estimates of annualized recharge from specific flood events (during the transient simulation) were simulated in the model using the recharge package.

### *Natural Recharge*

Natural recharge includes mountain front recharge and stream infiltration recharge. Natural recharge in the study area was simulated through the MODFLOW recharge (RCH package) and was applied to the uppermost active model layer. Mountain front recharge was primarily simulated along the mountain front of the Picacho Mountains. The total mountain front recharge of 500 AFY was simulated through 30 model cells at a constant rate of 16.67 AFY per cell (Figure 51).

As mentioned previously, recharge from the infiltration of Gila River flood flows was simulated differently in the model during the steady-state, and transient calibration periods. Gila River recharge at steady-state was simulated using the stream package. For the transient period, the maximum potential Gila River recharge from spills at Ashurst-Hayden Dam (generally flood events) was estimated using the difference of the Gila River Inflow and the Gila River outflow. The Inflow refers to the annual volume of Gila River surface water spilled and sluiced at the Ashurst-Hayden Dam and can be found in the SCIP annual reports. Gila River outflows were available at USGS gage 09478500 near Laveen for the periods before 1995. Gila River outflows after 1995 became available at USGS gage 09479350 near Maricopa. When the outflow data were missing or when outflow was larger than Inflow, the Gila River recharge was estimated to be 65 percent of the Gila River inflow. The estimated Gila River recharge showed large variability over time, ranging from 290 AFY in 2002 to 745,223 AFY in 1993. The average recharge (1934 ~2009) was 40,704 AFY and the median recharge was only 9,627 AFY.

Annual Gila River recharge was estimated at maximum potential levels. Recharge for some years was adjusted during model calibration. The relative distribution of Gila River

recharge to different reaches of the river was handled differently during “wet” and “dry” years. For dry years, the estimated Gila River recharge was simulated along the first (most upstream) 117 out of 150 Gila River cells. Recharge was not simulated for the 33 remaining Gila River cells west of Pima Butte; except for wet years since water levels along the Gila River west of Pima Butte are generally very shallow, and the Gila River is normally a gaining stream in that area. In general, it was assumed that the spatial distribution of Gila River recharge follows a decay curve from upstream to downstream, larger recharge rates were assigned in up-gradient recharge cells, and the recharge rate gradually declined to zero when approaching the reach near Pima Butte.

Stream recharge from the Santa Cruz River was considered negligible except in wet/flood years. Recharge after 1980 was mainly due to effluent from the Tucson AMA for non-wet years. The portion of recharge occurring on the Santa Cruz River inside the Pinal model area was estimated from flow volumes entering the Pinal model area from the Tucson AMA. These volumes were estimated for the recent update of the ADWR Tucson AMA model (Mason and Hipke, 2013). Santa Cruz River recharge was distributed differently depending on whether it was a wet year or dry year. During dry years, when the estimated Santa Cruz recharge was small, the total recharge was simulated only in the Eloy sub-basin. During flood years, estimated Santa Cruz River recharge was distributed along a greater reach, crossing the Eloy sub-basin and extending into the Maricopa-Stanfield sub-basin. The locations of model cells corresponding to the channel of the Santa Cruz River were approximated based on the most recent aerial photography. Figure 51 presents the recharge cells used to simulate the Gila and Santa Cruz River infiltration recharge during the transient period.

### ***Incidental Recharge***

Incidental recharge in this study includes agricultural recharge, canal recharge, urban irrigation recharge, Picacho Reservoir recharge, effluent recharge, and artificial recharge. In this model incidental recharge was simulated using the MODFLOW recharge (RCH) package.

### **Agricultural Recharge**

Agricultural recharge is the dominant component of simulated recharge in the Pinal model area. The methodology used to estimate and “lag” agricultural recharge was discussed earlier in the conceptual water budget section. Before 1983, agricultural recharge in non-SCIP project area was uniformly distributed based on irrigation maps of 1947, 1954, 1963 and 1973. Starting in 1984, agricultural recharge was distributed based on the areal extent of the irrigation districts including MSIDD, CAIDD, HIDD, the AK-Chin Indian Reservation, the Gila River Indian Community and non-district farming areas (Figure 52). In the SCIP project area, agricultural recharge was distributed based on the SCIP project boundary. Figure 53 shows the maximum extent of agricultural recharge simulated in Pinal model area.

As mentioned previously, agricultural recharge may take several years to percolate through the vadose zone to the aquifer. The agricultural recharge that was applied with the MODFLOW recharge package used the option that applied recharge to the uppermost active model cell in a given row and column. Since this MODFLOW option does not simulate unsaturated flow through the vadose zone, the estimated agricultural recharge was “lagged” manually with initial lag times calculated based on a combination of depth-to-water and an estimated average lag rate of 20 feet per year (Corell and Corkhill, 1994). It should be noted that during the transient model calibration the initial estimates of “lagged” agricultural recharge were

modified as necessary to achieve a better overall model calibration. Although following this empirical approach to estimate agricultural recharge improved the model calibration, it also made it more difficult to calculate any direct functional relationship between lag time, lag rate and depth-to-water. Regardless, of the complications encountered, the overall model calibration was improved by lagging the agricultural recharge. Agriculture was the only recharge component that was lagged.

### **Canal Recharge**

Canal recharge represents water seepage through the SCIP main canals and laterals, and the CAP main aqueduct. Figure 54 shows the locations of canals that had recharge simulated in the model. The SCIP canals and laterals are shown on Figure 54 as SCIP for the portion on the GRIC (the Agency Part) and SCIDD (the District Part) for the portion not on Indian land. CAP canal recharge began in 1987 when CAP water delivery started. Since the CAP aqueduct and laterals are lined, CAP recharge is comparatively small. A total of 1,710 AFY CAP canal recharge was estimated and distributed through a network of 85 model cells representing the CAP main aqueduct inside Pinal model area. CAP irrigation district main canal and lateral recharge were very limited, and were combined with the agricultural recharge within each irrigation district.

SCIP canals are not lined, water seepage from SCIP canals are the primary source of canal recharge in the Pinal model. SCIP canal recharge includes main canal seepage and lateral seepage. These estimates were developed from SCIP annual reports which provided SCIP project data from 1934. SCIP main canal recharge ranged from 3,900 AFY in 1990 to 62,702 AFY in 1984, and the average is 25,124 AFY. A total of 326 model cells were used to distribute main canal seepage, and these model cells represent the Northside Canal, the Blackwater Lateral, the

Pima Lateral, the Southside Canal, the Casa Blanca Canal, the Santan Canal, the Florence Canal, Florence-Casa Grande Canal, Florence-Casa Grande Extension, and the Casa Grande Canal.

SCIP lateral recharge consists of two components, the SCIDD lateral recharge and the GRIC lateral recharge. The total of SCIP lateral recharge ranged from 27, 848 AFY in 1934 to 180,724 AFY in 1981, and the average is 73,843 AFY. A total of 515 model cells were used to distribute the canal lateral recharge with 257 model cells for the GRIC part and the remaining 258 model cells in the SCIDD area.

### **Picacho Reservoir Recharge**

The Picacho Reservoir recharge ranged from 394 AFY in 2002 to 14,116 AFY in 1942 with an average recharge of 5,606 AFY. Figure 55 shows the location of the 16 model cells that were used to simulate this source of recharge.

### **Effluent Recharge**

Effluent recharge represents the recharge generated by waste water treatment and is delivered to various users, including municipal golf courses, an electric power generating station, farmlands and discharged to the Santa Cruz River channel (Burgess and Niple, 2004). The effluent generated from the Casa Grande Wastewater Treatment Facility accounts for most of the effluent recharge simulated in the model. This recharge was estimated to range from 1,230 AFY to 1,496 AFY. A total of 9 model cells were used to distribute this source of recharge (Figure 55).

### **Urban Irrigation Recharge**

The simulation of turf and urban recharge represents golf courses, parks, and other areas where urban flood irrigation was applied. Due to the limited quantity, recharge related to residential flood irrigation recharge was not considered. Urban irrigation recharge was estimated

to range from 731 AFY to 1,362 AFY. A total of 40 model cells were used to distribute this recharge. Figure 55 shows the locations where urban irrigation recharge was assigned.

### **Artificial Recharge**

The majority of the artificial recharge is represented by the relatively small amount of effluent stored in several active USF facilities. These facilities include North Florence Recharge Facility, the Arizona City Sanitary District Recharge Facility, Sun lakes at Casa Grande Effluent Recharge Facility, and the Eloy Reclaimed Water Recharge Project. The total recharge volume from these facilities ranged from 31 AFY to 898 AFY. CAP water was also recharged at the currently inactive Hohokam recharge site in 2003 for a volume of 739.5 AFY. These recharge locations are shown on Figure 55.

### ***Land Subsidence and Aquifer System Compaction***

For groundwater systems that include compressible, fine-grained sediments, water may be released from inter-bed storage when water levels decline. When the release of water from inter-bed storage is inelastic, the groundwater flow system can be impacted on a permanent basis. When water levels decline over time, fine-grained sediments in the subsurface may compress due to changes in overlying stress. The draining or re-wetting of pore space in the zone of water table fluctuations result in a change in the geo-static stress on the underlying sediments in the unconfined and confined aquifers (Leake and Galloway, 2007). Changes in hydrostatic stress due to the lowering of water table and/or confined aquifers, results in a change in the effective stress of the effected aquifer; relations between groundwater level changes, geostatic stress, hydrostatic stress and effective stress are documented in Leake and Galloway (2007).

The compression of fine-grained subsurface materials can lead to changes in effective stress of an aquifer or water bearing unit, and subsequently result in the subsidence of land at the

surface. In the Pinal AMA, some areas have experienced significant groundwater decline and associated land subsidence (Laney and others, 1978; Strange, 1983; Slaff, 1993). Between 1952 and 1977 land subsidence exceeding 7 feet already occurred in the Eloy, Picacho and Stanfield areas (Figure 56); isolated locations had experienced more than 10 feet of land subsidence (Laney and others, 1978) during this period. By 1985, some localized areas had experienced more than 15 feet of subsidence (Slaff, 1993).

In addition to land subsidence, the compaction of fine-grained materials in the subsurface may result in the release of water from interbed storage. The release of water from interbed storage consequently affects the groundwater flow system including changes in groundwater level elevations over time. Accordingly, the release of water from interbed storage may affect the hydraulic mechanisms associated with groundwater flow, and how it is simulated. In some cases, the release of water from interbed storage is inelastic, consequently altering the affected media's hydraulic properties including storage and hydraulic conductivity.

The groundwater flow system in the Pinal AMA includes multiple aquifers systems and aquitards; the aquitard material may consist of either interbeds of fine grain materials or massive clay bodies, both of which occur in the Pinal model area (Figures 57 and 58). In this version of the Pinal Model, alterations in the groundwater flow system from chronic water level declines are simulated, including the release of water from interbed storage and land subsidence. To simulate the release of water from interbed storage and land subsidence, the USGS MODFLOW SUB-WT (Leake and Galloway, 2007) module was employed. It is understood that the compaction of subsurface sediments may alter other hydraulic properties such as hydraulic conductivity (Rivera and Ledoux, 1991; Helm, 1976). For example, the inelastic compression of fine-grained sediments may permanently reduce the vertical hydraulic conductivity and

consequently affect groundwater flow system. With this version of the Pinal model, however, any possible alteration of hydraulic conductivity from compaction has not been formally included in the simulation process. It should also be noted that, at the time of this writing, there is no formal (MODFLOW) module available for simulating changes in hydraulic conductivity over time. See sensitivity analysis for details on the sensitivity of model parameters including vertical hydraulic conductivity.

Many of the hydraulic properties explicitly associated with SUB-WT module are impractical to directly observe or measure in the field including effective stress, geostatic stress, compaction, void ratio, etc., without disruption of the subject media itself. However comparison between observed and simulated land subsidence - a byproduct of compaction - was used to provide guidance for the calibration of key SUB-WT parameters. Laney and others (1978) provides observed land subsidence calibration targets over time including areal distribution of measured subsidence between 1952 and 1977, as well as cross-sectional profiles of land subsidence adjacent to I-10 between Casa Grande and near Picacho Peak for different periods of time. For later time periods (2004 to 2009), Interferometric Synthetic Aperture Radar (InSAR) data were also used as a calibration guide.

In addition to observed land subsidence, observed groundwater levels also provide guidance for the calibration of SUB-WT parameters because water is released from interbed storage. During simulation, if the release of water from interbed is inelastic, the expelled water augments groundwater flow system. Note that for groundwater conditions where inelastic compaction has not occurred, water remains within the interbed pore spaces of fine grained materials. Therefore, simulating water released from interbed storage results in solutions that

differ from simulating process that do not include the inelastic release of water from interbed storage.

The simulation of land subsidence is functionally-dependent on the coupled groundwater flow model. That is, the model solution is dependent on a combination of model parameters and stresses including traditional model parameters as well as parameters exclusive to the SUB-WT package. Outputs from the groundwater flow model yield state variables (heads) that in turn impact responses in the SUB-WT; thus there are feedback mechanisms that exist between “traditional” groundwater flow processes and the release of water from interbed storage. A mathematical description of the incorporation of interbed storage into the groundwater flow equations can be found in Leake and Galloway (2007).

## **Chapter 4. Model Calibration**

Model calibration is one of the most critical processes of model development. During calibration, model inputs (both stresses and aquifer properties) were adjusted within acceptable ranges so that simulated outputs (i.e. water levels, fluxes, water budget, etc.) reasonably matched observed data and conceptual estimates. A major objective of the calibration process was to minimize the differences, also known as errors or residuals, between simulated model outputs and observed data.

### **Calibration Targets and Standards**

#### ***Water Level Targets***

The groundwater system in the Pinal model area has undergone significant changes over time. Historic water level trends following the pre-development era consist of a period of rapid water level decline (caused by groundwater development) followed by a more recent period of significant water level recovery (generally coincident with reduced groundwater pumping and the introduction of CAP water). To better understand the dynamic changes, several model calibration periods were selected so that different stages of the groundwater system development could be evaluated. A total of 8 calibration periods were selected, that had sufficient water level data for model calibration. The calibration periods include: steady-state (circa 1923 or before), 1941, 1952, 1963, 1976, 1984, 1988 and 2007.

The GWSI database was first queried for water levels for the 8 selected calibration years. Calibration targets were selected based on several criteria: data quality, location, well depth, and measurement date. It should be noted that little data were available in GWSI for the early 1920s (steady-state). However, Thomsen and Baldy's study (1985) consolidated the available water levels measured between 1897 and 1905, and used these data to derive a composite steady-state water level contour map. This map, showing both water level contours and water level data

points, was digitized, geo-referenced and used for initial conditions and calibration targets for the steady-state simulation. Vertical hydraulic gradients may have existed in some areas during the pre-development era. However, there were insufficient data to delineate a layer-specific steady-state water level contour map.

A limited number of water level observations were available in GWSI for 1963. A review of previous studies indicates that Hardt and Cattany (1965) developed a composite water level contour map for year 1963 in Pinal area. Water level data points used to derive the contour map were also posted on the map. To increase the calibration data coverage, this map was digitized and geo-referenced, and some of the data points added to the 1963 water level targets. It should be pointed out that the additional calibration targets lack well construction data, and uncertainty was introduced when assigning these data to specific model layers.

A distinctive characteristic of the Pinal groundwater flow system is the presence of vertical hydraulic gradients. In some areas significant vertical gradients exist within and between hydrogeologic units. Significant vertical gradients have been observed in the Maricopa-Stanfield sub-basin, south of the Casa Grande Mountain in Eloy, and south of the Casa Grande Mountain. Vertical gradients appear to have increased from the 1940s to early 1980s, and started to decrease with water level recovery. In some areas, such as portions of the central to southern Maricopa-Stanfield sub-basin, vertical hydraulic gradients of a few hundred feet have been observed between the UAU and LCU. Consequently, assigning water level targets to incorrect model layers could easily result in a head residual of a few hundred feet. Assigning water level targets to the correct model layers was a challenging task due to insufficient well construction data and the fact that the observed water levels sometimes represented a mixture (composite) of water level from multiple aquifers.

In an effort to assign the water level targets to different model layers, well construction database and model geology were used with water level data to assign the model layer for all the targets. More effort was spent on analyzing and assigning the water level targets in 1984 and 2007, when more data were available, than for other years, and the period from 1984 to 2009 is the primary focus of this model study.

A total of 4,566 targets were used for the 8 calibration periods. Table 10 summarizes the water level targets used in the Pinal model. Long-term hydrograph data from key wells were also included as calibration targets. Hydrograph wells were selected to provide a representative spatial distribution throughout the model domain. Wells that were screened in different hydrogeologic units at one well site were also used to calibrate the vertical gradient in the model domain. A total of 89 hydrograph wells were selected, that provided 3,465 additional data points, resulting in a total of 8,031 water level targets collected from 2,215 well sites. The hydrograph targets covered various time periods that covered the transient simulation period and are not necessarily coincident with the 8 calibration periods shown in Table 10.

Water level observations were often assigned to all applicable model layers if wells were perforated or open to multiple aquifer units. Wells with no construction information were also assigned to applicable layers based on the depth of the well. Of the 2,215 well sites used, 1,433 had heads assigned (for any given time period) to a single model layer, 562 sites have heads for two or more layers and 220 sites assign heads to all three model layers

### ***Land Subsidence Targets***

Land subsidence is an important physical process in the Pinal model area. The observed land subsidence provides critical calibration targets. The subsidence targets mainly consist of two types of data: the spatial extent of observed subsidence and the vertical profile along

leveling lines over time. The subsidence targets were primarily derived from Laney and others (1977) study. The subsidence map developed by Laney and others was geo-referenced. This map delineates the approximate area where subsidence of more than 7 feet occurred in the Eloy and Maricopa sub-basins between from 1952 to 1977. The spatial extent of more than 7 feet of subsidence was used as a qualitative calibration target in this Pinal Model. Laney's report also included a vertical cross-section illustrating how subsidence changed over time at several bench marks along the land subsidence survey line between Casa Grande and Picacho Peak. The original data used for the cross-section could not be obtained. However, some of the data points were estimated from other data sources, and a similar subsidence cross-section was reconstructed and used in the model as a quantitative calibration target. Additionally, ADWR InSAR data were used to delineate the approximate spatial extent of the recent subsidence, which was used as a "qualitative" calibration guide.

**Table 10 Pinal Model Water Level Calibration Targets**

Calibration Year and Period		Layers	Sub-Basins			Subtotal
Year	Stress Period		ESRV	ELOY	MARICOPA-STANFIELD	
Steady-state	1	1	5	62	14	81
		2	5	62	14	81
		3	5	62	14	81
		<b>Subtotal</b>	<b>15</b>	<b>186</b>	<b>42</b>	<b>243</b>
1941	20	1	0	56	12	68
		2	0	23	3	26
		3	0	1	5	6
		<b>Subtotal</b>	<b>0</b>	<b>80</b>	<b>20</b>	<b>100</b>
1952	31	1	3	68	6	77
		2	0	26	5	31
		3	0	5	30	35
		<b>Subtotal</b>	<b>3</b>	<b>99</b>	<b>41</b>	<b>143</b>
1963	42	1	28	135	28	191
		2	3	10	17	30
		3	0	0	62	62
		<b>Subtotal</b>	<b>31</b>	<b>145</b>	<b>107</b>	<b>283</b>
1976	55	1	1	37	2	40
		2	0	38	17	55
		3	4	23	30	57
		<b>Subtotal</b>	<b>5</b>	<b>98</b>	<b>49</b>	<b>152</b>
1984	63	1	25	482	86	593
		2	25	448	83	556
		3	24	207	181	412
		<b>Subtotal</b>	<b>74</b>	<b>1,137</b>	<b>350</b>	<b>1,561</b>
1988	67	1	1	255	13	269
		2	0	249	64	313
		3	0	85	173	258
		<b>Subtotal</b>	<b>1</b>	<b>589</b>	<b>250</b>	<b>840</b>
2007	86	1	5	397	78	480
		2	8	387	74	469
		3	7	145	143	295
		<b>Subtotal</b>	<b>20</b>	<b>929</b>	<b>295</b>	<b>1,244</b>
Hydrograph Targets	1 ~ 88	1	0	1,272	218	1,490
		2	0	488	638	1,126
		3	90	250	509	849
		<b>Subtotal</b>	<b>90</b>	<b>2,010</b>	<b>1,365</b>	<b>3,465</b>
<b>TOTAL</b>			<b>239</b>	<b>5,273</b>	<b>2,519</b>	<b>8,031</b>

### ***Water Budget Comparisons***

The model simulated groundwater budget provided another dataset to compare to conceptual estimates, and thereby evaluate the overall effectiveness of the calibration effort. Simulated pumping and non-head dependent recharge (all forms of incidental, artificial and flood recharge) were compared with conceptual totals to assure these stresses were simulated by the model with reasonable accuracy. Head dependent boundary fluxes (constant head cells) and other head dependent budget components (evapotranspiration, interbed storage, stream discharge) were compared to conceptual estimates, if available. However, since conceptual estimates for most head-dependent budget components were either unavailable or associated with a high degree of uncertainty, these comparisons were mainly used as a check to determine if the respective MODFLOW packages generally functioned as expected.

### ***Residuals and Calibration Statistics***

Calibration targets are evaluated to assess whether or not a model adequately replicates the flow system being modeled. These calibration targets include individual calibration targets and more generalized systemic targets. Individual calibration targets can include water levels, estimated fluxes, or land subsidence that has a measured or estimated value and an associated acceptable calibration tolerance (or error). More generalized targets consist of localized or regional water budget estimates that can have a wider range of acceptance tolerances.

Several statistical-based measures are commonly used to evaluate model errors (Anderson and Woessner, 1992). These measures are defined below:

- Residual Mean (RM): the average of residuals
- Absolute Residual Mean (ARM): the average of the absolute value of residuals

- Root Mean Squared Error (RMSE): the square root of the average of the square of the residuals, which quantify the variability of the residuals
- Scaled RMSE: RMSE is scaled with the total model-wide head range

During the model calibration head residuals were first calculated as the difference between the observed water levels and the model simulated water levels at the same location. A positive head residual indicates that the observed water level is higher than the model simulated, a negative residual indicates that the observed water level is lower than the model simulated water level. A residual of zero represents an exact match between observed and simulated water levels. Once head residuals were calculated, the accuracy of the model calibration was evaluated using the above mentioned statistical measures.

The residual mean (RM) describes the mean error of a simulation and indicates whether the model is over or under simulating heads. The closer the RM is to zero, the better. An even more useful measure of model error is the mean of the absolute value of the head residuals (ARM) as the ARM uses the absolute values of the head residuals, it indicates how close model simulated heads are to observed heads no matter if they are over-simulated or under-simulated. The RMSE is a measure of the spread of the residuals about the mean (Helsel and Hirsch, 2002). The scaled RMSE is another useful measure of model error, which is calculated as the ratio of the RMSE to the total head loss in the system being modeled. If the scaled RMSE is low (less than 10 percent is a generally accepted threshold) then the model error is considered to represent only a small part of the overall model response (Anderson and Woessner, 1992).

## **Modifications of Model Inputs (Steady-State and Transient Calibrations)**

### ***Agricultural Recharge***

In most years agricultural recharge is generally the largest inflow to the Pinal model area aquifer system, averaging 57 percent of total conceptual model inflow throughout the model simulation. In non-flood years agricultural recharge accounted for up to 82 percent of the total estimated inflow. The large volume of agricultural recharge as well as the uncertainty associated with its estimate and distribution made it an important variable to evaluate during the transient model calibration. The simulation of agricultural recharge was complicated in the Pinal model area due to the substantial depth-to-water under many agricultural areas. In such areas the water that is recharged often takes many years to percolate downward through the vadose zone. The lagging of agricultural recharge was a critical factor that was evaluated during the transient model calibration.

The estimated agricultural recharge was initially distributed evenly based on irrigation maps or irrigation district boundaries. Based on head residuals, the spatial distributions and the rates of the agricultural recharge was then modified, with higher recharge rates being assigned to areas where water levels were under-simulated and lower rates to areas where water levels were over-simulated. During this redistribution, the total conceptual volume of agricultural recharge for each sub area or irrigation district was kept more or less the same. During the 1940s, water levels started to decline rapidly, and generally continued to decline until the late 1970s. Available data indicate that the full volume water that infiltrated beneath farmland in a given year did not reach the water table until sometime well after it was applied as irrigation. Instead, only a portion of the total estimated agricultural recharge arrived at the water table, and the remaining water continued to percolate downward.

During the model calibration, the impact of the lagged agricultural recharge was mainly simulated through shifting the timing of the recharge arrival at the water table without substantially modifying the cumulative total volume of the recharge. Specifically, in Maricopa-Stanfield and Eloy sub-basins, it was assumed that an average of about 80 percent of the conceptual annual agricultural recharge reached water table in the same year during the period of 1948 to 1983, and the remaining 20 percent arrived at the water table at much later years. In areas where depth-to-water table was shallow, the agricultural recharge was not lagged.

### ***Canal Recharge***

Canal recharge simulated in the model mainly refers to the main and lateral canal losses reported in SCIP annual reports. Since the SCIP main canals and laterals are unlined; loss rates of 30 to 50 percent of water were often reported in SCIP annual reports. The conceptual estimates of canal recharge were based on the difference between total water delivered and the total water applied to the field at both the GRIC (agency part) and SCIDD (district part). Therefore, the conceptual canal recharge represents the maximum potential canal recharge. During model calibration, it was observed that water levels along the Gila River Corridor, where most canal recharge was assigned, were consistently over-simulated. In that area, canal recharge was reduced by about 10 percent on average to account for the potential evaporation loss and errors in estimation.

The CAP lateral recharge was considered small and lumped with the agricultural recharge for each irrigation district. The recharge from the CAP main aqueduct was not adjusted during model calibration.

### ***Stream Recharge***

Recharge from stream channel infiltration recharge was a significant inflow component to the Pinal model area especially during flood years. Initially, Gila River stream recharge was assumed to only occur from the first up-gradient Gila River cell to the reach in the vicinity of Pima Butte for all the years simulated. During model calibration, it is found that the stream recharge should be distributed throughout the entire reach for flood years (based on available water level data). A similar approach was applied to distribute Santa Cruz River recharge. When recharge was limited, it was distributed along the well-defined Santa Cruz River channel in the southern Eloy sub-basin. During wet years, the stream recharge was extended to include tributary or ancestral channels from Eloy sub-basin to the Maricopa-Stanfield sub-basin where Santa Cruz River channel meets the Gila River channel. The Santa Cruz River recharge was distributed based on aerial photos showing the channel locations (Figure 51). The volume of the stream recharge was adjusted around the conceptual values based on head residuals.

### ***Other Recharge Components***

Other recharge components are small in volume and they were not adjusted during the transient model calibration. These components include mountain front recharge, Picacho Reservoir recharge, urban irrigation recharge, effluent recharge and artificial USF recharge.

### ***Pumping***

Total pumping in the Pinal model consists of four components, ROGR pumping, SCIP pumping, non-SCIP GRIC pumping and the pre-1984 pumping. The ROGR and SCIP pumping data were reported as well-specific annual totals and were considered to be the most accurate of all pumping data available. Consequently, those volumes were not adjusted during the model calibrations. Although non-SCIP GRIC pumping volumes were estimated, the volumes were

relatively small compared to other pumping totals, and therefore were not adjusted during model calibrations. The vertical distribution of pumping was adjusted for all four categories during the model calibration.

Pre-1984 pumping was a dominant outflow component which created cones of depression and altered flow directions in both the Eloy and Maricopa-Stanfield sub-basins. However, since pre-1984 pumping information were only available as the estimated basin-wide totals, the spatial and vertical distribution of those data are unknown, and the estimate of these distribution inevitably involves substantial uncertainties. During the transient model calibration, the horizontal and vertical distributions of pre-1984 pumping were extensively modified for the three model sub-areas. However, the total model-wide pumping was maintained at levels that closely matched USGS estimates of total pumping for the lower Santa Cruz basin (Anning and Duet, 1994).

### ***Hydraulic Conductivity***

The hydraulic conductivity distribution estimated from the steady-state calibration was fine-tuned during the transient model calibration. It is believed that aquifer compaction in Pinal model area not only caused significant land subsidence, but also permanently reduced aquifer hydraulic conductivities and storage properties. Since the aquifer compaction took place slowly and lasted a long period of time, these aquifer parameters vary in time accordingly. Currently, available model code simulates constant aquifer parameters over the simulation period. As a trade-off, during transient model calibrations, the hydraulic conductivity was calibrated to represent the most recent conditions. Therefore, more emphasis was placed on ensuring better calibration results at later simulation times than at steady-state or early times. In areas where aquifer test results were available, the horizontal hydraulic conductivities were adjusted to honor

the measured conductivities. In data deficient areas, conductivities were modified based on head residuals and other available hydrogeologic data.

Based on observed water level data, vertical gradients started to form as early as the 1940s. Comparison of unit-specific water level contour maps from 1984 and 2007 clearly and consistently indicate the presence of significant vertical gradients in three major areas: southwest of Eloy, southwest of Maricopa-Stanfield, and north of the Casa Grande Mountains. In some locations, vertical head differences between model layer 1 and model layer 2, or between layer 1 and layer 3 were as much as a few hundred feet during the 1960s to the early 1980s. The existence of the vertical gradients of this magnitude posed a great challenge for the model calibration. The vertical hydraulic conductivity was found to be the most critical and sensitive model parameter affecting the simulation of vertical gradients.

### *Vertical Conductance*

As discussed earlier, the Pinal model was developed using MODFLOW 2005 with the LPF package. In MODFLOW 2000 and other early versions, the Block Centered Flow (BCF) package was implemented with the vertical conductance term ( $V_{cont}$ ) ( $\text{day}^{-1}$ ) calculated independently from the model and based on the harmonic mean of vertical hydraulic conductivities between vertically adjacent model layers. In model simulations developed using MODFLOW 2000 or earlier versions, the  $V_{cont}$  term is held constant for the entire model simulation, regardless of any changes in the saturated thickness of the upper model layer (which, in theory should affect the calculated value of  $V_{cont}$ ). When the LPF package is used, the vertical hydraulic conductivity is a direct model input and the vertical conductance between model layers is calculated by the model as the harmonic mean based on the simulated saturated

thickness and the vertical hydraulic conductivity of each model layer. During model simulations, the vertical conductance is updated at every time step.

In the Pinal model area, water levels declined rapidly in many locations and large portions of model layers 1 and 2 became dewatered. The dynamic changes in aquifer saturated thickness affected the calculated vertical conductance and caused numerical instability and inaccurate model results. During the period of rapid water level declines, the aquifer system compacted, and the vertical conductance was conceptualized to become smaller (because the aquifer system compaction would theoretically decrease the vertical hydraulic conductivity) and limit the hydraulic connection between hydrogeologic units; thus creating a vertical hydraulic gradient between model layers. However, the LPF package provides no option to decrease vertical hydraulic conductivity, and instead increased the vertical conductance term at each time step as the saturated thickness of the uppermost active model layer decreased. This feature of the LPF package actually enhanced the vertical hydraulic connection between model layers. Specifically, water levels in Layer 1 were under simulated while water levels in layer 3 were over-simulated, the vertical gradient between layer 1 and layer 3 was simulated to be much smaller than observed.

To overcome this problem, the constant vertical conductance option of the LPF package was invoked (Nelson, 2012). The constant vertical conductance option assumes that the initial vertical conductance was calculated internally using vertical conductivity and model cell thickness instead of saturated aquifer thickness. As a result, the vertical conductance remained constant and was not recalculated with updated water levels during each time step. Vertical hydraulic conductivity or vertical conductance is minimally tested in field, and estimating this parameter involves substantial uncertainty. The observed vertical hydraulic gradient supports the

assumption that the hydraulic connection between model layers was limited, and the use of the constant vertical conductance option made it possible for the Pinal model to simulate the large vertical gradient in the three areas mentioned above. The model indicated that in areas where the vertical hydraulic gradient was small, the choice of whether the vertical hydraulic conductivity was updated, or not, had little impact on model results.

### ***Storage Coefficient***

Storage coefficients were less sensitive than many other model parameters. The initial specific yield and specific storage were estimated based on the original 1990 ADWR Pinal model and other previous studies in this area. During transient model calibrations, specific storage and specific yield were adjusted toward lower values for clay and other fine-grained material in model layers 2 and 3 to account for aquifer system compaction and inelastic compression of pore space.

### ***SUB-WT package parameters***

During the model development process the sensitivity of numerous SUB-WT parameters were evaluated. Calibration targets include both observed heads and observed land subsidence. Five SUB-WT parameters were identified as sensitive and deemed important to the model calibration process including:

- 1) The thickness of compressible sediments (b)
- 2) The compression Index (Cc)
- 3) The recompression index (Cr)
- 4) The starting preconsolidation stress offset (Precon)
- 5) The void ratio.

The final calibrated SUB-WT parameters were based on 4 general criteria: 1) plausible estimates of SUB-WT parameters based on estimates from the field where available (i.e., interbed thickness, void ratio, etc.) or plausible conceptual estimates from literature (i.e.,  $C_c$ ,  $C_r$ , and  $Precon$ ); 2) simulated head calibration to observed groundwater levels over space and time (i.e., water released from interbed storage generally increases water levels); that is simulated water levels provided another constraint for calibrating the SUB-WT parameters; 3) simulated subsidence – both relative and absolute land subsidence - calibrated to observed land subsidence (i.e., the spatial pattern and the land subsidence rate over time); and 4) the principal of parsimony: all the SUB-WT parameters were assigned single values per layer except the assignment of compressible sediments. Tradeoffs were made in order to balance the calibration objectives with the understanding that simulated subsidence was dependent on – and in a feedback loop with - the groundwater model solution. Furthermore is it assumed that there is unavoidable and inherent model error. As such, it is understood that in some cases final “calibrated” WT parameters may - to an extent deviate from conceptual estimates (i.e., estimate of thickness associated with compressible sediments) in order to meet the collective calibration objectives.

The thickness of compressible sediments,  $b$ , was defined as an array within the WT package. In general, the magnitude and distribution of assigned compressible sediment thickness reflects the distribution of the known, or assumed, fine-grained materials including the massive clay units in the general Picacho, Eloy and Maricopa-Stanfield areas (Figures 57 and 58). The most widespread areas of thick compressible sediments were assigned to model layer 2, including the massive clay bodies found in the Picacho-Eloy area. For model-calibration purposes, arrays defining zones of varying compressible sediments of were also assigned to

model layers 1 and 3. Furthermore, “default” compressible sediment thickness were assigned to model layers 1, 2 and 3 to represent naturally-occurring fine grain sediments inter-bedded within coarser-grained aquifer material. Default values for layers 1, 2 and 3 were assigned at 65 feet, 30 feet and 99 feet, respectively. During model development and calibration, assigning “default” compressible sediment thicknesses throughout the active model cells tended to stabilize the model solution. While the release of water from the compression of sediments seemed to lessen the occurrence of “dry” model cells, consequently lessening the frequency of cell re-wetting (a known MODFLOW difficulty), it is not exactly clear why this calibration adjustment helped stabilize solutions. Assigned thickness for layers 1, 2 and 3 varied from 65- 399 feet, 30 - 1,600 feet and 99-599 feet, respectively. The combined thickness of compressible sediments defined for all three model layers exceeds 2,000 feet in limited area around Picacho (Figure 58).

Assuming all other model parameters held constant - including parameters associated with the SUB-WT package - the areas / zones having the greatest assigned interbed thickness in combination with areas undergoing significant simulated head declines, consequently, results in the larger values of compaction, water released from interbed storage and land subsidence.

During model development, spatial distributions for other important SUB-WT parameters (i.e., Cc) were explored. However because of possible parameter combination non-uniqueness and / or uncertainty, constant values were ultimately assigned to simplify the model for Cc, Cr, Precon and void ratio for each of the three model layers.

The Cc and Cr are dimensionless compression and recompression indices, respectively, and relate to changes in effective stress. Calibrated values for Cc and Cr were assigned at 0.3 and 0.1, respectively. For comparative purposes, the magnitude of Cc assigned to two SUB-WT zones in the adjusted Antelope Valley Groundwater Model were 0.25 and 0.375 (Leake and

Galloway, 2010). The magnitude of Cr assigned in the adjusted Antelope Valley Groundwater Model was 0.0025 (Leake and Galloway, 2010). The preconsolidation stress is defined as the offset from the initial effective stress to initial preconsolidation stress, and is assigned in units of feet of a column of water. The calibrated value for Precon was 80 feet for all three model layers. For comparative purposes, the preconsolidation offset in the adjusted Antelope Valley Groundwater Model varied between zero feet and 160 feet for various zones (Leake and Galloway, 2010). The void ratio, defined as the ratio of the volume of voids to volume of solids, was assigned a value of 0.82, consistent with the test simulation value assigned in Leake and Galloway (2007). For comparative and reference purposes, the void ratio parameter for the Antelope Valley Groundwater Model was assigned a value of 0.724 (Leake and Galloway, 2010). For more details about the function of the SUB-WT parameters, see Leake and Galloway (2007). It should be noted that the coordinated adjustment of SUB-WT parameters as well as other parameters associated with the other key MODFLOW packages (i.e., LPF package, Kx; Kz; etc.) may render solutions that are comparable to the final calibrated model. In other words there may be combinations of SUB-WT parameters as well as other model parameters (i.e., Kz; Sy, etc.) that yield equally plausible solutions. Accordingly, the evaluation of all parameter combinations - by zone - has not been exhaustively explored.

## **Calibration Results**

### ***Steady-State Water Budget***

Limited hydrologic data were available for the pre-development period. However, independent analyses and reviews of previous studies resulted in a range of conceptual estimates for most groundwater flow components presented in the steady-state water budget (Chapter 2). The conceptual water budget was used to constrain the steady-state model calibration.

During steady-state, the primary inflow component to the groundwater system in the Pinal model area was Gila River stream infiltration recharge and the primary groundwater outflow was from evapotranspiration along the Gila River corridor. Thomsen and Eychaner's 1991 study provided critical information to estimate the spatial extent of ET, the volume of ET during pre-development, the average Gila River surface inflow, Gila River stream infiltration recharge and groundwater discharge. ET rate, ET extinct depth, and stream bed conductance were calibrated so that simulated ET and stream recharge and discharge reasonably matched the conceptual values. Other model parameters, such as horizontal hydraulic conductivity, were also adjusted to improve the correspondence between model simulated and the measurement-based 1900 water level contours developed by Thomsen and Baldys (1985).

The water budget for steady-state groundwater conditions was compiled from the calibrated model output for stress period 1 from both the base solution and the solution with the subsidence package. Inclusion of the sub-water table package introduced some mass balance errors to the steady-state solution. Table 11 compares the model simulated steady-state budget from both solutions. Since land subsidence was not assumed to occur during steady-state,, the budget from the base solution was compared to the conceptual steady-state budget (Table 12). Model simulated steady-state groundwater underflow into the Pinal model area was about 38,000 AFY which was about 7,000 acre-feet less than the conceptual estimate of about 45,000 acre-feet per year (Table 2). Gila River stream recharge was simulated at about 92,650 AFY, which was about 1,350 AFY less than the conceptual value (Table 5). Conceptual and simulated mountain front recharge was 500 acre-feet per year. The total simulated inflow of about 131,000 AFY, was about 6.5 percent less than the conceptual estimate. Simulated groundwater discharge to the Gila River was nearly identical to the conceptual value. Simulated evapotranspiration and

groundwater underflow from the model area acceptably corresponded to conceptual estimates. As mentioned previously, the simulation of closely related, head-dependent groundwater discharge components (stream discharge, riparian evapotranspiration and groundwater underflow leaving the model area) can be problematic for numerical model simulation. Although these components of groundwater discharge may be independently estimated from available data, each component's individual simulation using a groundwater model is complicated due to their interactive head-dependency. Therefore, in some areas the model simulated total for these three components may be more accurate than their individual simulated values.

Public Comment Draft - Subject to Revision

**Table 11 Pinal Model Simulated Steady-State Water Budget (With and Without the SUB-WT)**

Water Budget Component	Base Solution (AFY)	Solution with Subsidence (AFY)
IN		
Storage	0	0
Constant Head	29,370	29,357
Wells	8,424	8,424
ET	0	0
Recharge	499	499
Stream Leakage	92,642	92,813
Total Inflow	130,935	131,094
Out		
Storage	0	0
Constant Head	14,688	14,787
Wells	0	0
ET	95,870	95,890
Recharge	0	0
Stream Leakage	20,377	21,976
Total Outflow	130,935	132,653

**Table 12 Conceptual and Model Simulated Steady-State Water Budgets<sup>1</sup>**

	Conceptual Steady-state Budget (AFY)	Model Simulated Steady-state Budget (Base Solution) (AFY)
Inflow		
Total Underflow	45,600	37,794
Mountain Front Recharge	500	499
Stream Infiltration recharge	94,000	92,642
Total Inflow	140,100	130,935
Outflow		
ET	97,100	95,870
Stream Discharge	21,300	20,377
Total underflow	16,800	14,688
Total Outflow	135,200	130,935

1 Components of the Conceptual Water Budget Were Estimated Independently and Therefore the Total Conceptual Steady-state Inflow and Outflow Does Not Match Exactly

### ***Transient Water Budget***

The steady-state calibration provided calibrated hydraulic conductivities, streambed conductances and evapotranspiration parameters for the transient calibration. The steady-state calibration also provided initial conditions (starting heads) for the transient calibration. During the transient calibration the magnitude and distributions of aquifer storage properties (specific yield and storage coefficient), compressible sediment characteristics (pre-consolidation stress, clay thickness, compression indices, void ratio) and the vertical hydraulic conductivity were modified to improve the agreement between model simulated heads and fluxes and observed or estimated data.

During the transient calibration, additional inflow and outflow components were introduced that included recharge from agricultural irrigation, canals, flood events and other incidental and artificial sources and groundwater pumping. Groundwater released from the compression of fine-grained materials related to aquifer system compaction and land subsidence was also accounted for during the transient calibration period.

The simulated water budget from the model simulation period of 1923 to 2009 is presented in Table 13. This table shows a comparison of simulated water budgets with and without the SUB-WT package. Results indicate that the overall model-wide change in storage was about -16.2 to -16.9 million acre-feet, for the 87 year transient calibration period (depending upon whether the SUB-WT package was used, or not). The results also indicated a larger, but still acceptable, model-wide mass balance error for the model simulation that included the SUB-WT package.

**Table 13 Model Simulated 1923 – 2009 Water Budgets (With and Without SUB-WT)**

1923 - 2009 Simulated Water Budget (No SUB-WT Simulation)	87 Year Cum. Total	Annualized Volume Over 87 Years	1923 - 2009 Simulated Water Budget (With SUB-WT Simulation)	87 Year Cum. Total	Annualized Volume Over 87 Years	87 Year Difference (No SUB-WT - SUB-WT)
	AF	AFA		AF	AFA	AF
<b>STORAGE</b>	26,069,789	299,653	<b>STORAGE</b>	23,601,928	271,287	2,467,860
<b>CONSTANT HEAD</b>	2,742,529	31,523	<b>CONSTANT Head</b>	2,651,417	30,476	91,112
<b>WELLS</b>	1,222,018	14,046	<b>WELLS</b>	1,183,118	13,599	38,900
<b>ET</b>	0	0	<b>ET</b>	0	0	0
<b>RECHARGE</b>	39,086,318	449,268	<b>RECHARGE</b>	39,086,318	449,268	0
<b>STREAM LEAKAGE</b>	84,415	970	<b>STREAM Leakage</b>	105,928	1,218	-21,513
<b>INTERBED Storage</b>	0		<b>INTERBED Storage</b>	3,063,095	39,270	-3,063,095
<b>TOTAL IN</b>	69,203,398	795,441	<b>TOTAL IN</b>	69,690,083	801,035	-486,685
<b>OUT:</b>			<b>OUT:</b>			
----						
<b>STORAGE</b>	9,844,526	113,155	<b>STORAGE</b>	9,113,814	104,756	730,713
<b>CONSTANT HEAD</b>	1,912,784	21,986	<b>CONSTANT Head</b>	2,028,463	23,315	-115,679
<b>WELLS</b>	55,275,482	635,350	<b>WELLS</b>	55,397,153	636,289	-121,671
<b>ET</b>	1,202,102	13,817	<b>ET</b>	1,278,522	14,696	-76,421
<b>RECHARGE</b>	0	0	<b>RECHARGE</b>	0	0	0
<b>STREAM LEAKAGE</b>	963,036	11,069	<b>STREAM Leakage</b>	1,038,626	11,938	-75,590
<b>INTERBED Storage</b>	0		<b>INTERBED Storage</b>	627,669	7,215	-627,669
<b>TOTAL OUT</b>	69,198,806	795,388	<b>TOTAL OUT</b>	69,483,471	890,813	2,467,860
<b>IN - OUT</b>	5,296	61	<b>IN - out</b>	206,686	2,376	-201,390
<b>PERCENT DISCREPANCY</b>			<b>PERCENT Discrepancy</b>			
<b>Change in Storage</b>	-16,225,262	-186,497	<b>Change in Storage</b>	-14,488,115	-166,503	-1,737,148
<b>Change in Interbed Storage</b>	0	0	<b>Change in Interbed Storage</b>	-2,435,426	-27,993	2,435,426
<b>Total change in storage</b>	-16,225,262	-186,497	<b>Total change in storage</b>	-16,923,540	-194,523	698,278

**Table 14 Conceptual and Simulated (With SUB-WT) Pinal Model Water Budgets 1923 to 2009**

<b>Inflows</b>	<b>Conceptual</b>	<b>Simulated With SUB-WT</b>	<b>Conceptual/ Simulated Ratio</b>
<b>Groundwater Underflow</b>	4,446,000	3,834,535	1.16
<b>Total Recharge</b>	38,531,500	39,192,246	.98
<b>Outflows</b>			
<b>Groundwater Underflow</b>	1,590,000	2,028,463	.78
<b>Pumping</b>	56,743,200	55,397,153	1.02
<b>Evapotranspiration</b>	2,350,100	1,278,522	1.84
<b>Total Inflow – Outflow For Budget Components Shown</b>	-17,705,800	-16,923,540	1.05

Table 14 shows a comparison between the simulated cumulative transient budget for 1923 to 2009 that included the SUB-WT package and the conceptual cumulative estimates for major model budget components. The comparison indicates that model simulated groundwater underflow into the model area of about 3.8 million acre-feet (MAF), was about 86 percent of conceptual estimates (4.4 MAF). Total simulated recharge of about 39.2 MAF was about 2 percent greater than conceptual estimates (38.5 MAF). The total simulated groundwater underflow from the model area of about 2.0 MAF was about 28 percent greater than conceptual estimates (1.6 MAF). Total simulated groundwater pumping of about 55.3 MAF was about 2 percent less than the conceptual estimate of 56.7 MAF. Total simulated evapotranspiration of about 1.28 MAF was approximately 54 percent of the conceptual estimate of about 2.4 million acre-feet (Table 14). Although the model simulated evapotranspiration was substantially less

than the conceptual estimate, the difference is acceptable considering the general level of uncertainty of the conceptual estimate and also because it is a relatively small percentage of the overall model outflow. The total simulated inflow minus outflow of about -16.9 MAF for the budget components listed in Table 14 was about 4 percent less than the conceptual estimates (-17.7 MAF). The overall mass balance error for both transient model simulations (with and without the SUB-WT) is within acceptable limits and the high degree of correspondence between conceptual and simulated model budget components indicates the model successfully simulated the applied stresses.

### ***Head Residuals***

Table 15 summarizes the general calibration statistics for the error analysis of both the steady-state and transient model simulations. The mean error (ME), mean absolute error (MAE) and the root mean squared error (RMSE) for the steady-state calibration were 4.8 feet, 8.3 feet and 12.1 feet, respectively. The RMSE was 1.8 percent of the total head change in the steady-state model. All steady-state calibration statistics are within commonly accepted limits of model error.

The mean error (ME), mean absolute error (MAE) and the root mean squared error (RMSE) for 2007, the stress period 86 of transient model calibration period were -3.1 feet, 29.3 feet and 40.9 feet, respectively. The RMSE was 3.7 percent of the total head change in the transient model. All transient calibration statistics are within commonly accepted limits of model error.

The statistical methods described above give an indication of the average error of a model simulation. However, it is also important to examine the spatial distribution of model error to determine if there are areas in the model with excessive spatial bias. Figures 59 – 66 plot

residuals for each calibration. Examination of the residual maps reveals changing patterns of spatial bias over time. During many time periods there are large areas of the model that tend to have over-simulated or under-simulated heads in one or more model layers. Inspection of the changing patterns of spatial bias suggests that some of the model error is related to the simulated distribution and magnitude of the major model stresses (pumping and recharge). For example, in many time periods most of the area covered by one or more of the major farming entities (irrigation districts and areas of Indian agriculture) may tend to be positively or negatively biased. The residual maps also show opposing (positive vs. negative) patterns of spatial bias for different model layers within the same general area. These results suggest that some of the model error in such locations may also be related to the vertical distribution of pumping and/or to the simulated vertical hydraulic conductivity of the aquifer.

The distribution of model error is also shown in Figure 67 which is a scatter plot of the observed vs. simulated head pairs, and Figure 68 which shows residuals vs. observed heads. The scatter plots confirm that the distribution of model residuals is generally uniform about a mean of zero over the range of observed heads. These plots indicate the largest model errors generally occurred in Layers 2 and 3, in areas where the model heads were in the range of 700 to 1,100 feet. Although the model shows some level of spatial bias the overall calibration statistics are low compared to most of the other sensitivity tests that were evaluated (Chapter 5), and automated calibration would likely be required to appreciably reduce or minimize these biases. Overall, the various statistics related to the magnitude and spatial distribution of model error indicates an acceptable model-wide calibration.

**Table 15 Pinal Model Steady-State and Transient Residual Summary**

Year	Stress Period	Number of Targets (ft)	Mean Error (ME) (ft)	Absolute Mean Error (MAE) (ft)	Standard Deviation (ft)	Minimum Residual (ft)	Maximum Residual (ft)	Root Mean Squared Error (RMSE) (ft)	RMSE as % of Total Head Change
Steady-state	1	243	4.8	8.3	11.1	-33.2	47.9	12.1	1.86%
1941	20	100	0.3	11.3	15.4	-33.4	40.4	15.4	2.83%
1952	31	143	-2.5	20.6	24.9	-54.4	79.5	25.0	4.21%
1963	42	283	-33.5	45.4	45.0	-203.4	107.5	56.1	6.97%
1976	55	152	-5.9	47.3	66.6	-272.5	223.0	66.6	7.06%
1984	63	1,561	-10.4	28.7	38.7	-184.8	189.3	40.1	4.05%
1988	67	840	0.1	35.0	48.0	-215.5	252.2	48.0	4.96%
2007	86	1,244	5.1	26.1	32.6	-107.3	166.1	33.0	3.68%
All Targets	1 ~ 88	8,031	-3.1	29.3	40.8	-272.5	252.2	40.9	3.69%

Note:

1. Head Residual = Observed Head – Model Simulated Head
2. All targets include the targets used for the selected calibration periods and the additional targets used for hydrographs in between the calibration years.

### ***Water Level Maps***

Figures 69 and 70 are composite water level maps that compare observed heads and model simulated heads for steady-state and 2007. The maps overlay contours of measured and simulated heads. These maps show that the model reasonably simulated hydraulic gradients and flow directions throughout most of the model area for both the pre-development and present time.

### ***Hydrographs***

The model calibration was also evaluated by comparing hydrographs of simulated time-series head data with observed water level elevations. The hydrograph (HYD) package was used, producing data at 89 locations. Of those, 14 locations with long term observed water level records were compared with simulated model heads as hydrographs presented in Appendix C. The hydrograph locations are shown on Figure 29. The observed water level elevations in the hydrographs were constructed using water level data from the ADWR's GWSI database. Water levels with remarks that indicate pumping or some other activity that would invalidate the measurement were removed from the analysis.

In general, the hydrographs show that the model reasonably matched the observed water level trends between 1923 and 2009 at most well sites. Hydrographs for most wells in the model area generally showed long-term water-level declines from 1940s into early 1980s, and then water level recoveries from 1980s to the present.

The vertical hydraulic gradients simulated by the model, based on the difference in head between layers at the same location, were generally larger during the period of rapid water level decline, than at any other time. The simulated vertical gradients decreased as water levels recovered. Figures 71 - 78 show the distribution of vertical head differences between model

layers for each calibration period for Layer 1 Head – Layer 2 Head, Layer 2 Head – Layer 3 Head and Layer 1 Head – Layer 3 Head. Early in the simulation, vertical gradients were small in all parts of the model area. By 1952 there was a significant increase in the head difference between layers, with some areas showing more separation, in particular the central west portion of the Maricopa-Stanfield sub-basin near hydrograph H47 and the lower east portion of the Eloy sub-basin, near hydrograph H16. In the Maricopa-Stanfield sub-basin, the upper unit heads during that time period were typically greater than the lower unit heads. However, in the Eloy sub-basin, the simulation indicates areas where heads in the lower layers were greater than overlaying layers. In most areas, the spatial distribution of vertical head differences between Layers 2 and 3 is similar to the distribution of vertical gradients between Layers 1 and 3.

#### Calibrated Hydraulic Parameters

The final calibrated hydraulic parameters including hydraulic conductivities, specific yield, and specific storage are shown on Figures (79-86).

#### ***Simulated Inter-bed Storage (IB Storage)***

Figures 87 and 88 show simulated IB storage over time. For reference purposes, simulated IB storage change is compared with net elastic change-in-storage (or “traditional” storage). During the 87 year transient simulations, the net cumulative change-in-IB storage totaled about 2.44 MAF, or about 17 percent of the elastic net cumulative change-in-storage, which totaled about 14.5 MAF.

The highest rates of IB storage loss occurred from the early 1950’s to the early 1980’s, when groundwater withdrawals and groundwater levels declines were maximized. Net IB storage losses peaked during the early 1960’s when the annualized rate of net IB storage loss was about 100,000 AFY. That is, water was being released from (largely inelastic) IB storage, at

annualized rates of about 100,000 AFY. In last couple of decades, IB storage loss rates have significantly decreased, while groundwater levels in most areas have significantly recovered resulting in small gains of water back into IB storage. Depending on locations, the increase in simulated heads due to water released from compressible interbed storage (largely inelastic) varied from being negligible to greater than 50 feet south of Eloy.

### ***Observed and Simulated Subsidence***

Observed land subsidence provided additional key target data for the calibrations of the SUB-WT parameters. Figure 89 shows the comparison between simulated and observed land subsidence between 1952 and 1977. Land subsidence targets were also compared with model simulated subsidence along a profile located adjacent to I-10 between Picacho and Casa Grande (Figures 15 and 90). Figure 91 shows total simulated land subsidence from 1923 to 2009.

Simulated subsidence was compared with InSAR data (Figure 92) over the recent period between 2004 and 2009 (Conway, 2013). Comparatively small rates of subsidence were observed from the INSAR data during this recent period, with most areas showing less than 3 cm of subsidence. Comparably small rates of subsidence were simulated between 2004 and 2009. The magnitude of recently-simulated subsidence was minor compared to earlier decades due to the significant water level recoveries that occurred in most parts of the model area. In large portions of the model area, minor “rebound” of the land surface was simulated between 2004 to 2009. However, actual “rebound” was observed from INSAR data only in some parts of the model area, and only on a seasonal basis in the spring of some years during that period (Conway, 2013). Although the model simulated more recent rebound than indicated by the INSAR data the occurrence of rebound is not unexpected considering the significant water level recoveries that have occurred over the last several years (Leake, 2013). Overall, the magnitude of simulated and

observed rebound is minor compared to the cumulative subsidence that has occurred over the transient calibration period.

*Public Comment Draft - Subject to Revision*

## Chapter 5. Sensitivity Analysis

A sensitivity analysis provides a means of evaluating the uncertainties associated with model inputs. The responses of a model to changes in the various input parameters can be used to evaluate the sensitivity of a model solution to a particular model input parameter. The Pinal model calibration was based, in part, on direct information collected through time, for example water levels, pumping totals, surface flow and survey data; and indirect information such as recharge estimates (mountain-front and stream infiltration, agricultural recharge), timing of agricultural recharge (the lag factor), and aquifer parameters (vertical hydraulic conductivity, and storage values). The interpretation of all data inputs introduces a source of uncertainty in the model. The effects of increasing or decreasing the value of these parameters on the model results help identify parameters that may have measurable impacts on the model simulation.

### Sensitivity Runs

Sensitivity model runs were performed to test the following model parameters:

- Subsidence
- Non-lagged agricultural recharge
- Vertical hydraulic conductivity (Kz)
- Total recharge
- Specific yield (Sy)
- Pumping
- Total recharge and pumping combined
- Pumping and specific yield combined

## **Sensitivity Analysis Methods**

The sensitivity of model results to changes in model input parameters was evaluated using the following methods:

1. The model's sensitivity to changes in various input parameters and stresses was evaluated using heads simulated throughout the entire active model domain for the final model stress period (SP 88), which represents the year 2009. Specifically, for each sensitivity run, the model simulated water levels for each cell in each layer were compared to those of the calibration model run, and the head changes were calculated for all the active model cells in each model layer. Upon the completion of the head change calculations, the mean change in simulated heads was calculated for the entire model area, for each model layer and for selected sub-basins. The calculated mean changes in simulated heads for each category (model wide, layer specific, sub-basins) were then plotted against the parameter changes to indicate the sensitivity trend. Appendix D provides maps showing the spatial distribution of simulated head changes per layer for each sensitivity run and trend charts based on the tabulated data are included within this section of the report.
2. The sensitivity analysis also evaluated changes in simulated water levels at 14 wells located throughout the model area (Figure 29). The 14 wells were selected for this purpose based on well location and the availability of water level observations. Specifically, the model simulated hydrograph for the sensitivity run and the calibration model run were both compared to the observed data collected at the selected monitor wells. The comparisons of the water level trends graphically depict the sensitivity variations over time with respect to the same perturbation on tested model parameters. These hydrographs are also included in the appendix.

3. Sensitivity trends were also examined for the 8,031 individual head calibration targets. These targets have a model-wide distribution and cover both the steady-state and transient calibration periods. The head residuals for each sensitivity run were calculated for each target observation and then compared to the corresponding residuals from the calibration run to calculate the change in simulated residuals.

### **Sensitivity Analysis Procedures**

Alternative data outputs were selected in the MODFLOW name file to obtain different types of results to analyze the sensitivity of each tested model parameter. Vertical hydraulic conductivity, recharge, and specific yield were all altered by a percentage up or down for the active model cells using a multiplier in their respective packages. For example, a multiplier of 0.5 would reduce the original parameter values of the calibrated simulation by 50 percent and a multiplier of 1.5 would increase them by 50 percent. A multiplier of 1 is the default value within these packages and was used in the calibrated simulation. Groundwater pumping was simulated in the MODFLOW Well package that has a “list-type” input file format that cannot be altered with a multiplier like the other “array-type” input packages. Therefore a custom program was used to increase or decrease the pumping values assigned in the calibration model run. Care was taken to not increase or decrease well package values assigned to cells used to represent a boundary condition, but rather to simulate increases and decreases in actual pumping from wells as a water supply.

Results from the sensitivity runs were exported in the default model output formats for heads and cell-by-cell flows into Groundwater Vistas to obtain calibration statistics including mean, standard deviation, mean absolute error (MAE) and root mean square error (RMSE). Complete results of all sensitivity runs are included in Appendix D.

## **Sensitivity Results**

In addition to changing selected model array input multipliers or pumping rates, two simulations were run to evaluate the model's sensitivity to the simulation of aquifer-system compaction and also to evaluate the model's sensitivity to the lagged recharge inputs. To test these sensitivities, a simulation that did not include the SUB-WT package and a simulation that used a non-lagged version of the recharge package were included in the sensitivity analysis.

### ***Simulation without subsidence***

Table 16 presents the model-wide change in simulated heads and simulated residuals statistics for the sensitivity run that was made that did not include the SUB-WT Package. Changes in simulated heads were calculated for all active model cells at the end of the transient simulation period (SP88) using the relationship:

$$\text{Sensitivity Run Head (Without SUB-WT)} - \text{Calibrated Head (With SUB-WT)}$$

Changes in simulated residuals were calculated for the 8,031 individual water level observations using the relationship:

$$\text{Calibrated Residual (With SUB-WT)} - \text{Sensitivity Residual (Without SUB-WT)}$$

Removal of the subsidence package resulted in an average model-wide reduction of head of 12.38 feet (for all active model cells) at the end of the transient simulation period (SP 88). The removal of the subsidence package resulted in an average lowering of 17.07 feet in simulated heads compared to the simulation with the subsidence package, for the 8,031 calibration targets. The trend is further illustrated by comparing the simulated heads at each of

14 hydrograph locations with the simulated heads without the subsidence package (see Appendix D). A typical pattern is illustrated at hydrograph well H76 (D-08-08 10CDD) (Figure 93). The simulation without subsidence mirrors the calibrated simulation but the heads are approximately 15 feet lower and not as close to observed values.

**Table 16 Model Sensitivity to Subsidence (Without SUB-WT)**  
**Mean Change in Simulated Heads and Mean Change in Simulated Residuals \***

Area		Mean Change in Simulated Heads SP 88 (feet)	Mean Change in Simulated Residuals (feet)
Model-wide		-12.38	-17.07
Layers	Layer 1	-7.21	-10.27
	Layer 2	-10.93	-20.03
	Layer 3	-17.88	-24.06
Sub-Basins	East Salt River Valley	-2.66	-3.23
	Eloy	-17.03	-17.63
	Maricopa- Stanfield	-8.45	-17.20

\* Mean Change in Simulated Heads Calculated as:  
(Sensitivity Head [Without SUB-WT] – Calibrated Head [With SUB-WT])  
Mean Change in Simulated Residuals Calculated as:  
(Calibrated Residual [With SUB-WT] – Sensitivity Residual [Without SUB-WT])

### ***Simulation using Non-Lagged Recharge***

An alternative recharge package was produced that removed the agricultural recharge lag factor described in Chapter 2. In this test, the total quantity of water recharged into the system over the transient simulation remained the same at about 40 million acre-feet but the timing of the water from agricultural recharge reaching the water table was set to the same year the water was applied for irrigation (that is, the recharge was not lagged). The original crop and water use data were used but totals had to be adjusted to match the adjustments made during the trial and error calibration. The other types of recharge were unchanged. Using the non-lagged recharge package resulted in an average model-wide decrease of only 1.32 feet at the end of stress period 88 (2009). However, a comparison of residuals from the lagged and non-lagged recharge model simulations, showed that the non-lagged recharge package resulted in an average model-wide increase in head elevations of nearly 9 feet over the span of the transient simulation. So, although the use of the non-lagged dataset *did not make a significant impact on the final heads at the end of the transient simulation*, over the span of the transient simulation, some differences were significant and these differences exhibited an apparent trend where heads were usually over-simulated during early times and under-simulated during later times. Non-lagged heads resulted in higher residuals. The non-lagged simulation statistics were compared to corresponding values from the calibrated model run to further evaluate model sensitivity. Those values are presented in Table 17. This can be observed at hydrograph location H36, D-05-08 31DDD (Figure 94). The non-lagged recharge simulation has higher head elevations during most of the early years, but eventually, the heads recover in the lagged scenario, when the water that was estimated to have been recharged in earlier years is finally simulated to reach the water table. *The results of the sensitivity analysis indicate that it was critical to simulate lagged*

agricultural recharge over the transient calibration period. However, the results also suggest that it probably wouldn't be necessary to lag agricultural recharge for long-term future projection scenarios, assuming the final projected heads were the main model output to be evaluated. The following table summarizes the sensitivity statistics for model-wide mean change in simulated heads at the end of SP 88 and the mean change in simulated residuals for the 8,031 target observations on a model-wide, per layer and per sub-basin basis.

**Table 17 Model Sensitivity to Lagged and Non-Lagged Agricultural Recharge Mean Change in Simulated Heads and Mean Change in Simulated Residuals \***

Area		Mean Change in Simulated Heads SP 88 (feet)	Mean Change in Simulated Residuals (feet)
Model-wide		-1.32	8.93
Layers	Layer 1	-5.13	4.64
	Layer 2	-3.66	6.83
	Layer 3	3.93	18.53
Sub-Basins	East Salt River Valley	-2.21	4.05
	Eloy	-2.99	5.91
	Maricopa- Stanfield	2.19	15.71

\* Mean Change in Simulated Heads Calculated as:  
 (Sensitivity Head [Non- Lagged] – Calibrated Head [Lagged])  
 Mean Change in Simulated Residuals Calculated as:  
 Calibrated Residual [Lagged] – Sensitivity Residual [Non-lagged]

### ***Vertical Hydraulic Conductivity (Kz)***

The vertical hydraulic conductivity is specified in the MODFLOW LPF package. A Kz value is assigned to each active cell in the model with a heading that includes the multiplier. The default value of the multiplier is 1 and that was the value used for the calibration run. For each sensitivity run, the multiplier was adjusted up or down ranging from 0.05 to 20. Table 18, provides comparisons between the mean change in simulated heads at the end of SP 88 and the mean change in simulated residuals for the entire model area and for each model layer and sub-basin.

The changes in vertical hydraulic conductivity caused changes in vertical hydraulic gradients and vertical groundwater flow between model layers. For example, in the sensitivity runs where Kz was lowered (by .05 and .80) the simulated heads were higher in Layer 1 and lower in Layers 2 and 3. This occurred mainly because there is generally a downward vertical hydraulic gradient throughout most of the model domain that is caused by a combination of recharge being applied to the upper portion of the aquifer (usually in Layer 1) and also by proportionately more overall pumping coming from wells producing groundwater from the MSCU and LCU (Layers 2 and 3). Since the normal direction of groundwater flow is usually downward, any reduction in vertical hydraulic conductivity will limit vertical groundwater flow from upper model layers. In general, Layer 3 heads showed the highest level of sensitivity to reductions in vertical hydraulic conductivity (Table 18).

The opposite effect occurred when Kz was increased over calibrated values (by 1.2 and 20.). In those runs the groundwater flowed more easily from Layer 1 compared to the calibrated run and simulated heads were higher in Layers 2 and 3. Figure 95 shows the average change in head at the end of stress period 88 by layer and Figure 96 shows the average change in head at the end of stress period 88 by sub-basin.

**Table 18 Model Sensitivity to Vertical Hydraulic Conductivity**  
**Mean Change in Simulated Heads and Mean Change in Simulated Residuals\***

Area		(Kz) Multiplier							
		0.05		0.80		1.20		20.00	
		Mean Change in Simulated Heads SP 88 (feet)	Mean Change in Simulated Residuals (feet)	Mean Change in Simulated Heads SP 88 (feet)	Mean Change in Simulated Residuals (feet)	Mean Change in Simulated Heads SP 88 (feet)	Mean Change in Simulated Residuals (feet)	Mean Change in Simulated Heads SP 88 (feet)	Mean Change in Simulated Residuals (feet)
<b>Model-wide</b>		-41.68	-40.18	-3.29	-3.04	2.62	2.39	25.43	19.46
<b>Layers</b>	<b>Layer 1</b>	48.49	20.62	2.83	1.30	-1.97	-0.95	-10.36	-9.21
	<b>Layer 2</b>	-27.09	-33.28	-0.74	-0.59	0.63	0.47	8.97	-3.01
	<b>Layer 3</b>	-129.92	-146.53	-10.65	-13.18	8.16	10.24	65.26	94.74
<b>Sub-Basins</b>	<b>East Salt River Valley</b>	-18.19	-12.74	-1.09	-0.74	0.87	0.61	6.84	3.79
	<b>Eloy</b>	-47.46	-19.84	-4.23	-1.52	3.45	1.35	26.32	10.24
	<b>Maricopa-Stanfield</b>	-42.29	-85.37	-2.59	-6.43	1.91	4.72	33.74	40.25

\* Mean Change in Simulated Heads Calculated as:  
(Sensitivity Head [Variable Kz] – Calibrated Head)  
Mean Change in Simulated Residuals Calculated as:  
Calibrated Residual – Sensitivity Residual [Variable Kz]

## ***Recharge***

Recharge is specified in the MODFLOW RCH package. A recharge rate is assigned to each active cell in the model with a heading that includes the multiplier. The default value of the multiplier is 1 and that was the value used for the calibrated simulation. For each sensitivity run, the multiplier was adjusted up or down by 10 and 20 percent (0.8, 0.9, 1.10 and 1.20). Table 19 provides comparisons between mean sensitivity and calibrated head values at the end of SP 88 and the mean change in simulated residuals for the entire model area and for each model layer and sub-basin. The mean change in simulated heads at the end of SP 88 corresponds to the mean change in simulated residuals over the span of the simulation. Figure 97 shows the mean change in simulated head at the end of stress period 88 by layer and Figure 98 shows the mean change in simulated head at the end of stress period 88 by sub-basin.

As expected, increases in recharge caused simulated sensitivity heads to be higher than calibrated heads, and decreases in recharge had the opposite effect (Table 19). It should be noted that the sensitivity runs that had reduced recharge had more cells go dry than the calibrated model run. However, since the average changes in heads and residuals were only calculated for active (non-dry) cells, the model's apparent sensitivity to reduced recharge was less than its sensitivity to increased recharge (see flat portions of response of curves on Figures 97 and 98).

## ***Specific Yield (Sy)***

The specific yield (Sy) is defined in the MODFLOW LPF package. A Sy value is assigned to each active cell in the model with a heading that includes the multiplier. The default value of the multiplier is 1 and that was the value used for the calibrated simulation. For each sensitivity run, the multiplier was adjusted up or down ranging from 0.50 to 1.50 (-50 percent to +50 percent). The simulation failed to converge for the attempted multipliers 0.60 and 0.70 but

did converge for 0.5. Table 20 provides comparisons between mean sensitivity and calibrated head values at the end of SP 88 and the mean change in simulated residuals for the entire model area and for each model layer and sub-basin. In general, reduced specific yield resulted in lower simulated heads and increased specific yield resulted in higher simulated heads, regardless of layer and location (Figures 99 and 100). These results are generally consistent with the overall reduction of groundwater storage in the model area during the transient calibration period, and also due to the fact that reductions in specific yield cause the model to calculate more change in simulated water levels per unit change in groundwater storage, and increases in specific yield cause the model to calculate less change in simulated water levels per unit change in groundwater storage (regardless of whether the change in storage is positive or negative).

The differences in the sensitivity heads and calibrated heads were about 30 to 50 percent greater for the 8,031 targets where residuals were calculated, than for differences that were calculated for all active model cells at the end of SP 88. This is probably due to the fact that a larger percentage of the overall groundwater storage depletion and aquifer compaction in the model area occurred in earlier years of groundwater development (as opposed to current or recent times) and the 8,031 target measurements include those times while the simulated heads at the end of SP 88 do not.

**Table 19 Model Sensitivity to Recharge**  
**Mean Change in Simulated Heads and Mean Change in Simulated Residuals\***

AREA		Recharge Multiplier							
		0.80		0.90		1.10		1.20	
		Mean Change in Simulated Heads SP 88 (feet)	Mean Change in Simulated Residuals (feet)						
<b>Model-wide</b>		-18.63	-29.99	-19.00	-14.66	18.25	14.72	25.52	29.11
<b>Layers</b>	Layer 1	-12.27	-26.03	-17.03	-12.97	16.40	12.84	31.84	25.33
	Layer 2	-15.60	-28.06	-17.81	-14.10	16.97	14.43	33.13	28.30
	Layer 3	-26.45	-38.86	-21.66	-18.09	20.94	18.09	40.18	36.21
<b>Sub-Basins</b>	East Salt River Valley	-7.91	-20.03	-14.14	-10.00	9.04	9.02	6.84	16.97
	Eloy	-20.71	-29.33	-21.03	-14.63	21.01	14.86	26.49	29.21
	Maricopa-Stanfield	-19.96	-32.32	-17.66	-15.17	17.57	14.96	33.74	30.05

\* Mean Change in Simulated Heads Calculated as:  
(Sensitivity Head [Variable Recharge] – Calibrated Head)  
Mean Change in Simulated Residuals Calculated as:  
Calibrated Residual – Sensitivity Residual [Variable Recharge]

**Table 20 Model Sensitivity to Specific Yield  
Mean Change in Simulated Heads and Mean Change in Simulated Residuals\***

Area		Sy Multiplier					
		0.75		1.25		1.50	
		Mean Change in Simulated Heads SP 88 (feet)	Mean Change in Simulated Residuals (feet)	Mean Change in Simulated Heads SP 88 (feet)	Mean Change in Simulated Residuals (feet)	Mean Change in Simulated Heads SP 88 (feet)	Mean Change in Simulated Residuals (feet)
<b>Model-wide</b>		-12.92	-25.63	12.47	18.51	23.18	32.25
<b>Layers</b>	<b>Layer 1</b>	-6.33	-16.41	7.84	11.57	14.64	20.10
	<b>Layer 2</b>	-9.62	-22.32	10.51	17.89	19.49	30.60
	<b>Layer 3</b>	-21.10	-44.71	18.06	30.44	33.54	53.86
<b>Sub-Basins</b>	<b>East Salt River Valley</b>	-3.71	-7.74	2.73	5.92	4.69	10.30
	<b>Eloy</b>	-16.03	-21.49	15.57	16.20	28.93	27.90
	<b>Maricopa-Stanfield</b>	-11.64	-35.99	11.38	24.55	21.32	43.45

\* Mean Change in Simulated Heads Calculated as:  
(Sensitivity Head [Variable Sy] – Calibrated Head)  
Mean Change in Simulated Residuals Calculated as:  
Calibrated Residual – Sensitivity Residual [Variable Sy]

## ***Pumping***

Pumping is defined in the MODFLOW WELL package. The volume of water pumped was modified using custom well packages that were built to represent increases and decreases of up to 20 percent (0.80, 0.85, 0.90, 0.95, 1.05, 1.1, 1.15 and 1.2) of the calibrated pumping totals. Pumping rates were adjusted only for cells that represented actual wells. Pumping rates were not adjusted for cells that were used to represent constant flux boundary conditions.

Table 21 compares mean changes in simulated heads at the end of SP 88 and the mean change in simulated residuals over the span of the model calibration period. Figure 101 shows the mean change in simulated heads at the end of stress period 88 by layer and Figure 102 shows the mean change in simulated heads by sub-basin. As expected, increases in pumping caused the simulated sensitivity heads to be lower than the calibrated heads, and decreases in pumping caused the simulated sensitivity heads to be higher than the calibrated heads.

The sensitivity analysis shows that equal positive and negative percentage changes in pumping rates cause almost identical, but opposite, changes in simulated heads and residuals (Table 21). The analysis also shows that the greatest changes in simulated heads and residuals occurred in Layers 2 and 3; layers that typically have lower values of specific yield and storage coefficient. These results suggest that, in most areas, the applied changes in pumping rates probably did not cause the water table to drop below or rise above the model layer(s) that it was in during the transient calibration period. Otherwise, there would have been conversions from confined to unconfined conditions (and the opposite) that would have resulted in very different storage properties being applied for the calculation of model heads, thus making it unlikely that there would have been the near equal and opposite changes that were observed in the sensitivity analysis.

**Table 21 Model Sensitivity to Pumping**  
**Mean Change in Simulated Heads and Mean Change in Simulated Residuals\***

Area		Change Percentage											
		-20%		-10%		-5%		+5%		+10%		+20%	
		Mean Change in Simulated		Mean Change in Simulated		Mean Change in Simulated		Mean Change in Simulated		Mean Change in Simulated		Mean Change in Simulated	
		Heads SP 88 (Feet)	Residuals (Feet)										
<b>Model-wide</b>		56.82	58.54	28.58	29.48	14.22	14.62	-13.94	-14.45	-27.70	-29.77	-49.04	-55.75
<b>Layers</b>	<b>1</b>	39.65	37.88	19.86	19.12	9.69	9.56	-9.14	-9.46	-17.76	-19.73	-29.37	-36.33
	<b>2</b>	48.56	52.05	24.48	26.90	12.03	13.55	-11.55	-13.05	-23.27	-26.12	-40.20	-48.66
	<b>3</b>	63.88	100.10	39.48	49.41	19.93	24.11	-19.99	-24.30	-39.62	-50.63	-60.24	-96.08
<b>Sub-Basins</b>	<b>ESRV</b>	14.97	19.58	9.33	10.51	5.25	5.29	-6.43	-5.42	-12.58	-10.62	-24.71	-20.76
	<b>Eloy</b>	65.78	50.65	33.42	26.03	16.50	13.09	-15.78	-12.70	-31.59	-26.02	-54.41	-48.07
	<b>M-S</b>	60.17	78.75	28.82	38.48	14.27	18.71	-14.16	-18.99	-27.88	-39.45	-51.24	-75.14

\* Mean Change in Simulated Heads Calculated as:  
(Sensitivity Head [Variable Pumping Rate] – Calibrated Head)  
Mean Change in Simulated Residuals Calculated as:  
Calibrated Residual – Sensitivity Residual [Variable Pumping Rate]

### ***Combined Pumping and Recharge***

Recharge adds water to the system, typically at the top layer. Pumping removes water from all layers. Both stresses were simultaneously changed up and down by 10 and 20 percent. By simultaneously changing both pumping and recharge by the same percentage it is possible to determine which of the two stresses has the greatest impact on the simulation results. Furthermore, conducting sensitivity tests that combine two or more parameters may enable reviewers to better understand how parameters interact directly in a system that may be highly non-linear. In this sense, the combined (global) sensitivity analysis is superior to even inverse model products, such as covariance matrices, which depend on certain linearity assumptions.

Table 22 compares model-wide mean changes in simulated heads for the sensitivity and calibrated model runs at the end of SP 88 and the mean change in simulated residuals during the transient model calibration period for each layer and each sub-basin. Figure 103 shows the mean change in simulated heads, by layer, at the end of stress period 88, and Figure 104 shows the mean change in simulated heads by sub-basin. Changing both pumping and recharge simultaneously resulted in a trend, where a decrease in both stresses caused a model-wide increase in head and an increase in both stresses caused a model-wide decrease in head, similar to the way the model reacted to the individual changes in pumping stresses. These results are consistent with the fact that about 30 percent more water was pumped (about 55.2 MAF) than recharged (about 39.1 MAF) over the transient calibration period. The results show that simultaneous and equal percentage changes in the total volumes of these applied stresses exaggerate the impacts of the dominant stress to the model (pumping). This is shown in Figure 105 which provides a model-wide average at the end of the simulation.

**Table 22 Combined Model Sensitivity to Pumping and Recharge  
Mean Change in Simulated Heads and Means Change in Simulated Residuals**

Area		Pumping and Recharge Multiplier							
		0.80		0.90		1.10		1.20	
		Mean	Mean	Mean	Mean	Mean	Mean	Mean	Mean
		Change in Simulated Heads SP 88 (feet)	Change in Simulated Residual (feet)						
<b>Model-wide</b>		20.71	29.34	9.78	15.03	-8.91	-14.54	-17.32	-29.30
<b>Layers</b>	<b>Layer 1</b>	6.25	12.71	2.53	6.37	-1.35	-5.80	-1.79	-12.48
	<b>Layer 2</b>	14.25	24.76	6.65	13.15	-5.54	-11.66	-10.35	-23.82
	<b>Layer 3</b>	38.42	61.94	18.58	31.36	-18.16	-32.31	-36.19	-63.39
<b>Sub-Basins</b>	<b>ESRV</b>	-0.98	2.30	-0.56	0.92	0.38	-1.45	0.69	-2.00
	<b>Eloy</b>	24.84	22.39	11.81	11.71	-10.57	-10.56	-20.17	-21.95
	<b>Maricopa-Stanfield</b>	23.36	46.47	10.94	23.32	-10.30	-24.14	-20.72	-47.27

\* Mean Change to Simulated Heads Calculated as:  
(Sensitivity Head [Variable Pumping and Recharge Rates] – Calibrated Head)  
Mean Change to Simulated Residuals Calculated as:  
Calibrated Residual – Sensitivity Residual [Variable Pumping and Recharge Rates]

### ***Combined Pumping and Specific Yield***

In a similar manner to the pumping and recharge combination, pumping and specific yield parameters were simultaneously increased and decreased by 10 percent. They were also decreased by 20 percent, but the model failed to converge when both parameters were increased by 20 percent. The results indicate that a decrease in both parameters yield similar results to the decrease in pumping alone, while an increase in both causes heads to fall generally midway between the effects of the two.

Table 23 compares mean changes in simulated heads between the sensitivity and calibrated runs at the end of SP 88 and the mean change in simulated residuals by model layer and by sub-basin. Figure 106 shows the average change in head at the end of stress period 88 by layer and Figure 107 shows the average change in heads by sub-basin.

Model-wide, the effects of the combined Sy and Pumping parameter modification appears to closely follow the change in pumping alone. This is shown in Figure 108 which provides a model-wide average at the end of the simulation.

**Table 23 Combined Model Sensitivity to Pumping and Specific Yield  
Mean Change in Simulated Heads and Mean Change in Simulated Residuals\***

Area		Multiplier			
		0.90		1.10	
		Mean Change in Simulated Heads SP 88 (feet)	Mean Change in Simulated Residuals (feet)	Mean Change in Simulated Heads SP 88 (feet)	Mean Change in Simulated Residuals (feet)
<b>Model-wide</b>		24.56	22.41	-21.57	-18.83
<b>Layers</b>	<b>Layer 1</b>	17.33	14.75	-14.65	-12.57
	<b>Layer 2</b>	20.98	20.47	-18.30	-16.70
	<b>Layer 3</b>	33.76	37.23	-30.13	-31.61
<b>Sub-Basins</b>	<b>East Salt River Valley</b>	8.83	8.06	-11.04	-7.94
	<b>Eloy</b>	28.13	20.17	-24.12	-16.75
	<b>Maricopa-Stanfield</b>	25.49	28.47	-21.94	-24.21

\* Mean Change in Simulated Heads Calculated as:  
(Sensitivity Head [Variable Pumping and Sy] – Calibrated Head)  
Mean Change in Simulated Residuals Calculated as:  
Calibrated Residual – Sensitivity Residual [Variable Pumping and Sy]

### *Sensitivity Analysis of the SUB-WT Parameters*

The sensitivity of the four key SUB-WT parameters including  $C_c$ ,  $C_r$ , void ratio and preconsolidation offset were also tested. Although a formal analysis of the model's sensitivity to changes in compressible sediment thickness was not conducted, it is generally known that increasing the compressible sediment thickness result in 1) additional water being released from interbed storage; 2) increases in simulated heads (in affected areas); and 3) increases in simulated land subsidence. However because of the complex feedback patterns which exist between the dynamic flow model as well as other SUB-WT parameters, it is difficult to quantify the true nature of the sensitivity of the complex compressible thickness array. It is assumed that changes in the non-uniform compressible thickness array result in non-linear model responses, in terms of resulting simulated heads and simulated land subsidence. Because of the complexity and interaction associated among model variables the most rigorous way to understand the model parameter sensitivity is to conduct a global sensitivity analysis (Saltelli, et al, 2004), which is beyond the scope of this first generation model.

Because of the complex interactions between the SUB-WT parameters and other fundamental parameters, the sensitivity analysis was limited to evaluating  $C_c$ ,  $C_r$ , void ratio and Precon and the associated response for each model layer with respect to simulated heads. The sensitivity of the SUB-WT parameters with respect to simulated subsidence was not evaluated because the release of water from interbed storage is generally more sensitive to head changes than with respect to simulated land subsidence. Furthermore, the sensitivity of  $C_c$ ,  $C_r$ , void ratio and Precon were evaluated on a relative simulated head basis, with respect to the Base model calibrated heads using the final calibrated values of interbed thickness (assigned in an array format for all three model layers),  $C_c$  (constant for all three layers),  $C_r$  (constant for all three

layers), Precon (constant for all three layers) and void ratio, b (constant for all three layers). SUB-WT parameter sensitivity was strictly based on the total cumulative simulated head difference between the adjusted SUB-WT parameter and the calibrated base model after stress period 88, or simulation year 2009. The results of the SUB-WT parameter sensitivity are shown in Figures 109 - 115. In general, the analysis showed that changes in Cc, Cr, Precon and Void ratio produced similar responses for all model layers. Overall the model showed the most sensitivity to the applied changes in Cc and Precon.

## 6. Model Summary and Recommendations

### Model Summary and Results

An updated groundwater flow model has been developed that covers the groundwater basin portions of the Eloy and Maricopa-Stanfield sub-basins of the Pinal AMA and a portion of the East Salt River Valley sub-basin of the Phoenix AMA. The model was calibrated to steady-state conditions (early development - circa 1922) and transient conditions from 1923 to 2009. The model simulates regional groundwater flow and aquifer system compaction in three model layers that represent the UAU, MSCU and LCU aquifer units.

The development of this model produced a large data repository which covers a long period of time (1900~ 2009) for Pinal AMA for the first time. Numerous studies from a variety of sources including studies performed by USGS, ADWR, BOR, and other non-agency companies were reviewed. All the groundwater flow components as well as geology, hydrogeology, groundwater level conditions, and land subsidence in Pinal AMA were estimated, interpreted, and compiled into geodatabases, which will greatly facilitate the data sharing with all future users of this modeling report. This modeling study established the foundation of data for improved groundwater systems in Pinal AMA and future modeling efforts.

The transient model calibration covers a full range of the Pinal AMA groundwater development history, from the significant groundwater development to recent groundwater recovery. During the significant groundwater development period, groundwater pumping increased from less than 100,000 AFY in 1923 to over 1,400,000 AFY in 1953. Agricultural activity and groundwater pumping slowly diminished from the 1960s through the 1980s and has averaged between 400,000 to 500,000 AFY since the late 1980s when CAP water became readily

available. The model simulates large annual volumes of agricultural recharge that are sometimes lagged by several years to improve model calibration.

The Pinal model is the first regional groundwater flow model developed by ADWR to account for the impacts of land subsidence. Model results greatly improve our understanding of the effects of aquifer compaction on the aquifer systems in the Pinal model area, and quantify the volume of water released over time from the inter-bed storage. Model results also include estimates of simulated land subsidence which are of interest to water resource managers and water facility managers.

The updated Pinal AMA groundwater flow model was generally successful in replicating significant long-term water level trends and changes in groundwater flow patterns and aquifer storage. However, the accurate simulation of extreme vertical gradients and absolute water level elevations was less successful in some parts of the model area. The model reasonably replicated regional patterns and amounts of land subsidence. Model-wide residual analysis indicated that the mean absolute error (MAE) for all time periods was about 29 feet and the root mean squared error (RMSE) was about 41 feet which is about 3.7 percent of the total head change in the model. Both these statistics indicate an acceptable model-wide simulated head distribution. Water budget data show that the total simulated pumping and recharge were within 2 percent of conceptual estimates.

Sensitivity analysis indicated that the model's overall head calibration was improved by including land subsidence and lagged agricultural recharge. However, the sensitivity analysis indicated that it might not be necessary to "lag" agricultural recharge for future long-term projection scenarios. The model was shown to be comparatively sensitive to changes in vertical hydraulic conductivity (Figure 116), and less sensitive to changes in specific yield. The model's

sensitivity to changes in compressible sediment parameters  $C_c$ ,  $C_r$ , Precon and void ratio was similar for all model layers.

In general, the Pinal model was most sensitive to changes in pumping and vertical hydraulic conductivity. The comparative model responses to changes in pumping, recharge and specific yield are shown in Figure 117. Figure 118 shows that the mean absolute error of the base model was the lowest of all conceptual models tested.

### **Model Limitations and Uses**

The updated Pinal AMA groundwater flow model provides a useful analytical tool to study various hydrologic features and processes within the model area. The model is well-suited to study the regional impacts of future water use scenarios, potentially including: significant reductions in CAP water-use, increased or decreased groundwater pumping and future flood events on the Gila and Santa Cruz Rivers. The model is capable of providing useful estimates of future regional land subsidence. The accumulated hydrologic, geologic, pumping and recharge data also comprise a valuable database for other regional and sub-regional hydrologic studies and models.

Although the updated model may be well-suited for many uses it may not be appropriate for site-specific applications in areas of data deficiency and/or poor model calibration. Additionally, the current .5 square mile model grid may be too coarse for certain types of well drawdown or groundwater mounding studies or analyses. Other factors that may affect model use for long-term projections include mass balance, cell de-watering and numerical stability issues related to cell wet/dry conversions, subsidence simulation and numerical solver limitations.

Since each ADWR model has its own unique character and areas of data deficiency, poor calibration or marginal boundary conditions it should not be assumed that a model can be used,

as is, without first reviewing it to determine if it is a suitable tool to be used for a specific task. In many cases, a model may be sufficient to use, as is; however, it is contingent on the user of the model to review the model for their specific purpose and address any issues before the model can be used to conduct hydrologic analysis required to support applications submitted to the Department. If an ADWR model is used in conjunction with an application, it should be reviewed for suitability before proceeding with the analysis.

### **Recommendations**

The update of the Pinal AMA groundwater flow model has provided an improved understanding of hydrogeology of the AMA's regional aquifer system and also provided a useful analytical tool to study, test and evaluate various future water use strategies and conditions. As with all ADWR models the Pinal model will be periodically updated in the future to improve reliability and maintain current pumping and recharge information. The following recommendations are provided to help guide future model improvements and data collection activities.

1. New pumping and recharge data should be collected and run in the model at least every 5 years to keep the model up to date.
2. The current GWSI annual index line water level measurement network should be maintained and potentially expanded in the AMA to include more unit-specific wells (particularly MSCU and LCU wells) and add more measurements in data deficient areas. Periodic sweeps of a larger percentage of the measureable wells in the AMA should be reinstated as Departmental priorities and resources allow.
3. Continued collection and analysis of land subsidence data should be maintained using the Department's InSAR program.

4. Periodic microgravity measurements to support the AMA's aquifer storage monitoring program should continue at a frequency appropriate to maintain program continuity and reliability. This data should be integrated into future model updates and calibration.
5. An important part of future model calibrations should be to improve the simulation of significant vertical hydraulic gradients (where they may exist), and the reduction of major "offset-residuals" between simulated and observed water levels in some areas. This may require local grid refinements in some "problematic" areas.
6. Further analysis and quantification of agricultural recharge and the "lagging" of simulated agricultural recharge is also advised. Based on model sensitivity analysis it is suggested that lagging projected agricultural recharge is not necessary for long-term future simulations.
7. A future update and analysis of riparian evapotranspiration in the model area is recommended.
8. Future model updates should potentially include the adaption of the Pinal AMA model to newer versions of MODFLOW such as the Newtonian (NWT) or Unstructured Grid (USG) versions.
9. Future model calibrations should also be based, at least in part, on automated calibration methods such as PEST (Watermark Numerical Computing, 2010).

## References

ADWR 1996. Hydrographic Survey Report for the Gila River Indian Reservation, In Re The General Adjudication of the Gila River System and Source. Watershed File Report No. L8-58-001.

ADWR, 1999. Third Management Plan for Pinal Active Management Area 2000-2010.

ADWR, 2013. Miscellaneous aquifer test data for Pinal model area from ADWR Assured and Adequate Water Supply and Well Impact Files. Compiled and Stored in ADWR Modeling Section Files.

Anderson, M., and Woessner, W., 1992. Applied Groundwater Model: Simulation of Flow and Advective Transport, Academic Press Inc. Harcourt Brace Jovanich Publishing.

Anderson, T.W., 1968. Electric-Analog Analysis of Ground-Water Depletion in Central Arizona. U.S. Geological Survey Water Supply Paper 1860.

Anning, D.W., and Duet, N.R., 1994. Summary of Ground-Water Conditions in Arizona, 1987-90. United States Geological Survey Open-File Report 94-476.

Arizona Agricultural Statistics, 1966. Arizona Agricultural Statistics 1867 to 1965. Arizona Crop and Livestock Reporting Service.

Arizona Agricultural Statistics, 1966-2009. Arizona Agricultural Statistics Bulletins [various annual bulletins and reports from 1966 to 2009]. Prepared in cooperation with the United States Department of Agriculture, University of Arizona and the Arizona Department of Agriculture.

Arizona Department of Water Resources, 1999. Third Management Plan For Pinal Active Management Area 2000-2010.

Bartlett, D., and Corell, S., 2003. City of Peoria Groundwater Flow Model of the West Salt River Valley. Developed by Clear Creek Associates for the City of Peoria (P02-0064).

Bota, L, Jahnke, P. and Mason, D., 2004.. SRV Model Calibration Update 1983-2002. Memo to the Salt River Valley Model File. Arizona Department of Water Resources, Hydrology Division.

Burgess and Niple, 2004. Professional Review of the Pinal Active Management Area's Groundwater Budget, Arizona Department of Water Resources.

City of Scottsdale (2003). Regional Groundwater Flow Model, City of Scottsdale, Arizona. Appendix E: Summary of Model Modifications to the City of Scottsdale Groundwater Flow Model. Prepared by Brown and Caldwell.

Conway, B. 2013. ADWR INSAR data and analysis.

Cooper, H.H. and Jacob, C.E., 1946. A generalized graphical method for evaluating formation constants and summarizing well field history, Am. Geophys. Union Trans., vol. 27.

Corell, S., and Corkhill, E.F., 1994. A Regional Groundwater Flow Model of the Salt River Valley Phase II, Phoenix Active Management Area, Numerical Model, Calibration, and Recommendations. Arizona Department of Water Resources. Model Report No. 08.

Corkhill, E.F., Hill, B.M., 1990. Pinal Active Management Area Regional Groundwater Flow Model Phase Two: Numerical Model, Calibration, Sensitivity and Recommendations. Arizona Department of Water Resources Modeling Report No. 2.

Corkhill, E.F., Corell, S., Hill, B., and Carr, D. 1993. A Regional Groundwater Flow Model of the Salt River Valley – Phase I, Phoenix Active Management Area, Hydrogeologic Framework and Basic Data Report. Arizona Department of Water Resources Model Report No. 06.

Driscoll, F.G., 1986. Groundwater and Wells: 2<sup>nd</sup> Edition. Johnson Division, St. Paul, Minnesota.

Dubas, L., Davis, T., 2006. Arizona Department of Water Resources Salt River Valley Model Geology Update Model Report No. 16.

Dubas, L., and Liu, S., 2010. Arizona Department of Water Resources Regional Groundwater Flow Model of the Pinal Active Management Area Provisional Report Geology Update – Modeling Report No. 20.

Duffield, G.M., and Rumbaugh, J.O., 1991. AQTESOLV, Aquifer Test Solver Version 1.1, Geraghty & Miller Inc.

Epstein, V.J., 1987. Hydrologic and geologic factors affecting land subsidence near Eloy, Arizona: U.S. Geological Survey Water-Resources Investigations Report 87-4143.

ESRI, 2011. ARCGIS Version 10 Software from Environmental Systems Research Institute, Inc. <http://www.esri.com/>.

Evans, D. and Pool, D. 2000. Aquifer Compaction and Ground-water Levels in South-Central Arizona. United States Geological Survey Water-Resources Investigation Report 99-4249.

Freihoefer, A., Mason, D., Jahnke, P., Dubas, L., Hutchinson, K., 2009. Regional Groundwater Flow Model of the Salt River Valley, Phoenix Active Management Area, Model Update and Calibration. Arizona Department of Water Resources Modeling Report 19.

Freethy, G.W., and Anderson, T.W., 1986. Pre-development Hydrologic Conditions in the Alluvial Basins of Arizona and Adjacent Parts of California and New Mexico. United States Geological Survey Hydrologic Investigations Atlas HA-664.

GRIC, circa 1980. Documents and data sent to ADWR by (Mr. Cox?) on behalf of Gila River Indian Community listing GRIC well locations and pumping capacities for years 1975-1979.

Halpenny, L., and others, 1952. Ground water in the Gila River basin and adjacent areas, Arizona – A summary: U.S. Geological Survey open-file report.

Hammett, B., R. Herther (1995). Hydrologic Map Series No. 27, Maps showing groundwater conditions in the Phoenix Active Management Area, Maricopa, Pinal and Yavapai Counties, Arizona 1992.

Hantush, M.S. and Jacob, C.E. 1955. Non-steady radial flow in an infinite leaky aquifer, Am. Geophys. Union Trans., vol. 36, no. 1, pp. 95-100.

Hantush, M.S., 1960. Modification of the theory of leaky aquifers, Jour. of Geophys. Res., vol. 65, no. 11, pp. 3713-3725.

Haneberg W., Gomez, P., Gibson, A. and Allred, B, 1998. Preliminary Measurements of stress-dependent hydraulic conductivity of the Santa Fe Group aquifer system sediments from the 98<sup>th</sup> St. core hole Albuquerque, New Mexico. February 1998 New Mexico Geology.

Harbaugh, A.W. (1990). A computer program for calculating subregional water budgets using results from the U.S. Geological Survey modular three-dimensional ground-water flow model: U.S. Geological Survey Open-File Report 90-392.

Harbaugh, A.W., E. Banta, M. Hill, M. McDonald (2000). MODFLOW-2000, The U.S. Geological Survey Modular Ground-Water Flow Model – User Guide to the Observation, Sensitivity, and Parameter-Estimation Process and Three Post-Processing Programs: U.S. Geological Survey Open-File Report 00-184.

Harbaugh, A.W., 2005. MODFLOW-2005, The U.S. Geological Survey Modular Ground-Water Model – The Groundwater Flow Process. Chapter 16 of Book 6. Modeling techniques, Section A. Ground Water.

Harbaugh, A.W. (2008). “Zonebudget Version 3.” Program documentation, U.S Geological Survey.

Hardt, W.F., Cattany, R.E., and Kister, L.R., 1964. Basic Ground-Water Data for Western Pinal County, Arizona. ASLD Water Resources Report Number Eighteen. Prepared for Arizona State Land Department by the USGS.

Hardt, W.F., and Cattany, R.E. 1965. Description and Analysis of the Geohydrologic System in Western Pinal County, Arizona. United States Geological Survey Open File Report.

Helm, D.C., 1976. One-dimensional simulation of aquifer system compaction near Pixley, California: 2. Stress-Dependent Parameters. *Water Resources Research* Vol. 12, NO. 3, PP. 375-391, 1976 doi:10.1029/WR012i003p00375

Helsel, D., and Hirsch, R., 2002. *Statistical Methods in Water Resources*. Techniques of Water Resources Investigations, Book 4, chapter A3. U.S. Geological Survey.

Hill, M., 1998. *Methods and Guidelines for Effective Model Calibration*. U.S. Geological Survey Water-Resources Investigation Report 98-4005.

Hipke, W., F.Putman, J. Holway, M. Ferrell (1996). *Analysis of Future Water Use and Supply Conditions: Current Trends Alternative 1989-2025*. Arizona Department of Water Resources. Model Report No. 11.

Holzer, T.L., 1981, Preconsolidation stress of aquifer systems in areas of induced land subsidence: *Water Resources Research*, v. 17, no. 3, p. 693-704. 25.

Konieczki, A.D., and English, C.S. 1979. *Maps Showing Ground-Water Conditions in the Lower santa cruz Area, Pinal, Pima, and Maricopa County, Arizona – 1977*. U.S. Geological survey Water-Resources Investigations 79-56 Open-File Report.

Laney, R.L., Raymond, R.H., Winikka, C.C., 1978. *Maps Showing water-level declines, land subsidence, and earth fissures in south-central Arizona*. USGS Water-Resources Investigations Report: 78-83.

Leake, S.A., 2013. Personal communication between Stan Leake and Keith Nelson regarding simulated and observed subsidence data and trends in the Pinal AMA.

Leake, S.A., and Galloway, D.L., 2007. *MODFLOW Ground-Water Model-User Guide to Subsidence and Aquifer-System Compaction Package (SUB-WT) for Water-Table Aquifers*. United States Geological Survey Chapter 23 of Section A, Ground Water, of Book 6, Modeling Techniques. Techniques and Methods 6-A23.

Leake, S., and Galloway, D., 2010. *Use of SUB-WT Package for Modflow to Simulate aquifer-system compaction in Antelope Valley, California, USA. Land Subsidence, Associated Hazards and the Role of Natural Resources Development (Proceedings of EISOLS 2010, Queretaro, Mexico, 17-22 October 2010)*. IAHS Publ. 339, 2010.

Lee, W. T., 1904. *The underground waters of Gila Valley, Arizona*: U.S. Geological Survey Water-Supply and Irrigation Paper 104.

Long, M., and Erb, S., 1980. *Computerized Depth Interval Determination of Groundwater Characteristics from Driller Logs*. Hydrology and Water Resources in Arizona and the Southwest. Arizona-Nevada Academy of Science. Volume 10.

Long, M., M.Niccoli, R.Hollander, J.Watts (1982). Salt River Valley Cooperative Study Model Effort.

Mason, D., and Hipke, W., 2013. Regional Groundwater Model of the Tucson Active Management Area, Arizona, Model Update and Calibration. Arizona Department of Water Resources Modeling Report No. 24.

Moench, A.F., 1985. Transient flow to a large-diameter well in an aquifer with storative semiconfing layers, Water Resources Research, vol. 21, no. 8, pp. 1121-1131.

Nelson, K., 2011. ADWR Internal Memo from Keith Nelson (dated March 16, 2011) "Leaky\_Aquifer\_Test\_Results\_03\_16-2011.pdf".

Nelson, K., 2012. ADWR Internal Memorandum from Keith Nelson (dated July 12, 2012). "Comparison showing how alternative MODFLOW solvers can affect the same model including 1) Prescott Model: The comparison of simulated heads with and without the CONSTANTCV NOCORRECTION Optim in the LPF Package; 2) Pinal Model: The Comparison of Simulation".

Pool, D.R., Carruth, R.L., and Meehan, W.D., 2001. Hydrogeology of Picacho Basin, South-Central Arizona. United States Geological Survey Water-Resources Investigations Report 00-4277.

Prudic, D.E., 1989. Documentation of a computer program to simulate stream-aquifer relations using a modular, finite-difference, ground-water flow model: U.S. Geological Survey Open-File Report 88-729.

Rascona, S.J. (2005). Hydrologic Map Series No. 35, Maps showing groundwater conditions in the Phoenix Active Management Area, Maricopa, Pinal and Yavapai Counties, AZ, Nov. 2002-Feb 2003.

Richard, S.M., Reynolds, S.J., Spencer, J.E., and Pearthree, P.A. 2000. AZGS Geologic Map of Arizona, scale 1:1,000,000.

Rivera A., Ledoux, E., 1991. Nonlinear Modeling of Groundwater Flow and Total Subsidence of the Mexico City Aquifer-Aquitard System. Land Subsidence (Proceedings of the Fourth International Symposium on Land Subsidence, May 1991. IAHS Publ. no. 200, 1991.

Robinson, G.M., and Peterson, D.E., 1962. Notes on earth fissures in southern Arizona: U.S. Geological Survey Circular 466.

Rumbaugh, and others, 2011. Groundwater Vistas Version 6 ESI (Environmental Simulations Incorporated) Software and manuals. <http://www.groundwatermodels.com>

Saltelli, A., Tarantola, S., Campolongo, F. and Ratto, M. 2005. Sensivity Analysis in Practice. A Guide to Assessing Scientific Models. Jon Wiley & Sons Ltd.

Slaff, S., 1993. Land Subsidence and Earth Fissures in Arizona. Arizona Geologic Survey Down-to-Earth Series 3.

Smith, G.E.P., 1940. The groundwater supply of the Eloy District in Pinal County, Arizona: University of Arizona, College of Agriculture, Agricultural experiment station Technical Bulletin 87.

SCIP, 1934-2009. United States Department of Interior San Carlos Irrigation Project Coolidge, Arizona - Annual Reports (1934-2009).

Stetson Engineers 1981. Historic Groundwater Depletion Beneath the Gila River Indian Reservation Arizona.

Theis, C.V., 1935. The relation between the lowering of the piezometric surface and the rate and duration of discharge of a well using groundwater storage, Am. Geophys. Union Trans., vol. 16, pp. 519-524.

Thomsen, B.W., and Baldys, S, III, 1985. Groundwater conditions in and near the Gila River Indian Reservation, south-central Arizona: U.S. Geological Survey Water-Resources Investigations Report 85-4073.

Thomsen, B.W., and Eychaner, J.H., 1991. Pre-development Hydrology of the Gila River Indian Reservation, South-Central Arizona. United States Geological Survey Water-Resources Investigations Report 89-4174.

Thomsen, B.W., and Porcello, J.J, 1991. Pre-development Hydrology of the Salt River Indian Reservation, South-Central Arizona. United States Geological Survey Water-Resources Investigations Report 91-4132.

Turner, S.F., and others, 1943. Groundwater Resources of the Santa Cruz Basin Arizona. United States Department of the Interior Geological Survey.

US Bureau of Reclamation, 1976. Central Arizona Project, Geology and Groundwater Resources Report, Maricopa and Pinal Counties, Arizona. Vols. 1 and 2.

U.S. Geological Survey (1973). Map of Irrigated Land in the Phoenix Area, Arizona from USGS, USDA, and Arizona Water Commission. USGS Map I-845-B.

USGS, 1989. Floods of October 1983 in Southeastern Arizona. USGS Water-Resources Investigations Report 85-4225-C.

Watermark Numerical Computing, 2010. PEST Model-Independent Parameter Estimation User Manual 5<sup>th</sup> Edition. <http://www.pesthomepage.org>

Wickham, M.P., and Corkhill, E.F., 1989. Pinal Active Management Area Regional Groundwater Flow Model Phase One: Hydrogeologic Framework, Water Budget and Phase One Recommendations. Arizona Department of Water Resources Modeling Report Number 1.

Public Comment Draft - Subject to Revision